Application of PC-SAFT equation of state in the carbon dioxide capture and the gasoline desulfurization

Yushu Chen

UNIVERSITÉ DE LORRAINE

Ecole Doctorale RP2E : Ressources, Procédés, Produits, Environnement
Laboratoire Réactions et Génie des Procédés – UMR 7274 CNRS – ENSIC

THÈSE

Présentée par

Yushu CHEN
Ingénieur CPE LYON

Pour l'obtention du grade de

Docteur de l'Université de Lorraine
Spécialité : Génie des procédés et des produits

Application de l'équation PC-SAFT à la capture du dioxyde de carbone et à la désulfuration des essences

Soutenue publiquement le 26 septembre 2013 devant la commission d'examen :

Rapporteurs :	Mme. Pascale HUSSON
	M. Jean-Philippe PASSARELLO
Examinateurs :	Mme. Isabelle CHEVALOT
	M. Jean-Noël JAUBERT (directeur de thèse)
	M. Rafael LUGO
	M. Fabrice MUTELET (co-directeur de thèse)
Invité :	M. Romain PRIVAT

Remerciements

Ce travail a été réalisé au laboratoire Réactions et Génie des Procédés (LRGP-UPR 7274 CNRS) à Nancy. Je tiens tout d'abord à remercier Monsieur Laurent FALK, directeur du LRGP, pour m'avoir accueilli et intégré dans son laboratoire.

Je tiens à exprimer mes sincères remerciements à mon directeur de thèse : Monsieur Jean-Noël JAUBERT, Professeur à l'Université de Lorraine/LRGP, pour la confiance qu'il m'a accordée durant ces trois années et pour avoir réuni les conditions nécessaires au bon déroulement de mes travaux.

J'adresse mes plus vifs remerciements à Monsieur Fabrice MUTELET, Maître de Conférences-HDR à l'Université de lorraine/LRGP, qui m'a encadré tout au long de cette thèse. Je le remercie pour ses encouragements, sa compréhension, sa grande disponibilité et son aide indispensable qui ont rendu ce travail de thèse très enrichissant sur le plan scientifique.

Que Madame Pascale HUSSON, Maître de Conférences-HDR à l'Université de Blaise Pascal et Monsieur Jean-Philippe PASSARELLO, Professeur à l'Université Paris 13 trouvent ici l'expression de ma sincère gratitude pour avoir accepté de juger ce travail en tant que rapporteurs. Leur présence dans le jury m'honore. J'assure ma profonde gratitude à Madame Isabelle CHEVALOT, Professeur à l'Université de Lorraine pour avoir accepté de présider cette commission d'examen. Je souhaite également remercier sincèrement Monsieur Rafael LUGO, chef de projet IFP EN, ainsi que Monsieur Romain PRIVAT, Maître de Conférences à l'Université de lorraine, pour m'avoir fait l'honneur de participer à mon jury de thèse.

Un grand merci à tous les membres du laboratoire : Dominique ALONSO, Mohammed BOUROUKBA, Patrick CARRE, Michel DIRAND, Ludivine FRANCK-LACAZE, Nathalie HUBERT, Jean-Charles MOÏSE, Viviane RENAUDIN, Roland SOLIMANDO. Je voudrais aussi remercier tous les stagiaires, thésards, ex-thésards et post-doc qui ont su faire de ces trois ans une expérience agréable et enrichissante,

pour leur sympathie, leur générosité et le partage de leur savoir : Afef ATTIA, Daniela BELTRAN, Pablo FERNANDEZ, Yingying GU, Elsayed Rabie HASSAN, Niramol JUNTARACHAT, Karolina KEDRA-KROLIK, El Shaimaa Abou MANDOUR, Virginia ORTEGA-VILLA…

Pour terminer, sans doute le plus important, je voudrais remercier mes parents ainsi que ma femme, qui de près ou de loin, ont toujours su m'offrir leur soutien, leurs encouragements et leur affection.

Table des matières

Nomenclature et symboles

Abréviation

AAD%	Erreur relative moyenne (Absolute Average Deviation)
CPA	Cubique plus association
EoS	Equation d'état
NRTL	Non-Random Two Liquid Model
UNIQUAC	Universal Quasi-Chemical Approach
PPR78	Predictive Peng-Robinson 1978
PC-SAFT	Perturbed Chain Satatistical Associating Fluid Theory
tPCP-SAFT	Truncated Perturbed Chain Polar- SAFT
VLE	Equilibre liquide-vapeur
LLE	Equilibre liquide-liquide
LIs ou ILs	Liquides ioniques
FO	Fonction objectif

Symboles

a et b	Paramètre de l'équation de type cubique (paramètre énergétique et covolume respectivement)
$\tilde{a}$	Energie molaire résiduelle d'Helmholtz
C_1	Coefficient de PC-SAFT
d	Diamètre des sphères dures
f	Fugacité
g	Fonction de distribution
g^E	Energie de Gibbs molaire d'excès
I	Intégrale adimensionnelle utilisée dans l'équation PC-SAFT
i et j	Indices représentant les constituants i et j
k_B	Constante de Boltzmann

k_H	Constante d'Henry
k_{ij}	Paramètre d'interaction
m	Nombre de segments
M_w	Masse moléculaire
M_i	Nombre de sites d'association du composé i
n_c	Nombre de constituants dans un mélange
N_{avog}	Nombre d'Avogadro
P	Pression
P_c	Pression critique
R	Constante des gaz parfaits
T	Température
T_c	Température critique
v	Volume molaire
x	Composition globale/ fraction molaire en phase liquide
X	Fraction des molécules non associées
y	Fraction molaire en phase vapeur
Z	Facteur de compressibilité

Lettres grecques

Δ^{AB}	Intensité d'association
ε	Energie d'interaction
ε^{AB}	Energie d'association
η	Densité réduite du fluide
φ	Coefficient de fugacité
κ^{AB}	Volume d'association
μ	Potentiel chimique
ζ	Paramètre binaire utilisé dans les règles de combinaison

	de Lorentz-Berthelot
γ	Coefficient d'activité
ρ	Densité molaire
$\tilde{\rho}$	Densité nombre
σ	Diamètre des segments
θ	Fraction surfacique
ϕ	Fraction volumique
ω	Facteur acentrique

Indices et Exposants

att	Attraction
A et *B*	Site associatif
assoc	Contribution de l'association dans l'équation PC-SAFT
c	Critique
cal	Calculée
disp	Contribution de la dispersion dans l'équation PC-SAFT
exp	Expérimentale
hc	Contribution de la chaîne dure dans l'équation PC-SAFT
hs	Contribution de la sphère dure dans l'équation PC-SAFT
ideal	Idéale
LJ	Lennard-Jones
liq	Phase liquide
polar	Polaire
res	Résiduelle
rép	Répulsive
sat	Saturation
vap	Phase vapeur

Introduction

L'utilisation continue de grandes quantités de solvants organiques en tant que milieu réactionnel est une préoccupation majeure dans l'industrie chimique d'aujourd'hui. Les effets délétères remarquables de ces solvants sur la santé humaine, la sécurité et l'environnement combinés avec leur volatilité et leur inflammabilité ont fait naître une prise de conscience pour réduire au maximum leur utilisation.

Alors que la chimie de base a trouvé une solution qui consiste en la conception de procédés de fabrication alternatifs avec des risques réduits et de faibles rejets d'effluents, la chimie verte cherche des solutions plus efficaces qui consistent à substituer les solvants organiques par des solvants plus respectueux de l'environnement. Parmi ces derniers, on trouve les liquides ioniques, sels fondus à température ambiante, dont la propriété la plus intéressante est leur faible tension de vapeur.

Ces dernières années, l'attention prêtée par la communauté scientifique vers l'utilisation des liquides ioniques en tant que solvants innovants est très importante. Leur usage industriel reste toutefois limité pour des raisons financières mais aussi par un manque de connaissances fondamentales lié à une importante diversité des liquides ioniques. De plus, la quantité de données disponibles est parfois limitée par rapport à ce qui serait théoriquement nécessaire, si bien qu'il est difficile de dégager une vision d'ensemble de leurs domaines d'applications. Il est donc évident qu'un effort tout particulier doit être fait en vue de comprendre et de prédire les relations entre structure et propriétés des liquides ioniques.

Les objectifs de cette thèse s'insèrent dans un projet de mise en place de cartographie des liquides ioniques purs permettant d'établir leur domaine d'applications dans le génie des procédés. Pour ce faire, nous avons choisi deux domaines d'applications des liquides ioniques : la capture des gaz à effet de serre et la désulfurisation des essences. Deux approches seront utilisées : une expérimentale avec la détermination

de propriétés thermodynamiques des liquides ioniques et de mélanges et une autre théorique faisant appel à la modélisation de ces données expérimentales par le modèle thermodynamique PC-SAFT. Les performances de l'équation d'état PC-SAFT seront évaluées dans un premier temps.

Dans le chapitre I, nous nous intéresserons en premier lieu à la présentation des liquides ioniques en insistant sur leurs définitions, leurs propriétés physico-chimiques et leurs applications. Une fois ce travail préliminaire effectué, différents modèles thermodynamiques capables de représenter les propriétés des liquides ioniques seront décrits.

Après ce premier chapitre de synthèse bibliographique, une étude expérimentale et théorique sur la solubilité du CO_2 dans les liquides ioniques à l'aide de l'équation PC-SAFT sera présentée dans les chapitres II et III. Plus concrètement, les objectifs concernent l'étude des interactions entre liquides ioniques et CO_2 au travers de mesures d'équilibre liquide-vapeur et de leur corrélation par le modèle PC-SAFT.

Le chapitre IV est consacré à l'étude expérimentale de la solubilité des gaz à effet de serre principaux (CO_2, CH_4, N_2O) dans différents liquides ioniques. Cette étude met en évidence l'importance de la structure du liquide ionique sur la solubilité de ces gaz. Nous nous efforçons de développer une méthode de contribution de groupes afin de déterminer la constante d'Henry du CO_2 dans les liquides ioniques.

Enfin, le dernier chapitre est dédié la désulfurisation extractive des essences à l'aide des liquides ioniques. L'ensemble de ces données expérimentales sont modélisées par le modèle PC-SAFT.

Chapitre I. Synthèse bibliographique

Les liquides ioniques sont des sels qui ont la particularité d'être liquides à température ambiante. Ils possèdent une température de fusion inférieure à 100 °C et une tension de vapeur très faible voire non mesurable. Ce caractère non volatil offre un avantage pour la séparation des produits et évite l'exposition non contrôlée aux vapeurs. Ils ont une stabilité chimique-thermique élevée et sont relativement peu coûteux et faciles à synthétiser. De plus, les liquides ioniques ont un fort pouvoir solvant car ils sont capables de dissoudre un grand nombre de composés organiques ou inorganiques et présentent des spécificités intéressantes par rapport aux solvants organiques classiques. L'ensemble de ces propriétés en font des milieux de choix pour le développement de la chimie verte.

En outre, les propriétés thermodynamiques des liquides ioniques peuvent être mesurées par des techniques expérimentales puis utilisées pour développer des modèles fiables. L'utilisation de modèles thermodynamiques permet ensuite de prédire les comportements de phases des systèmes contenant les liquides ioniques à n'importe quelle température et n'importe quelle pression comprises dans les intervalles de température et pression expérimentales. En conséquence, un modèle thermodynamique fiable est nécessaire pour prédire les équilibres entre phases de systèmes contenant des liquides ioniques. Après avoir défini les liquides ioniques et présenté quelques-unes de leurs applications, nous présenterons un bref bilan sur les performances des différents modèles thermodynamiques (g^E, équation d'état cubique et modèle de type SAFT) utilisés pour la représentation des équilibres entre phases de systèmes contenant des liquides ioniques.

I.1 Généralités sur les liquides ioniques

I.1.1 Définition

Les liquides ioniques (LIs) sont des sels liquides se différenciant de l'ensemble des sels fondus classiques par une température de fusion inférieure à 100 °C. La plupart d'entre eux sont liquides à température ambiante [1]. Les LIs sont constitués d'un cation le plus souvent organique, associé à un anion organique ou inorganique. De plus les combinaisons possibles entre cation et anion sont très nombreuses ($>10^6$).

Les cations rencontrés sont généralement volumineux et dissymétriques. Les plus classiques sont des ammoniums, imidazoliums, pyridiniums, pyrolidiniums, phosphoniums et sulphoniums (Figure I.1). Les plus étudiés sont les sels d'imidazoliums substitués sur les atomes d'azote et de carbone. Les chaînes R1 et R2 sont le plus souvent des chaînes alkyles, cependant, il existe également des structures de liquides ioniques sur lesquelles nous pouvons introduire des groupes fonctionnels particuliers tels que des groupements amines [2], alcools [3,4], acides carboxyliques [5], thiols [6] et alcynes [7] afin de définir des liquides ioniques à tâche spécifique ou des liquides ioniques fonctionnalisés.

Par contre la plupart des anions mis en œuvre peuvent être inorganiques comme le Fluor, le Chlore, l'Iode et le Brome ou organiques comme le tétrafluoroborate $[BF_4]^-$ et le hexafluorophosphate $[PF_6]^-$. Les anions $[BF_4]^-$ et $[PF_6]^-$ très utilisées en chimie organique ou organométallique sont à la base de nombreux sels liquides. Actuellement, d'autres anions avec des propriétés spécifiques ont été développés tels que des anions chiraux [8] ou des anions fonctionnalisés par des nitriles [9] ou par des bases de Lewis [10]. Des systèmes anioniques à base d'hétéropolyanions ou de sels métalliques sont également étudiés [11,12].

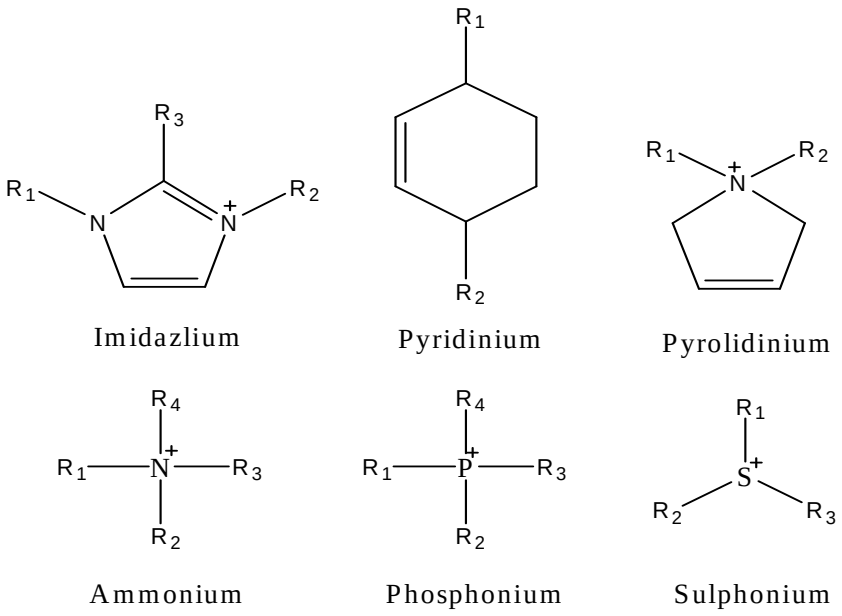

Figure I.1 – Cations des liquides ioniques

I.1.2 Propriétés physico-chimiques des liquides ioniques

Les LIs présentent de nombreuses propriétés physico-chimiques intéressantes qui en font une classe de solvants verts très prometteurs pour de nombreuses applications [13,14]. De plus, leurs caractéristiques physico-chimiques peuvent être ajustées en jouant sur le choix de l'anion et/ou du cation mais également en modifiant les substituants sur le cation. La pureté du liquide ionique est aussi un facteur pouvant influencer leurs propriétés de manière significative [15].

I.1.2.1 Point de fusion

Les LIs sont caractérisés par un point de fusion relativement bas (inférieur à 100 °C). La température de fusion des LIs dépend de la nature du cation mais surtout de celle de l'anion [16].

I.1.2.2 Densité et viscosité

Les LIs sont en général plus denses et visqueux que l'eau ou les autres solvants organiques. Leur densité est comprise entre 1 et 1.6 $g.cm^{-3}$. Leur viscosité généralement dix fois supérieure à celle des solvants organiques classiques est

essentiellement déterminée par leur tendance à former des liaisons hydrogène ou par leur force d'interaction de Van der Waals [17].

I.1.2.3 Stabilité thermique

La stabilité thermique des LIs est fixée par leur température de décomposition. Généralement, le cation imidazolium présente une température de décomposition élevée ce qui permet de les utiliser à des températures supérieures à 250 °C et dans certains cas supérieures à 400 °C [13]. De plus, pour un liquide ionique constitué d'un cation imidazolium, la stabilité thermique dépend essentiellement de la structure de l'anion. Ainsi, les anions engendrant les plus faibles interactions intermoléculaires induisent les températures de décomposition les plus élevées.

I.1.2.4 Solubilité dans l'eau et les solvants organiques

La solubilité des LIs dans l'eau est déterminée par leur caractère hydrophile ou hydrophobe qui est une donnée importante dans l'étude de leurs propriétés de solvatation. La miscibilité des LIs, notamment les LIs dialkylimidazolium dans l'eau, a été largement étudiée [18][19]. Leurs solubilités dans l'eau sont principalement gouvernées par la nature de l'anion et la longueur de la chaîne alkyle greffée sur le cation. En règle générale, les solvants organiques sont d'autant plus miscibles avec les LIs qu'ils sont polaires. Donc les LIs sont miscibles avec les alcools à courte chaîne et les cétones, le dichlorométhane et l'acétonitrile. En revanche, par un choix judicieux de la nature du cation et/ou de l'anion, les LIs peuvent être non-miscibles avec les alcanes, le dioxane, le toluène et l'éther [13,20].

I.2 Applications des liquides ioniques

I.2.1 Utilisation des liquides ioniques dans les procédés de séparation : extraction liquide-liquide

Les procédés de séparation sont le cœur de l'industrie chimique dans des domaines variés tels que la pétrochimie, l'hydrométallurgie, les industries pharmaceutiques ou l'agroalimentaire. Les LIs sont envisagés pour l'extraction liquide-liquide de solutés d'intérêt dans diverses applications grâce à leurs propriétés. La désulfuration des carburants par l'extraction liquide-liquide utilisant les LIs est de plus en plus étudiée. L'extraction des composés organiques soufrés à l'aide des LIs a été proposée pour la première fois par Bössman et al. [21] et a été suivie par de nombreuses autres études [22-27]. Dans ces études, l'effet de la nature du liquide ionique sur la performance de l'extraction a été présenté. Les résultats de ces travaux montrent que le choix de l'anion semble être plus important que le choix du cation pour l'extraction. A titre d'exemple, les LIs constitués du cation alkylméthylpyridinium présentent des taux d'extraction supérieur à 70 % pour les composés organiques soufrés [26]. Ce résultat peut être amélioré en couplant ce cation avec des anions tels que le thiocyanate.
De nombreuses études expérimentales des équilibres de phases ont été réalisées afin d'évaluer la capacité des liquides ioniques à extraire divers solutés gazeux ou liquides. La majorité des données expérimentales est corrélée à l'aide de modèles thermodynamiques tels que : NRTL, UNIQUAC ou électrolyte-NRTL [28-30,23,31-34]. L'étude de Simoni et al. a démontré que ces modèles peuvent être utilisés pour présenter les équilibres de phases moyennant quelques améliorations [33].

I.2.2 Utilisation des liquides ioniques pour la capture des gaz à effet de serre

Les inquiétudes liées au réchauffement climatique, dû aux émissions des gaz à effet de serre issus de la combustion des énergies fossiles, doivent mener au développement de nouvelles technologies destinées à la réduction et à la capture de ces gaz. Parmi les principaux gaz à effet de serre, on note la vapeur d'eau (H_2O), le dioxyde de carbone (CO_2), le méthane (CH_4) et le protoxyde d'azote (N_2O). Ces

dernières années, une attention particulière a été dédiée aux réductions des émissions de CO_2 à cause des activités humaines.

Parmi les différentes approches possibles pour la capture du CO_2, l'absorption utilisant des absorbants liquides est de plus en plus utilisée et fait l'objet de nombreux développements [35]. Il existe actuellement trois catégories de solvants d'absorption connues et utilisées pour la capture du CO_2 : les solvants chimiques (monoéthanolamine-MEA); les solvants physiques (N-méthylpyrrolidone, méthanol et diméthyléther de polyéthylène glycol); les solvants hybrides (mélanges de solvant chimique et de solvant physique). Bien que ces trois catégories de solvants soient très efficaces pour absorber le CO_2, l'utilisation de ces solvants présente plusieurs inconvénients. Les LIs peuvent être considérés comme de bons candidats pour l'absorption des gaz à effet de serre notamment du CO_2 grâce à leurs propriétés intéressantes [36,37] et sans les inconvénients des absorbants classiques. En outre, l'absorption du CO_2 par les LIs est un phénomène physique qui ne met en jeu que des interactions de faible énergie et sans réaction chimique.

I.3 Modèles thermodynamiques pour présenter les propriétés thermodynamiques des liquides ioniques

L'étude des opérations unitaires des procédés industriels telles que la distillation, l'absorption, l'extraction liquide-liquide, etc. nécessite la prédiction et la corrélation des propriétés thermodynamiques des fluides. Les équations d'état restent l'outil de choix à cet effet car elles permettent le calcul des propriétés thermodynamiques mais aussi des équilibres de phases. De nombreuses équations d'état sont dérivées du modèle cubique basé sur la théorie de Van Der Waals.

En 1873, Van der Waals [38] a proposé la première équation d'état cubique capable de prédire et représenter aussi bien les phases liquides que gazeuses. Cependant, l'équation de Van Der Waals est d'une précision insuffisante et uniquement applicable à des fluides simples, ce qui a conduit à de nombreuses modifications.

Actuellement le défi réside dans la modélisation de procédés complexes, de propriétés de fluides eux-mêmes complexes, tels que les systèmes polaires, les systèmes de macromolécules biologiques, les liquides ioniques, parfois en conditions supercritiques. Contrairement aux fluides simples, les fluides complexes contiennent des molécules qui interagissent les unes avec les autres au moyen d'interactions spécifiques comme les interactions polaires ou associatives. C'est le cas des LIs, qui sont considérés comme des composés associatifs ou polaires [39][40]. L'estimation de leurs propriétés par différents modèles thermodynamiques tels que les modèles de coefficient d'activité (NTRL et UNIQUAC), Cubique et SAFT seront présentés dans ce chapitre.

I.3.1 Modèle d'énergie de Gibbs molaire totale d'excès g^E

Les modèles d'énergie de Gibbs d'excès g^E, appelés modèles de coefficient d'activité sont essentiels pour calculer les équilibres de phases dans les régions sub-critiques. De nombreux travaux ont montré que les modèles de g^E tels que NRTL [41] et UNIQUAC [42] sont capables de représenter les propriétés des LIs en mélange et de simuler l'extraction liquide-liquide des systèmes ternaires.

A l'heure actuelle, la majorité des données d'équilibre liquide-liquide (ELL) de systèmes ternaires contenants un LI est corrélée à l'aide de modèles de g^E tels que NRTL et UNIQUAC [33,34,43-49]. Ces modèles donnent des résultats très satisfaisants pour la représentation des données expérimentales. Cependant, en 2008, les travaux de Simoni et al. ont montré que les modèles NRTL et UNIQUAC n'étaient pas complètement satisfaisants pour représenter simultanément des données d'équilibre liquide-vapeur et d'équilibre liquide-liquide.

I.3.2 Equation d'état cubique

Les équations d'état cubiques sont très utilisées dans le domaine de la thermodynamique des fluides. Parmi les plus connues, nous allons citer celle de

PPR78 [50]. Ce modèle utilise l'équation d'état de Peng-Robinson dans sa version de 1978, les règles de mélange de Van der Waals, et suppose que le coefficient d'interaction binaire k_{ij} est uniquement fonction de la température T. La méthode est rendue prédictive par le calcul de k_{ij} à partir d'une méthode de contributions de groupes [51, 52].

Dans les travaux de thèse de Revelli, PPR78 a été appliqué à la représentation des propriétés des LIs purs et en mélanges avec du CO_2. Dans ce cadre, il est nécessaire de connaitre les trois paramètres : la température critique Tc, la pression critique Pc et le facteur acentrique ω_i de chaque constituant. Malheureusement, il est impossible de mesurer expérimentalement les propriétés critiques des LIs car la plupart d'entre eux se décomposent avant d'atteindre le point critique. Ainsi, une méthode de contributions de groupes proposée par Valderrama et al. a été utilisée afin d'estimer ces propriétés critiques [53,54]. Les points expérimentaux d'équilibres liquide-vapeur du CO_2 dans plusieurs LIs ont été mesurés sous haute pression. Le modèle PPR78 a été utilisé pour prédire les pressions de bulle expérimentales. Les résultats indiquent que ce modèle est capable de décrire les diagrammes de phases des systèmes {CO_2+LIs} à condition que les propriétés critiques soient connues. Marina et al. [55] ont présenté l'importance de l'association intermoléculaire lors de leur étude de la solubilité du dioxyde de carbone dans les LIs. Cette étude a évalué trois équations d'état Peng-Robinson, Soave-Redilich-Kwong et l'équation cubique plus association (CPA) avec un paramètre d'interaction dépendant de la température. Les auteurs ont démontré que l'utilisation d'un terme associatif n'apportait pas d'avantage majeur pour l'étude des systèmes binaires {LIs+CO_2}.

I.3.3 Equation d'état SAFT

Ces dernières années, les équations d'état de type SAFT [56] (Statistical Associating Fluid Theory), en particulier PC-SAFT [57] et Soft-SAFT sont de plus en plus utilisées pour représenter les propriétés des LIs purs et en mélange. Le modèle Soft-SAFT

développé par Blas et Vega en 1997. [58] Récemment, Llovell et Vega [59] ont utilisé l'équation Soft-SAFT pour estimer les propriétés thermodynamiques des LIs purs et en mélanges. Les LIs purs ont d'abord servi à paramétrer le modèle et à évaluer sa fiabilité. Le comportement des LIs dans les mélanges binaires avec des autres composés associatifs ont alors été prédits. Llovell et Vega ont conclu que le comportement thermodynamique des LIs purs mais aussi des mélanges binaires peut être représenté avec une grande précision à l'aide de l'équation Soft-SAFT.

En 2012, Domanska et al. [60] ont appliqué le modèle PC-SAFT à l'étude de systèmes contenant des liquides ioniques. Les auteurs ont démontré que le modèle PC-SAFT permettait de représenter des équilibres liquide-vapeur ainsi que des équilibres liquide-liquide de systèmes constitués d'aromatiques et de liquides ioniques à base d'isoquinolium.

Conclusion

En conclusion, les modèles NTRL et UNIQUAC sont capables de présenter l'extraction liquide-liquide de systèmes ternaires contenant des LIs mais se montent insuffisants pour corréler certains systèmes binaires qui ont une lacune de miscibilité. Les équations d'état cubique semblent être de bons candidats pour représenter les propriétés des LIs purs mais aussi de mélanges constitués de {CO_2 + LIs}. Néanmoins, les propriétés critiques des LIs sont mal connues et les modèles cubiques ne prennent pas directement en compte les effets de la structure moléculaire et les interactions spéciales entre molécules. Les modèles SAFT sont de plus en plus appliqués aux fluides complexes comme les LIs. La nature des composés et les interactions spécifiques sont considérées ce qui conduit à une bonne représentation des diagrammes de phases de mélanges contenant des LIs. Dans ce cadre, l'équation d'état PC-SAFT a été choisie dans cette thèse afin d'évaluer sa capacité à reproduire les comportements thermodynamiques des LIs purs et de leurs mélanges.

Références bibliographiques

[1] Wasserscheid, P.; Welton, T., Ionic Liquids in Synthesis, Second Edition. Wiley-VCH, Weinheim, Germany. **2008**.

[2] Bates, E.; Mayton, R.; Ntai, I.; Davis, J. *J. Am. Chem. Soc*. **2002**, *124*, 926–927.

[3] Branco, L. C.; Rosa, J. N.; Ramos, J. J. M.; Afonso, C. A. M. *Chem. Eur. J.* **2002**, *8*, 3671–3677.

[4] Schrekker, H. S.; Stracke, M. P.; Schrekker, C. M. L.; Dupont, J. *Ind. Eng. Chem. Res.* **2007**, *46*, 7389–7392.

[5] Fei, Z. F.; Ang, W. H.; Geldbach, T. J.; Scopelliti, R.; Dyson, P. J. *Chem. Eur. J.* **2006**, *12*, 4014–4020.

[6] Itoh, H.; Naka, K.; Chujo, Y. *J. Am. Chem. Soc.* **2004**, *126*, 3026–3027.

[7] Fei, Z. F.; Zhao, D. B.; Scopelliti, R.; Dyson, P. J. *Organometallics.* **2004**, *23*, 1622–1628.

[8] Fukumoto, K.; Ohno, H. *Chem. Commun.* **2006**, *29*, 3081–3083.

[9] Zhao, D. B.; Fei, Z. F.; Ohlin, C. A.; Laurenczy, G.; Dyson, P. J. *Chem. Commun.* **2004**, *10*, 2500–2501.

[10] MacFarlane, D. R.; Pringle, J. M.; Johansson, K. M.; Forsyth, S. A.; Forsyth, M. *Chem. Commun.* **2006**, *18*, 1905–1917.

[11] Welton, T. *Coord. Chem. Rev.* **2004**, *248*, 2459–2477.

[12] Olivier-Bourbigou, H.; Magna, L. *J. Mol. Catal. A*. **2002**, *182*, 419–437.

[13] Bonhôte, P.; Dias, A. P.; Papageorgiou, N.; Kalyanasundaram, K.; Grätzel, M. *Inorg. Chem.* **1996**, *35*, 1168–1178.

[14] Huddleston, J. G.; Visser, A. E.; Reichert, W. M.; Willauer, H. D.; Broker, G. A.; Rogers, R. D. *Green Chem.* **2001**, *3*, 156–164.

[15] Seddon, K. R.; Stark, A.; Torres, M. J. *Pure Appl. Chem.* **2000**, *72*, 2275–2287.

[16] Hunt, P. A. *J. Phys. Chem. B* **2007**, *111*, 4844-4853.

[17] Greaves, T. L.; Drummond, C. J. *Chem. Rev.* **2008**, *108*, 206–237.

[18] Domanska, U. *Pure and Applied Chemistry* **2005**, *77*, 543-557.

[19] Domanska, U. *Thermochimica Acta* **2006**, *448*, 19-30.

[20] Welton, T. *Chem. Rev.* **1999**, *99*, 2071–2083.

[21] Bosmann, A.; Datsevich, L.; Jess, A.; Lauter, A.; Schmitz, C.; Wasserscheid, P. *Chem. Commun.* **2001**, 2494-2495.

[22] Esser, J.; Wasserscheid, P.; Jess, A. *Green Chem.* **2004**, *6*, 316–322.

[23] Alonso, L.; Arce, A.; Francisco, M.; Rodríguez, O.; Soto, A. *AIChE J.* **2007**, *53*, 3108–3115.

[24] Mochizuki, Y.; Sugawara, K. *Energy Fuels* **2008**, *22*, 3303–3307.

[25] Gao, H. S.; Luo, M. F.; Xing, J. M.; Wu, Y.; Li, Y. G.; Li, W. L.; Liu, Q. F.; Liu, H. Z. *Ind. Eng. Chem. Res.* **2008**, *47*, 8384–8388.

[26] Holbrey, J. D.; Lopez-Martin, I.; Rothenberg, G.; Seddon, K. R.; Silvero, G.; Zheng, X. *Green Chem.* **2008**, *10*, 87–92.

[27] Francisco, M.; Arce, A.; Soto, A. *Fluid Phase Equilib.* **2010**, *294*, 39-48.

[28] Simoni, L. D.; Chapeaux, A.; Brennecke, J. F.; Stadtherr, M. A. *Comput. Chem. Eng.* **2010**, *34*, 1406-1412.

[29] Arce, A.; Earle, M. J.; Rodriguez, H.; Seddon, K. R. *J. Phys. Chem. B.* **2007**, *111*, 4732–4736.

[30] Arce, A.; Earle, M. J.; Rodriguez, H.; Seddon, K. R.; Soto, A. *Green Chem.* **2008**, *10*, 1294–1300.

[31] Letcher, T. M.; Deenadayalu, N. *J. Chem. Thermodyn.* **2003**, *35*, 67–76.

[32] Meindersma, G. W.; Podt, A. J. G.; de Haan, A. B. *Fluid Phase Equilib.* **2006**, *247*, 158–168.

[33] Simoni, L. D.; Lin, Y.; Brennecke, J. F.; Stadtherr, M. A. *Ind. Eng. Chem. Res.* **2008**, *47*, 256–272.

[34] Alonso, L.; Arce, A.; Francisco, M.; Soto, A. *J. Chem. Thermodyn.* **2008**, *40*, 966–972.

[35] Pennline, H. W.; Luebke, D. R.; Jones, K. L.; Myers, C. R.; Morsi, B. I.; Heintz, Y. J.; Ilconich, J. B. *Fuel Process. Technol.* **2008**, *89*, 897–907.

[36] Anthony, J.; Aki, S.; Maginn, E.; Brennecke, J. *Int. J. Envir. Technol. Manage.* **2004**, *4*, 105–115.

[37] Baltus, R. E.; Counce, R. M.; Culbertson, B. H.; Luo, H. M.; DePaoli, D. W.; Dai, S.; Duckworth, D. C. *Sep. Sci. Technol.* **2005**, *40*, 525–541.

[38] Van der Waals, J. D. *Ph.D. thesis, Leiden* 1873.

[39] Kroon, M. C.; Karakatsani, E. K.; Economou, I. G.; Witkamp, G. J.; Peters, C. J. *J. Phys. Chem. B* **2006**, *110*, 9262-9269.

[40] Andreu, J. S.; Vega, L. F. *J. Phys. Chem. C* **2007,** *111,* 16028-16034.

[41] Renon, H.; Prausnitz, J. *AIChE J.* **1968**, *14*, 135–144.

[42] Abrams, D. S.; Prausnitz, J. M. *AIChE J.* **1975**, *21*, 116–128.

[43] Letcher, T. M.; Deenadayalu, N.; Soko, B.; Ramjugernath, D.; Naicker, P. K. *J. Chem. Eng. Data.* **2003**, *48*, 904–907.

[44] Meindersma, G. W.; Podt, A.; de Haan, A. B. *J. Chem. Eng. Data.* **2006**, *51*, 1814–1819.

[45] Domanska, U.; Pobudkowska, A.; Zolek-Tryznowska, Z. *J. Chem. Eng. Data.* **2007**, *52*, 2345–2349.

[46] Chapeaux, A.; Simoni, L. D.; Ronan, T. S.; Stadtherr, M. A.; Brennecke, J. F. *Green Chem.* **2008**, *10*, 1301–1306.

[47] Alonso, L.; Arce, A.; Francisco, M.; Soto, A. *Fluid Phase Equilib.* **2008**, *270*, 97–102.

[48] Pereiro, A. B.; Rodriguez, A. *J. Chem. Eng. Data.* **2008**, *53*, 1360–1366.

[49] García, J.; Fernández, A.; Torrecilla, J. S.; Oliet, M.; Rodríguez, F. *Fluid Phase Equilib.* **2009**, *282*, 117–120.

[50] Peng, D. Y.; Robinson, D. B. *Ind. Eng. Chem. Fundam.* **1976**, *15 (1)*, 59-64.

[51] Jaubert, J. N.; Mutelet, F. *Fluid Phase Equilib.* **2004**, *224*, 285–304.

[52] Vitu, S.; Privat, R.; Jaubert, J. N.; Mutelet, F. *J. Supercrit. Fluids.* **2008**, *45*, 1–26.

[53] Valderrama, J. O.; Sanga, W. W.; Lazzus, J. A. *Ind. Eng. Chem. Res.* **2008**, *47*, 1318–1330.

[54] Valderrama, J. O.; Rojas, R. E. *Ind. Eng. Chem. Res.* **2009**, *48*, 6890–6900.

[55] Manic, M. S.; Queimada, A. J.; Macedo, E. A.; Najdanovic-Visak, V. *J. Supercrit. Fluids* **2012**, *65*, 1-10.

[56] Huang, S. H.; Radosz, M. *Ind. Eng. Chem. Res.* **1990**, *29*, 2284-2294.

[57] Gross, J.; Sadowski, G. *Ind. Eng. Chem. Res.* **2001**, *40*, 1244-1260.

[58] Blas, F. J.; Vega, L. F. *Molecular Physics* **1997**, *92*, 135-150.

[59] Llovell, F.; Valente, E.; Vilaseca, O.; Vega, L. F. *J. Phys. Chem. B* **2011**, *115*, 4387-4398.

[60] Paduszynski, K.; Domanska, U. *J. Phys. Chem. B* **2012**, *116*, 5002-5018.

Chapitre II. Étude théorique sur la solubilité du dioxyde de carbone dans les liquides ioniques à l'aide de l'équation d'état PC-SAFT

The goal of this chapter is to check the ability of the PC-SAFT equation of state to represent the solubility of carbon dioxide (CO_2) in ionic liquids. Parameters of pure imidazolium based ionic liquids were estimated using experimental density in a large range of temperature and then correlated with respect to the molecular weight and the structure of the solvents. It is found that such a correlation is able to predict the density with high accuracy. The solubility of carbon dioxide in such ionic liquids is then studied. The binary interaction parameter k_{ij} needed for the representation of such binary systems was first fitted on experimental liquid-vapor equilibria data. In a second step, a correlation based on the group contribution concept is developed to determine this temperature-dependent parameter. The ability of the model to describe accurately carbon dioxide solubility in imidazolium based ionic liquids is demonstrated.

II.1 Introduction

Recent concerns over global warming due to greenhouse gas emissions from fossil fuel combustion have lead to develop technologies in order to reduce and capture these gases. The main greenhouse gases in the Earth's atmosphere are water vapor, carbon dioxide (CO_2), methane (CH_4), and nitrous oxide (N_2O). Currently, a particular attention is devoted to the CO_2 emission reduction. There are a number of different separation technologies that can be applied to carbon dioxide capture including solvent, membrane and adsorbent based processes.

One approach being considered for capturing CO_2 is the use of liquid absorbents designed to selectively solvate CO_2.[1] The alkanolamines are the most generally accepted and widely used of the various available solvents for removal of CO_2 from natural gas stream. The reactivity and availability at low cost of this family of compounds especially monoethanolamine and diethanolamine, have made the solvent achieved a pinnacle position in the gas processing industry. Although these aqueous alkanolamine solutions are industrially effective on CO_2 removal, this method presents several drawbacks such as the intensive energy consumption, cost increases, important losses of alkanolamine within relatively high vapor pressure and especially corrosion problems in the presence of high concentration acid gases.[2,3]

Another class of solvent named ionic liquids[4] (ILs) seems to be good candidates for capturing greenhouse gases because they have some advantages in comparison to other solvents. Indeed, these compounds have good thermal stability, negligible vapor pressure and are liquid in a large range of temperature. Furthermore, physical properties of ILs may be modified and adjusted by employing different cation-anion combinations.[5-8]Their use and application in industrial processes is somewhat limited due to numerous reasons. Thermodynamic properties of pure ionic liquids or dissolved in solution are not always available in the literature. While numerous thermodynamic models were evaluated for mixtures containing ionic liquids, no model is purely predictive.

The other background of this work is that the prediction or correlation of thermodynamic characteristics and phase equilibrium with equation of state remains an important goal in chemical and related industries. The use of equations of state has for a long time been restricted to systems of simple fluids, however, there is an increasing demand for models that are also suitable for even more complex fluids. Clearly, some early models derived from statistical mechanics were non-molecularly-based equations of state and only suitable for simple fluids. During the past few years, many studies assumed nonspherical molecules to be chains of freely jointed spherical segments. Despite its simplicity, this molecular model accounts for size and shape effects of molecules and has successfully been applied to simple species as well as large polymeric fluids and their mixtures.

A more recent molecularly based equation of state concept for chain molecules based on Wertheim's thermodynamic perturbation theory of first order[9-12] has been proposed by Chapman et al.[13,14] The essence of their approach. referred to as the Statistical Associating Fluid Theory (SAFT), is to use a reference fluid that incorporates both the chain length (molecular size and shape) and molecular association, in place of the much simpler hard sphere reference fluid used in most existing engineering equation of state. The advantage of these molecularly based equations of state not only provide a useful thermodynamic basis for deriving chemical potentials or fugacities that are needed for phase equilibrium simulations but also allow for separating and quantifying the effects of molecular structure and interactions on bulk properties and phase behavior.

Earlier works related to SAFT focused on the application of the equation to experimental systems[15] or on simplifying the equation to make it more tractable.[16,17]These simplifying versions allowed straightforward calculation and programming, however, the price paid was a poorer description of the experimental systems of interest. In the late 1990s, many studies and efforts were put into refining the equation, especially improving the accuracy of the term used for the reference fluid, in spite of the more complex mathematical form. This led to different version

of the equation with different acronyms, such as SAFT-VR[18], Soft-SAFT[19,20] and later, PC-SAFT.[21]

Recently, Llovell and Vega[22] used the Soft-SAFT equation to estimate the thermodynamic properties of pure ILs and of mixtures containing ILs. The model has been used in a predictive manner to check the capability of Soft-SAFT in capturing the thermodynamic behavior of several complex associating mixtures such as the behavior of binary mixtures of ionic liquids with different cations and anions, the vapor-liquid equilibria of mixtures containing short-chain alcohols and dialkylimidazolium [Tf_2N] and liquid-liquid equilibria of binary systems {water + ILs}. They showed that such phase equilibria could be represented with high accuracy using soft-SAFT.

The truncated perturbed-chain polar statistical associating fluid theory (tPC-PSAFT)[23,24] was also evaluated for the prediction of CO_2 solubility in dialkylimidazolium ionic liquids. In their works, Kroon et al.[25] and Karakatsani et al.[26] calculated the parameters of pure ionic liquids by fitting them to experimental liquid density data. In the case of pure ILs, the association contribution was not taken into account but dipolar interactions of ILs molecules and quadrupolar interactions of CO_2 molecule were considered. In the case of ILs, they assumed that their polarity was comparable to the polarity of lower to medium alcohols.

Then, Domanska et al.[27] proposed to represent LLE of binary systems containing aliphatic hydrocarbons and piperidinium based ionic liquids by the PC-SAFT equation and the nonrandom hydrogen-bonding theory (NRHB). Pure fluid parameters of the model were obtained from experimental liquid density and solubility parameter data at ambient pressure and tested against high pressure densities. The authors have shown that the PC-SAFT and NRHB models were both able to capture phase behavior in a qualitative manner.

In this work, the PC-SAFT (Perturbed-Chain SAFT) EoS was choosen to model both the pure components and the binary systems: {CO_2+ILs}. Indeed, a theory like PC-SAFT which is a molecularly based equation of state offers several advantages. The

first advantage is that each of the approximations made in the development of SAFT such as the chain, association term and polar term has been verified against molecular simulation results. In this way, the range of applicability and the shortcomings of each term in the equation of state have been assessed. A second advantage is that the SAFT parameters have physical meaning which can help us check the accuracy and the correctness of the parameters while modelling the pure components. A third advantage is that like all the molecularly based equations of state, the PC-SAFT is a useful tool in which the effects of molecular structure on the thermodynamic properties can be separated and quantified.

II.2 PC-SAFT modelling

The Pertubed Chain-Statistical Associating Fluid Theory (PC-SAFT) EoS which is similar to other SAFT type EoS has been developed in 2001 by Gross and Sadowski.[21] Applying a perturbation theory for chain molecules inspired from two papers of Barker and Henderson.[28,29] Gross and Sadowski derived a dispersion expression for chain molecules and used a hard-chain reference fluid, to compare with other classical SAFT EoS which use a hard-sphere reference meaning that the dispersion term accounts for attraction between spherical segments, not for attraction between hard chains.

PC-SAFT equation are usually written in terms of residual Helmholtz free energy. Each term in the equation represents different microscopic contributions to the total free energy of the fluid. The equation writes:

$$\tilde{a}^{res} = \tilde{a}^{hc} + \tilde{a}^{disp} + \tilde{a}^{assoc} \qquad \text{(II-1)}$$

where $\tilde{a}^{res}$ is the residual Helmholtz free energy of the system ($\tilde{a}^{res} = \tilde{a}^{total} - \tilde{a}^{ideal}$). The superscripts hc, disp and assoc refer to a reference hard chain contribution, a dispersion contribution and an associating contribution, where $\tilde{a} = a/RT$.

The hard-sphere chain contribution was provided and defined by Gross and Sadowski:[21]

$$\tilde{a}^{hc} = \bar{m}\tilde{a}^{hs} - \sum_{i=1}^{n_c} x_i \left(m_i - 1\right) \ln g_{ij}^{hs} \tag{II-2}$$

it depends on the radial pair distribution function for segments in the hard-sphere system(g_{ij}^{hs}), on the hard-sphere contribution ($\tilde{a}^{hs}$) and on the mean segment number ($\bar{m}$) which is a function of m: the number of segments per chain.

The radial pair distribution function (g_{ij}^{hs}) and the hard-sphere contribution ($\tilde{a}^{hs}$) were defined by:

$$g_{ij}^{hs} = \frac{1}{1-\zeta_3} + d_{ij}\frac{3\zeta_2}{(1-\zeta_3)^2} + d_{ij}^2\frac{2\zeta_2^2}{(1-\zeta_3)^3}, \quad \{i,j\} \in [\![1, n_c]\!]^2 \tag{II-3}$$

$$\tilde{a}^{hs} = \frac{1}{\zeta_0}\left[\frac{3\zeta_1\zeta_2}{1-\zeta_3} + \frac{\zeta_2^3}{\zeta_3(1-\zeta_3)^2} + \left(\frac{\zeta_2^3}{\zeta_3^2} - \zeta_0\right)\ln(1-\zeta_3)\right] \tag{II-4}$$

Where d_i and ζ_n were defined by:

$$d_i(T) = \sigma_i\left[1 - 0.12\exp\left(-\frac{3\varepsilon_i}{k_B T}\right)\right], \; i \in [\![1, n_c]\!] \tag{II-5}$$

$$d_{ij} = \frac{d_i d_j}{d_i + d_j} \tag{II-6}$$

$$\zeta_n = \frac{\pi}{6}\tilde{\rho}\sum_{i=1}^{nc} x_i m_i d_i^n \;, \; n \in [\![0,3]\!] \tag{II-7}$$

The dispersion contribution to the Helmholtz free energy $\tilde{a}^{disp}$ accounts for Van der Waals forces. In this work we use the dispersion expression defined by Gross and Sadowski:[21]

$$\tilde{a}^{disp} = -2\pi\tilde{\rho}I_1\overline{m^2\varepsilon\sigma^3} - \pi\tilde{\rho}\overline{m}C_1I_2\overline{m^2\varepsilon^2\sigma^3} \tag{II-8}$$

where the coefficient C_1 depends on the mean segment number($\overline{m}$) and on the reduced density η defined by: $\eta = \zeta_3$

$$C_1 = \left[1 + \overline{m}\frac{8\eta - 2\eta^2}{(1-\eta)^4} + (1-\overline{m})\frac{20\eta - 27\eta^2 + 12\eta^3 - 2\eta^4}{[(1-\eta)(2-\eta)]^2}\right]^{-1} \tag{II-9}$$

I_1 and I_2 are expressed by:

$$I_1 = \sum_{i=0}^{6} a_i\eta^i \tag{II-10}$$

$$I_2 = \sum_{i=0}^{6} b_i\eta^i \tag{II-11}$$

the quantities for $\overline{m^2\varepsilon\sigma^3}$ and $\overline{m^2\varepsilon^2\sigma^3}$ are defined by:

$$\overline{m^2\varepsilon\sigma^3} = \sum_{i=1}^{nc}\sum_{j=1}^{nc} x_i x_j m_i m_j \left(\frac{\varepsilon_{ij}}{k_B T}\right)\sigma_{ij}^3 \tag{II-12}$$

$$\overline{m^2\varepsilon^2\sigma^3} = \sum_{i=1}^{nc}\sum_{j=1}^{nc} x_i x_j m_i m_j \left(\frac{\varepsilon_{ij}}{k_B T}\right)^2\sigma_{ij}^3 \tag{II-13}$$

Conventional combining rules for ε_{ij} and σ_{ij} were employed:

$$\sigma_{ij} = \frac{\sigma_i + \sigma_j}{2} \tag{II-14}$$

$$\varepsilon_{ij} = \sqrt{\varepsilon_i \varepsilon_j}\left(1 - k_{ij}\right) \text{ where } k_{ij} \text{ is the binary interaction parameter} \tag{II-15}$$

For evaluating the VLE of normal fluids, inclusion of $\tilde{a}^{hc}$ and $\tilde{a}^{disp}$ in the PC-SAFT approach is sufficient. Three parameters, the segment number (m), the segment energy parameter (ε/k_B), and the segment diameter (σ) are required to characterize each compound. However, in alkanol or acid solution, hydrogen bonding contributes dominantly to the nonideality of these solutions and its contribution should be taken into account. The Helmholtz free energy due to association $\tilde{a}^{assoc}$ is defined by:[15,30]

$$\tilde{a}^{assoc} = \sum_{i=1}^{nc} x_i \left[\sum_{A_i} \left(\ln X^{A_i} - \frac{X^{A_i}}{2} \right) + \frac{1}{2} M_i \right] \tag{II-16}$$

where X^{A_i} is the mole fraction of molecules i not bonded at site A, M_i is the number of association sites on each molecule and $\sum_{A_i}$ represents a sum over all associating sites on each molecule. The parameter X^{A_i} is given by:

$$X^{A_i} = \left[1 + N_{AV} \sum_j \sum_{B_j} \rho_j X^{B_j} \Delta^{A_i B_j} \right]^{-1} \tag{II-17}$$

where the internal sum sign runs over all sites on molecule j, ρ_j is the molar density of component j:

$$\rho_j = x_j \rho \tag{II-18}$$

The association strength $\Delta^{A_iB_j}$ is given by:

$$\Delta^{A_iB_j} = g_{ij}^{hs}\left[\exp\left(\varepsilon^{A_iB_j}/k_BT\right)-1\right]\left(\sigma_{ij}^3 k^{A_iB_j}\right) \quad \text{(II-19)}$$

and depends on the association energy $\varepsilon^{A_iB_j}$ and the association volume $k^{A_iB_j}$ between associating substances i and j. The combining rules suggested by Wolbach and Sandler [31] are expressed by:

$$\varepsilon^{A_iB_j} = \frac{1}{2}\left(\varepsilon^{A_iB_i} + \varepsilon^{A_jB_j}\right) \quad \text{(II-20)}$$

$$k^{A_iB_j} = \sqrt{k^{A_iB_i}k^{A_jB_j}}\left(\frac{\sqrt{\sigma_{ii}\sigma_{jj}}}{0.5\left(\sigma_{ii}+\sigma_{jj}\right)}\right)^3 \quad \text{(II-21)}$$

were used. Hence, if one of the substances in a mixture is non-associating, $k^{A_iB_j}$ and $\Delta^{A_iB_j}$ will vanish consequently.

II.3 Molecular model for carbon dioxide and ionic liquids

Following Huang and Radoz[15] approach, the carbon dioxide molecule was modeled as a non-associating substance. This molecule was thus represented by three molecular parameters: m: the segment number; σ: the segment diameter; ε/k_B: the segment energy parameter. The used values are taken from the paper of Gross and Sadowski[21].

In this work, the PC-SAFT parameters of pure ILs were firstly determined considering ILs as non-associating compounds. The three pure-component parameters (m, σ, ε/k_B) were obtained by a fitting procedure on pure-component data. In a second step, ILs were considered as self-associating molecules. However,

in order to keep a minimum number of parameters to be fitted, the associating parameters ($\varepsilon^{A_iB_j}$ and $k^{A_iB_j}$) were transferred from those of 1-alkanols[32], i.e., $\varepsilon^{A_iB_j}$ =3450 [K] and $k^{A_iB_j}$ =0.00225 [-]. Both associating parameters were assumed constant for the whole ILs family because the alkyl chain length of the cation does not affect the strength of the associating bonds. These two sets of parameters were compared in order to determine whether the associating contribution of ILs should be or not taken into account.

We have focused on the most studied imidazolium-based ILs. These ILs are 1-alkyl-3-methyl-imidazolium tetrafluoroborate [C_n-mim][BF_4], 1-alkyl-3-methyl-imidazolium hexafluoroborate [C_n-mim][PF_6], 1-alkyl-3-methyl-imidazolium bistrifluoromethylsulfonylimide [C_n-mim][Tf_2N], 1-alkyl-3-methyl-imidazolium thiocyanate [C_n-mim][SCN], 1-alkyl-3-methyl-imidazolium ethylsulfate [C_n-mim][C_2SO_4], 1-alkyl-3-methyl-imidazolium trifluoromethanesulfonate [C_n-mim][CF_3SO_3], 1-alkyl-3-methyl-imidazolium dicyanmide [C_n-mim][DCA], 1-alkyl-3-methyl-imidazolium trifluoroacetate [C_n-mim][TFA], 1-alkyl-3-methyl-imidazolium nitrate [C_n-mim][NO_3], 1-alkyl-3-methyl-imidazolium methylsulfate [C_n-mim][C_1SO_4], 1-alkyl-3-methyl-imidazolium chloride [C_n-mim][Cl], 1-alkyl-3-methyl-imidazolium bromide [C_n-mim][Br] and 1-alkyl-3-methyl-imidazolium acetate [C_n-mim][AC].

Following the studies performed by Andreu and Vega[22,33] and Huang and Radosz[15], the ILs of the following families: [C_n-mim][BF_4], [C_n-mim][PF_6], [C_n-mim][SCN], [C_n-mim][Cl], [C_n-mim][Br] and [C_n-mim][DCA], were modelled as Lennard-Jones chains with one associating site in each molecule (Figure II-1a). This model thus considers the neutral pairs composed by the anion and the cation as a single chain molecule with this association site describing the specific interactions. For the [C_n-mim][Tf_2N] family, ILs were modelled as homonuclear chainlike molecules with three associating sites mimicking the strong interactions between the anion and the cation (Figure II-1b). The number of associating sites is chosen on the basis of the delocalization of the anion electric charge due to the oxygen groups, enhancing the possibility of interaction with the surrounding cations through them. As a

consequence, one associating A type site represents the nitrogen atom interaction with the cation, while two B sites represent the delocalized charge due to the oxygen atoms on the anion, allowing only AB interactions between different IL molecules. For the [C_n-mim][C_2SO_4], [C_n-mim][CF_3SO_3], and the [C_n-mim][C_1SO_4] families, ILs were modelled as chainlike molecules with three associating sites between the anion and the cation (Figure II-1c): one associating A type site represents the oxygen atom interaction with the cation and two B sites represent the delocalized charge due to the oxygen atoms on the anion and for the [C_n-mim][TFA] and [C_n-mim][NO_3] families, ILs were modelled as chain molecules with two associating sites (Figure II-1d): one associating A type site represents the oxygen atom interaction with cation; one associating B type site represents the oxygen atom on the anion interaction with cation.

(a)

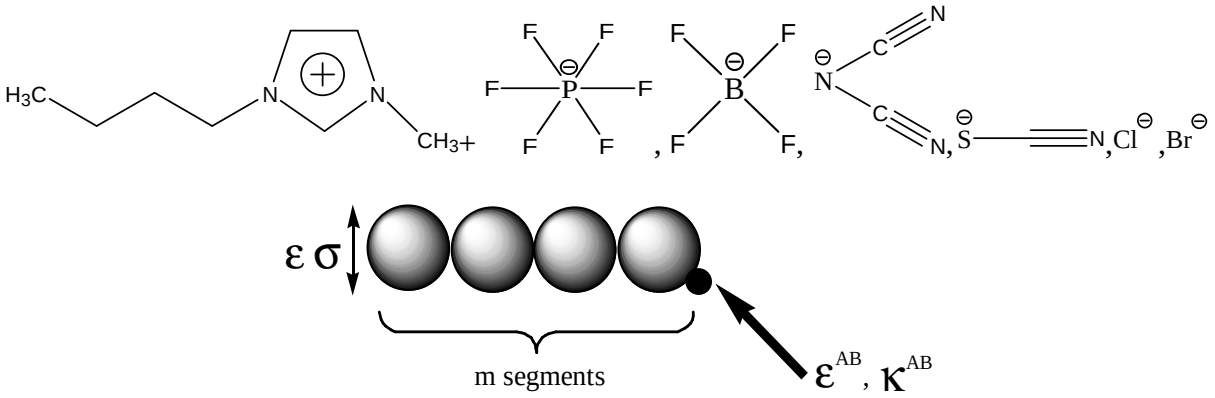

(b)

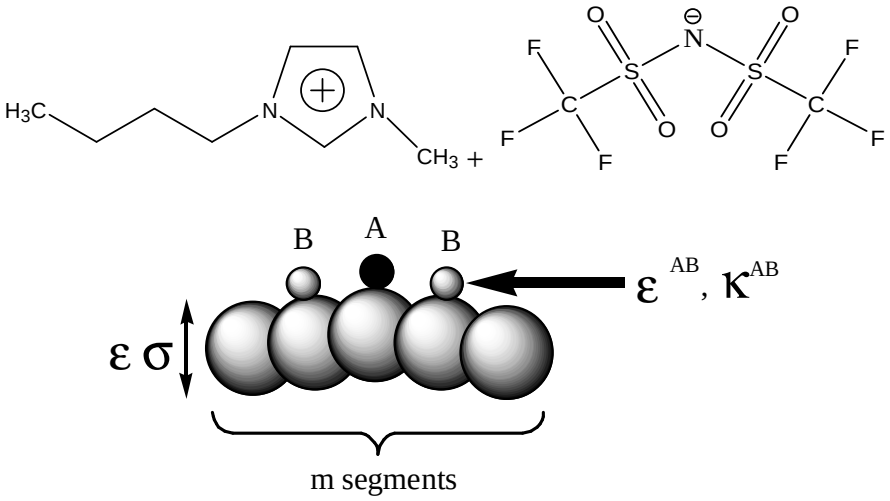

(c)

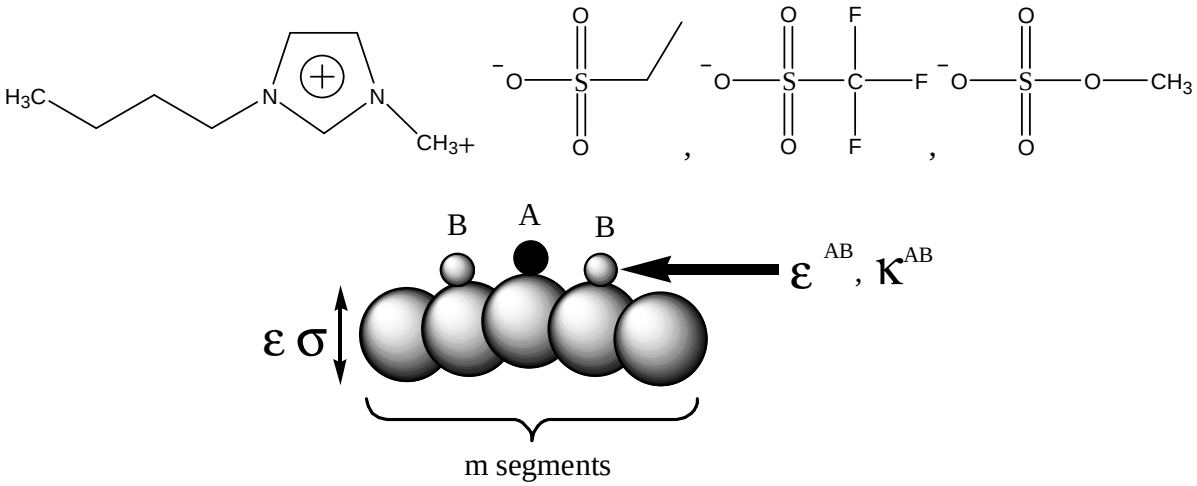

(d)

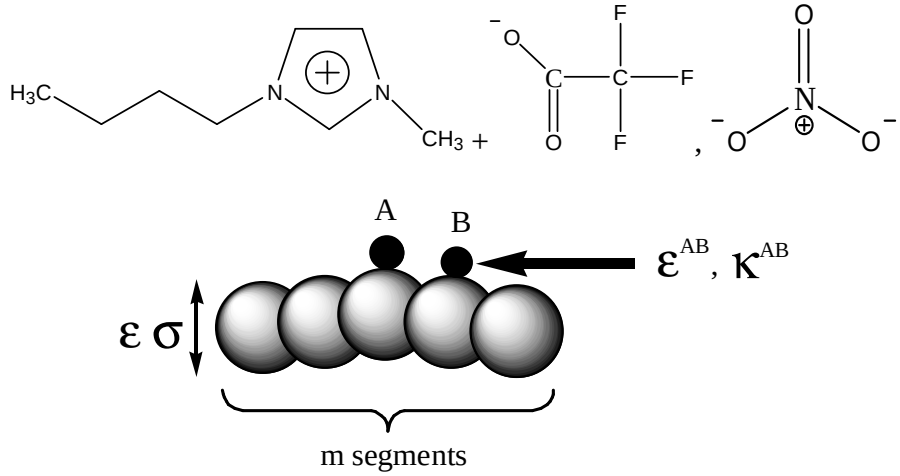

Figure II-1. Sketch of the model used to describe the ILs within the PC-SAFT approach: **(a)** [Cn-mim][BF_4], [Cn-mim][PF_6], [Cn-mim][SCN], [Cn-mim][Cl], [Cn-mim][Br] and [Cn-mim] [DCA]; **(b)** [Cn-mim][Tf_2N]; **(c)** [Cn-mim][C_2SO_4], [Cn-mim][CF_3SO_3] and [Cn-mim][C_1SO_4]; **(d)** [Cn-mim][TFA] and [Cn-mim][NO_3].

II.4 Results and discussion

II.4.1 Pure components

The PC-SAFT equation was evaluated in the representation of the thermodynamic properties of pure ILs such as temperature-dependent density. ILs were considered both as self-associating and non-associating molecules. The set of PC-SAFT

parameters for carbon dioxide was taken from the literature and is presented in Table II-1.[21] The parameters m, σ and ε/k_B of ILs were determined in order to minimize the following objective function (OF):

$$OF = \sum_{i=1}^{npts} \left(\frac{\rho_i^{sat,\exp} - \rho_i^{sat,cal}}{\rho_i^{sat,\exp}} \right)^2 \quad \text{(II-22)}$$

which takes into account the deviations between calculated and experimental liquid densities.

II.4.1.1 Ionic liquids as non-associating compounds.

In a first step, ILs were considered as non-associating compounds. Parameters m, σ and ε/k_B obtained after optimization for the ILs studied in this paper are provided in Table II-1. The resulting density-temperature diagrams are shown in Figure II-2a for the [Cn-mim][BF_4] family, Figure II-2b for the [Cn-mim][PF_6] family, Figure II-2c for the [Cn-mim][Tf_2N] family and Figure II-2d for the [Cn-mim][CF_3SO_3] family. The absolute average deviation (AAD %) on the density for all the ILs considered in this work is about 0.38%. We can thus conclude that the density is globally well correlated even if deviations are observed at high and low temperatures. A linear relationship between the three parameters of the ILs and their molecular weight was observed for each family of ILs studied in this work. As examples, $m\sigma^3$ and $m\varepsilon/k_B$ are depicted as a function of the molecular weight in Figure II-3 for the [Cn-mim][Tf_2N], [Cn-mim][BF_4] and [Cn-mim][PF_6] family. The corresponding equations for the [Cn-mim][Tf_2N] based ILs (with n=2, 4, 6 and 8) are:

$$\begin{aligned} m &= 0.0138\, M_w + 2.4503 \\ m\sigma^3 &= 1.958\, M_w - 366.23 \\ m\varepsilon/k_B &= 5.9721\, M_w + 726.42 \end{aligned} \quad \text{(II-23)}$$

These correlations were used to predict the experimental density of three other ILs not taken into account in the database: [C_3-mim][Tf_2N], [C_5-mim][Tf_2N] and [C_7-mim][Tf_2N]. The PC-SAFT parameters of these ILs are calculated using equation (II-23). A good agreement with experimental density data is observed and results of the AAD% on densities are given in Table II-1. Therefore, these correlations are useful since they give the possibility to predict the behavior of heavier members of a given family without needing experimental data.

TABLE II-1: Optimized PC-SAFT parameters of pure ILs considered as non-associating compounds.

ILs	M_w ($g \cdot mol^{-1}$)	σ (Å)	ε/k_B (K)	m	AAD%	Reference of experimental density data
[C_2-mim][BF_4]	197.97	3.48	354.39	5.45	0.5190	40-47
[C_4-mim][BF_4]	226.03	3.62	369	6.00	0.4047	34,40,42,43,45,48-64
[C_8-mim][BF_4]	282.13	3.81	389.4	7.14	0.4535	61,65-67
[C_4-mim][PF_6]	284.18	3.71	391.7	6.25	0.3254	42,43,48,49,53,54,57,59,63,67-81
[C_6-mim][PF_6]	312.24	3.81	395.6	6.74	0.3387	42,66,76,82-86
[C_8-mim][PF_6]	340.29	3.91	395.5	7.14	0.4400	42,65-67,75-77,85-87
[C_2-mim][Tf_2N]	391.32	3.71	390.60	7.83	0.4246	45,51,53,54,74,88-93
[C_3-mim][Tf_2N]	405.33	3.76	391.34	8.04	0.5998	88,94
[C_4-mim][Tf_2N]	419.37	3.81	393.80	8.23	0.2880	51,53,54,73,74,84,88-91,93,95,96
[C_5-mim][Tf_2N]	433.35	3.85	393.50	8.42	0.2994	88,95
[C_6-mim][Tf_2N]	447.36	3.90	395.00	8.59	0.1370	54,82,88,90,97-102
[C_7-mim][Tf_2N]	461.45	3.94	395.48	8.81	0.3824	88,92
[C_8-mim][Tf_2N]	475.48	3.97	396.40	9.00	0.2861	54,88,90,92,97,103,104
[C_2-mim][SCN]	169.25	3.48	346.7	5.3	0.5515	105
[C_4-mim][SCN]	197.3	3.68	356	5.5	0.4268	50,61,106,107
[C_2-mim][CF_3SO_3]	260.24	3.61	390	6.15	0.3065	58,108-112
[C_4-mim][CF_3SO_3]	288.29	3.82	392.3	6.1	0.3098	51,54,62,63,66,80,109,113
[C_6-mim][CF_3SO_3]	316.34	3.81	390.5	7.14	0.2691	114,115

[C_8-mim][CF_3SO_3]	345.41	3.91	398.9	7.54	0.2190	115
[C_4-mim][NO_3]	201.23	3.59	365.8	5.65	0.3705	42,116,117
[C_2-mim][TFA]	224.18	3.51	386	6.15	0.3136	112
[C_4-mim][TFA]	252.24	3.71	414	6.34	0.1162	54,80
[C_2-mim][DCA]	177.21	3.7	364	4.7	0.3825	45,111,118
[C_4-mim][DCA]	205.26	3.72	383.4	5.7	0.3764	51,61,118-120
[C_6-mim][DCA]	233.31	3.82	404	6.3	0.2212	120
[C_4-mim][C_1SO_4]	250.32	3.61	376.9	6.74	0.2612	43,58,61,63,76,109,121-125
[C_2-mim][C_2SO_4]	236.29	3.71	384	5.66	0.6024	53,58,74,89,93,96,111,112,117,125-132
[C_4-mim][Cl]	174.67	3.49	359	5.66	1.0250	133-135
[C_6-mim][Cl]	202.37	3.7	366.4	5.8	0.4177	42,126,135,136
[C_8-mim][Cl]	230.78	3.92	391.9	5.81	0.3476	42,135-138
[C_2-mim][AC]	170.21	3.48	364.5	5.5	0.4571	105,139,140
[C_4-mim][AC]	198.27	3.72	378	5.51	0.3299	141,142
[C_6-mim][Br]	247.18	3.61	374	6.54	0.2175	143
CO_2	44.01	2.0729	169.21	2.7852	0	21

$$AAD\% = \frac{100}{npts} * \sum_{i=1}^{npts} \left| \frac{\rho_i^{sat,\exp} - \rho_i^{sat,cal}}{\rho_i^{sat,\exp}} \right|$$

[a]For the family of [C_n-mim][NTf_2], parameters for the members n=2, 4, 6 and 8 were obtained by fitting to experimental data and parameters corresponding to n=3, 5 and 7 have been obtained using the correlations presented in Eq. 23

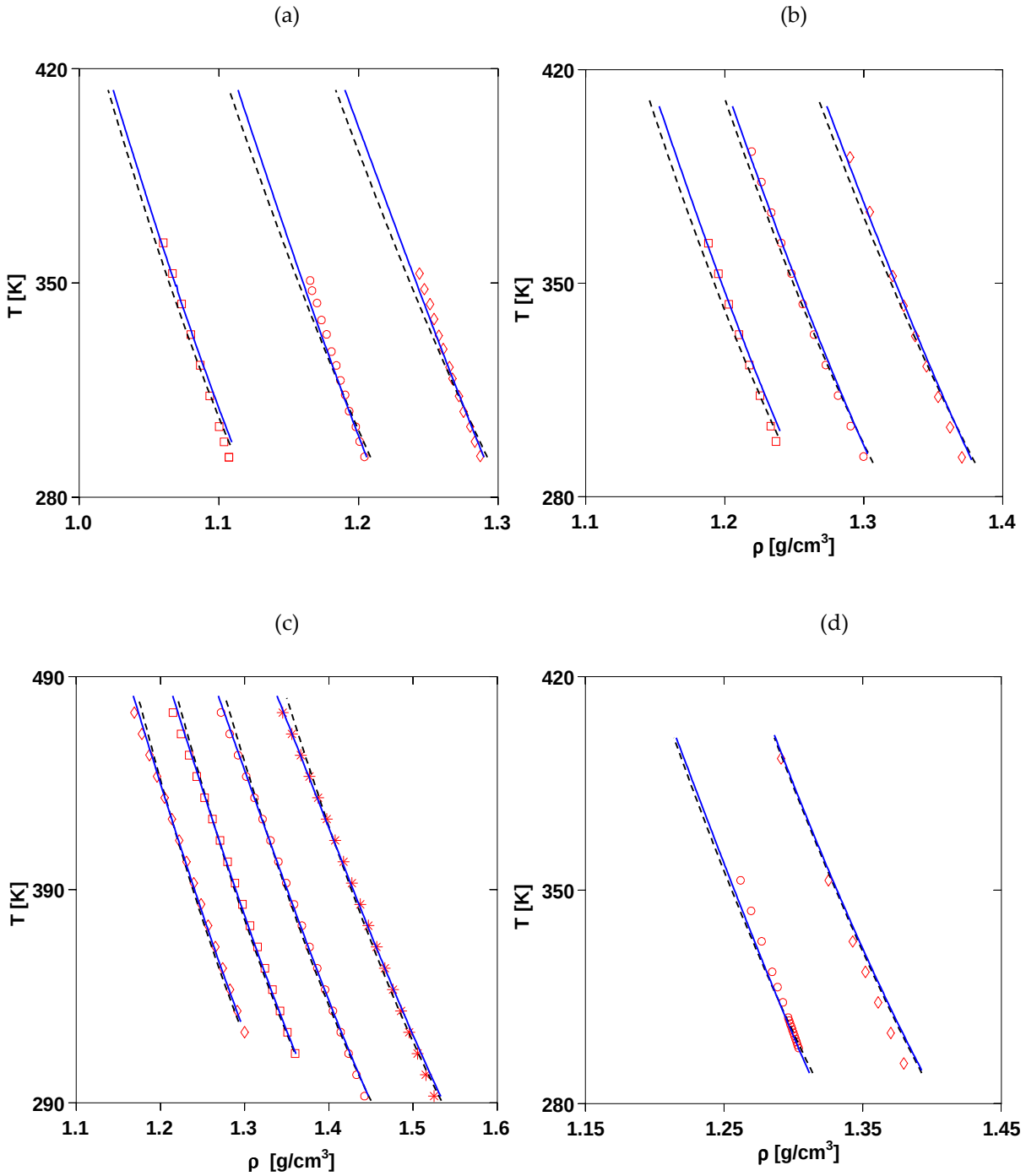

Figure II-2: Temperature-density diagrams for ILs considered as non-associating and self-associating compounds. Symbols: experimental data used in the parameter estimation. Solid lines: self-associating estimations. Dotted lines: non-associating estimations. **(a)** [C_2-mim][BF_4] (◊), [C_4-mim][BF_4] (○) and [C_8-mim][BF_4] (□); **(b)** [C_4-mim][PF_6] (◊), [C_6-mim][PF_6] (○) and [C_8-mim][PF_6] (□); **(c)** [C_2-mim][Tf_2N] (*), [C_4-mim][Tf_2N] (○), [C_6-mim][Tf_2N] (□) and [C_8-mim][Tf_2N] (◊); **(d)** [C_2-mim][CF_3SO_3] (◊), [C_4-mim][CF_3SO_3] (○).

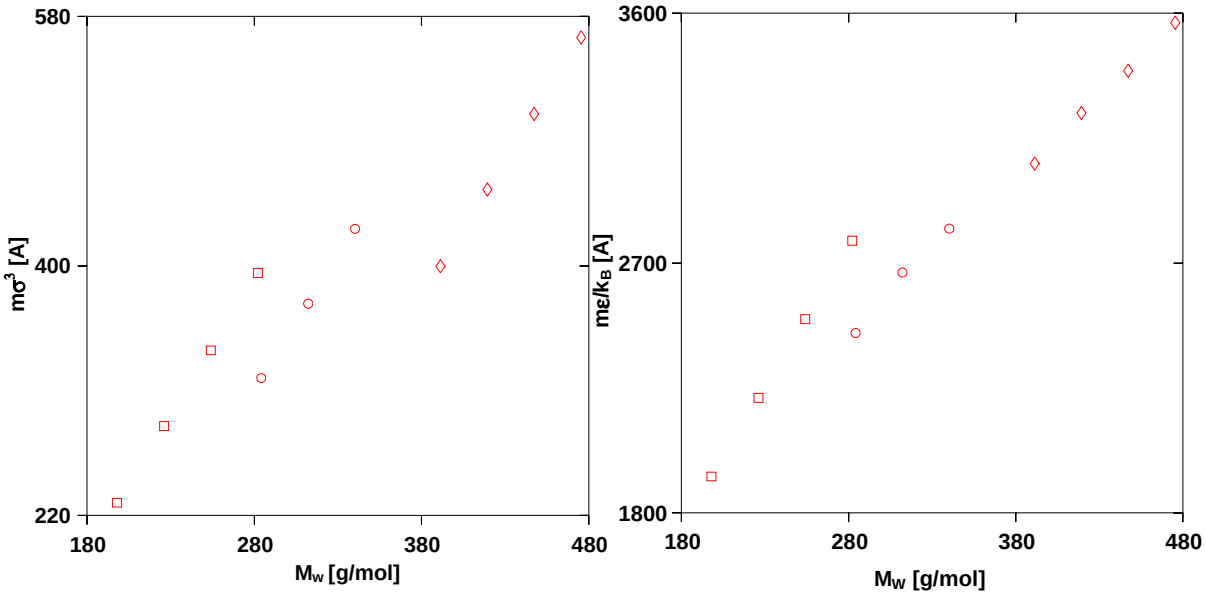

Figure II-3. Pure-component parameters: $m\sigma^3$ and $m\varepsilon/k_B$ of the PC-SAFT EoS for the [Cn-mim][Tf2N] (◊), [Cn-mim][BF4] (□) and [Cn-mim][PF6] (○) family as a function of the IL molecular weight.

II.4.1.2 Ionic liquids as self-associating compounds

Secondly, the parameters of ILs taken as self-associating compounds were estimated. As mentioned before, the association parameters: $\varepsilon^{A_iB_j}$ and $k^{A_iB_j}$ are kept constant and equal to those of 1-alkanols[32]. Parameters: m, σ and ε/k_B were estimated by minimizing equation 22. Results for molecular parameters and absolute average deviation (AAD %) on density are provided in Table II-2. The AAD% on the density for all the ILs is about 0.29%. The trend of deviations for each family of ILs is shown in Figure II-4. The largest deviations are obtained for the $[C_2SO_4]^-$ and $[Cl]^-$ based ILs. There is thus a great improvement by using self-associating parameters. Meanwhile, we can notice this significant improvement through the density-temperature diagrams shown in Figure II-2(a, b, c and d). We can thus conclude that the associating contribution should be taken into account in order to accurately correlate the properties of ILs.

TABLE II-2: Optimized PC-SAFT parameters of pure ILs considered as self-associating molecules.

ILs	M_w g·mol^{-1}	σ (Å)	ε/k_B (K)	m	K_{AB} (-)	ε_{AB}/k_B (K)	AAD%
[C_2-mim][BF_4]	197.97	4.23	408.1	3.13	0.00225	3450	0.2315
[C_4-mim][BF_4]	226.03	4.33	426.7	3.62	0.00225	3450	0.3019
[C_8-mim][BF_4]	282.13	4.32	434	5.03	0.00225	3450	0.1263
[C_4-mim][PF_6]	284.18	4.23	421	4.3	0.00225	3450	0.1870
[C_6-mim][PF_6]	312.24	4.32	431.8	4.73	0.00225	3450	0.1666
[C_8-mim][PF_6]	340.29	4.32	433.8	5.42	0.00225	3450	0.1430
[C_2-mim][Tf_2N]	391.32	4.18	360.5	5.38	0.00225	3450	0.1346
[C_3-mim][Tf_2N]	405.33	4.20	368.48	5.68	0.00225	3450	0.5014
[C_4-mim][Tf_2N]	419.37	4.21	375.2	6.05	0.00225	3450	0.1213
[C_5-mim][Tf_2N]	433.35	4.26	377.85	6.19	0.00225	3450	0.1599
[C_6-mim][Tf_2N]	447.36	4.31	385.2	6.35	0.00225	3450	0.1343
[C_7-mim][Tf_2N]	461.45	4.31	385.80	6.71	0.00225	3450	0.1731
[C_8-mim][Tf_2N]	475.48	4.32	386.9	7	0.00225	3450	0.1907
[C_2-mim][SCN]	169.25	4.22	383.8	3.05	0.00225	3450	0.3247
[C_4-mim][SCN]	197.3	4.21	383.5	3.77	0.00225	3450	0.2497
[C_2-mim][CF_3SO_3]	260.24	4.27	373.9	3.68	0.00225	3450	0.3165
[C_4-mim][CF_3SO_3]	288.29	4.43	392	3.92	0.00225	3450	0.2352
[C_6-mim][CF_3SO_3]	316.34	4.32	397.9	4.93	0.00225	3450	0.2374
[C_8-mim][CF_3SO_3]	345.41	4.41	398.1	5.26	0.00225	3450	0.2038
[C_4-mim][NO_3]	201.23	4.23	393.7	3.52	0.00225	3450	0.2417
[C_2-mim][TFA]	224.18	4.230	395.80	3.520	0.00225	3450	0.1636
[C_4-mim][TFA]	252.24	4.430	417.00	3.710	0.00225	3450	0.0627
[C_2-mim][DCA]	177.21	4.340	409.40	3.010	0.00225	3450	0.3855
[C_4-mim][DCA]	205.26	4.440	411.10	3.400	0.00225	3450	0.2102
[C_6-mim][DCA]	233.31	4.53	429.2	3.82	0.00225	3450	0.1173
[C_4-mim][C_1SO_4]	250.32	4.43	422.9	3.72	0.00225	3450	0.1682
[C_2-mim][C_2SO_4]	236.29	4.22	419	3.94	0.00225	3450	0.5331
[C_4-mim][Cl]	174.67	4.130	402.60	3.520	0.00225	3450	0.8482
[C_6-mim][Cl]	202.37	4.33	407.8	3.72	0.00225	3450	0.3351
[C_8-mim][Cl]	230.78	4.53	413.8	3.82	0.00225	3450	0.2506
[C_2-mim][AC]	170.21	4.23	405.70	3.130	0.00225	3450	0.3078

[C_4-mim][AC]	198.27	4.43	414	3.33	0.00225	3450	0.2402
[C_6-mim][Br]	247.18	4.210	391.90	4.170	0.00225	3450	0.1660
CO_2	44.01	2.0729	169.21	2.7852	0	0	0

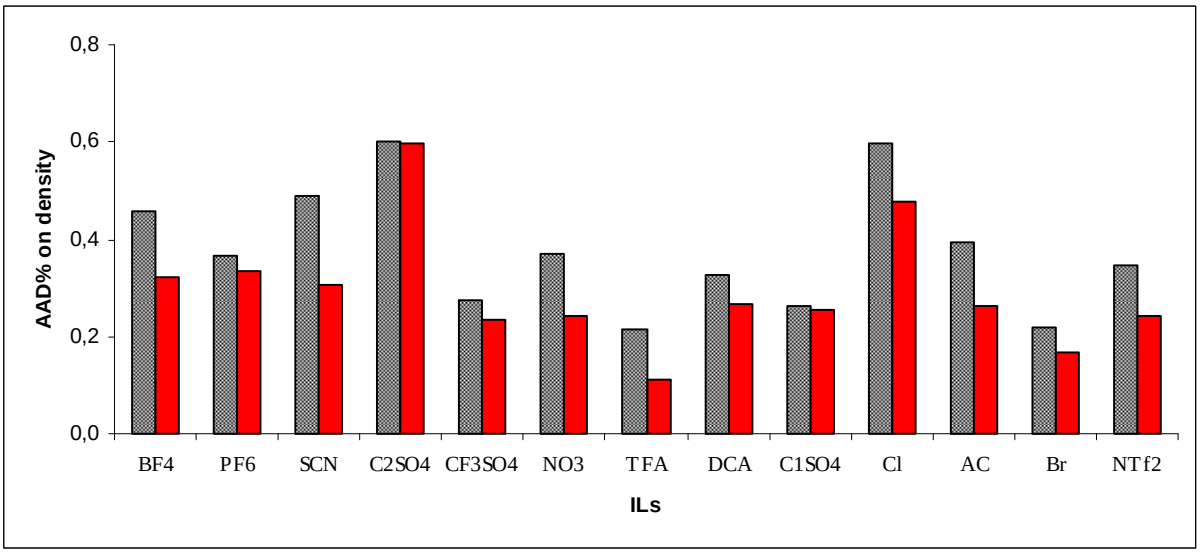

Figure II-4. Average absolute deviations obtained on density for different families of ILs. Black rectangles: ILs considered as non-associating compounds and red rectangles: ILs considered as associating compounds.

It was thus decided to develop simple correlations to predict the three molecular parameters: m, σ and ε/k_B of PC-SAFT model for the different families of ILs. The approach is based on the fact that m, $m\sigma^3$ or $m\varepsilon/k_B$ is linearly related to the molecular weight of ILs. Correlations are as follow:

$$m = a_i \cdot M_W + b_i$$
$$m\sigma^3 = c_i \cdot M_W + d_i \qquad \text{(II-24)}$$
$$m\varepsilon/k_B = e_i \cdot M_W + f_i$$

where a_i, b_i, c_i, d_i, e_i and f_i are the constants characterizing the family i of ILs. In this work, 9 families of [C_n-mim] ILs are defined depending on the associated anion (BF_4, PF_6, NTF_2, SCN, CF_3SO_3, TFA, DCA, AC and Cl). Parameters suitable for such

correlations are given in Table II-3. The average absolute deviation on density calculated using the parameters estimated from these correlations is equal to 0.29%. Therefore, the densities calculated from these parameters are globally accurate as compared to available experimental data. The approach was also evaluated through a new IL 1-hexyl-3-methylimidazolum tetrafluoroborate[34] not used to determine the parameters in equation 24. For such a IL, the parameters issued from equation 24 lead to AAD%=0.10%, to be compared with AAD%=0.06% calculated by a direct fit of the parameters on the experimental density data. In summary, PC-SAFT model provides the possibility to predict the behavior of new members of a given family with the help of the correlations developed in this work.

TABLE II-3: Parameters to be used in equation 24 in order to estimate m, σ, ε/k_B for [Cn-mim] families of ILs.

IL family	a_i	b_i	c_i	d_i	e_i	f_i
[Cn-mim][BF_4]	0.0224	-1.3539	2.0042	-159.6301	10.7046	-852.1832
[Cn-mim][PF_6]	0.0196	-1.3030	1.9890	-239.7743	9.4840	-893.8708
[Cn-mim][SCN]	0.0257	-1.2944	1.8592	-85.4749	9.7487	-478.6220
[Cn-mim][CF_3SO_3]	0.0200	-1.6170	1.9473	-220.2002	9.0532	-1001.8402
[Cn-mim][TFA]	0.0068	2.0020	1.9895	-179.4601	5.5205	155.1283
[Cn-mim][DCA]	0.0144	0.4550	1.9327	-97.1372	7.1208	-39.0765
[Cn-mim][Cl]	0.0054	2.5946	1.9157	-86.4376	2.9395	909.3006
[Cn-mim][AC]	0.0071	1.9168	1.8752	-82.2877	3.9254	601.0192
[Cn-mim][Tf_2N]	0.0184	-1.7982	2.0398	-404.7292	8.9773	-1549.9298

Moreover, we checked the validity of the adjusted parameters listed in Table II-2 to predict the vapour pressures of some ILs and compared the PC-SAFT calculations with available experimental data. Recently, Rocha et al.[144]and Zaitsau et al.[103] measured the vapour pressures of several imidazolium ILs ([Cn-mim][NTF_2] with n =

2,4,6 and 8). The vapor pressure was measured by the integral effusion Knudsen method in the temperature range T = 450−500 K.

Calculated vapour pressures and experimental data are plotted in the Figure II-5. The observed deviations from experimental data are particularly important. For ILs with short alkyl chains, the predicted vapor pressure is about 4 orders of magnitude higher than experimental data. The difference between calculated and experimental vapor pressure decreases when the alkyl chain increases. It is important to note that calculated vapour pressures of ILs is underestimated when ILs is taken as non associating fluid and overestimated when ILs are defined as associating fluid. Recently, Llovell et al:[22] presented similar calculations on [NTf_2] based ILs using the soft-SAFT equation of state. The authors obtained overestimated values of vapour pressure for all ILs, and the difference was about 2 orders of magnitude. Similar calculations were proposed by Paduszyński and Domanska[145] using the PC-SAFT model and 10-site model. The authors concluded that their approach tends to enhance the vapor pressure predictions of ILs. Therefore, we decide to determine the molecular parameters of PC-SAFT model for the family of [C_n-mim][NTf_2] using density and vapour pressure data. Molecular parameters and average absolute deviations on vapour pressure and density are given in Table II-4. In this case, vapour pressures and density of [NTf_2] based ILs are determined with good accuracy.

TABLE II-4: Optimized PC-SAFT parameters of the family [C_n-mim][NTf_2] using experimental density and pressure data.

ILs	M_w g·mol^{-1}	σ (Å)	ε/k_B (K)	m	K_{AB} (-)	ε_{AB}/k_B (K)	AAD%	
							Pressure	Density
[C_2-mim][Tf_2N]	391.32	4.28	457.40	5.67	0.00225	3450	11.81	1.28
[C_4-mim][Tf_2N]	419.37	4.37	458.90	5.72	0.00225	3450	9.41	4.29
[C_6-mim][Tf_2N]	447.36	4.47	460.30	5.78	0.00225	3450	6.49	1.66
[C_8-mim][Tf_2N]	475.48	4.63	461.60	5.83	0.00225	3450	5.14	2.89

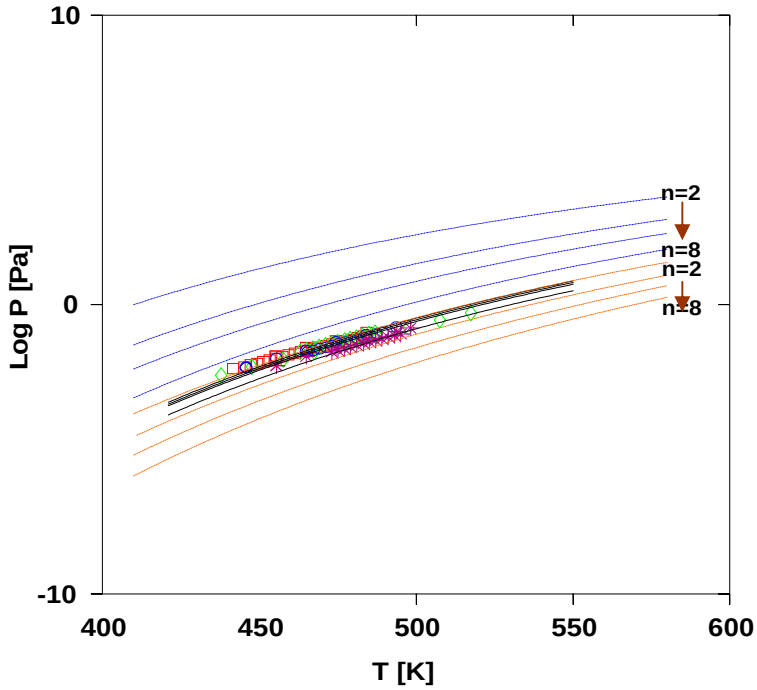

Figure II-5. Vapor pressures for [C2-mim][Tf2N](□), [C4-mim][Tf2N](◊), [C6-mim][Tf2N](○) and [C8-mim][Tf2N](∗). The symbols represent the experimental data. Blue dotted lines: ILs considered as associating compounds using PC-SAFT parameters adjusted on experimental density data only, orange dotted lines: ILs considered as non-associating compounds using PC-SAFT parameters adjusted on experimental density data only and black solid lines: ILs considered as associating compounds using PC-SAFT parameters adjusted on experimental pressure and density data.

II.4.2. Mixtures: solubility of carbon dioxide in ionic liquids

The use of PC-SAFT equation of state for mixtures requires the knowledge of a binary interaction parameter k_{ij}. Up to now, there is no general correlation to determine this parameter, which is generally, fitted on experimental VLE data. Many thermodynamic models can be used in a purely predictive manner by keeping k_{ij} constant (k_{ij} = 0 or 1) such as Soft-SAFT. However, it was demonstrated that better results are obtained when the interaction parameter is dependent temperature and different from zero (or one). As an example, {[C4-mim][BF4]+CO2} at T= 323 K with k_{ij} constant (k_{ij} = 0, 1) and k_{ij} fitted by VLE data. Results are shown in Figure II-6. A large

difference was found when k_{ij} equals to 0 or 1 as compared to experimental data. Therefore, in this work, the k_{ij} parameters of various binary mixtures containing IL and carbon dioxide were determined in order to minimize the deviations between calculated and experimental VLE data on an extended data base. A flash algorithm has been used to perform VLE calculations (for a selected binary system and a given T and P, we have found the composition of the liquid(x) and gas(y) phases in equilibrium). Values of interaction parameters k_{ij} at different temperatures are shown in Table II-5. Figures II-7 highlight that k_{ij} is a temperature-dependent parameter and increases linearly with temperature. A model based on the group contribution concept for the determination of the interaction parameter was thus developed. In our approach, each imidazolium based ionic liquids is characterized by two groups: one group for the anion and another group (-CH_3 or -CH_2-) to describe the alkyl chain grafted on the cation. Correlation is as follows:

$$k_{ij} = \left(a_i + n \cdot a_{CH_3/CH_2}\right) \cdot T + (b_i + n \cdot b_{CH_3/CH_2}) \qquad \text{(II-25)}$$

a_i and b_i are the contribution of the anion i, whereas $a_{CH3/CH2}$ and $b_{CH3/CH2}$ are used for describing the alkyl chain grafted on the cation, the length of which is characterized by n carbon atoms. Values of all parameters a_i, b_i, a_{CH_3/CH_2} and b_{CH_3/CH_2} are given in Table II-6.

Vapor-liquid equilibrium calculations of binary systems {CO_2 + ionic liquid} were performed using the interaction parameter issued from equation 25. The absolute average deviation on the estimated molar fraction of CO_2 at different temperatures using this approach is presented in Table II-5 and can be compared to the results obtained by a direct fit of the k_{ij} on experimental VLE data. This table clearly highlights that the proposed equation 25 is very accurate.

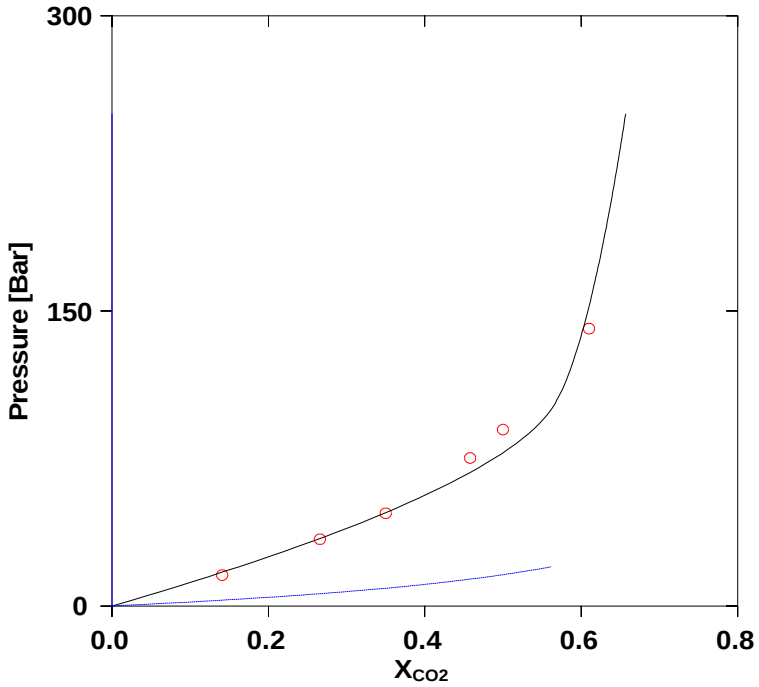

Figure II-6. Solubility of CO_2 in the [C_4-mim][BF_4] at temperatures: T=323K (○) obtained with different k_{ij} values. Symbols represent experimental data. Blue dotted lines: k_{ij}=0. Blue solid lines: k_{ij}=1. Black solid lines stand for k_{ij} fitted by experimental data.

TABLE II-5: k_{ij} interaction parameters at different temperatures for CO_2 + IL binary mixtures.

ILs	T/K	A		B	
		k_{ij}	AAD%	k_{ij}	AAD%
[C_2-mim][BF_4]	298.2	0.159	2.516	0.1588	2.521
	313.2	0.16	1.295	0.1594	1.586
[C_4-mim][BF_4]	303	0.142	5.883	0.1487	7.261
	313	0.146	5.097	0.1505	5.830
	323	0.151	3.974	0.1523	4.421
	333	0.154	3.876	0.1541	3.888
	343	0.157	3.709	0.1560	3.730
	353	0.161	3.210	0.1578	3.959
	363	0.163	3.316	0.1596	4.080
	373	0.165	1.872	0.1614	3.516
	383	0.172	2.310	0.1633	7.865
[C_4-mim][PF_6]	303	0.112	9.421	0.1217	11.001
[C_2-mim][NTf_2]	303.85	0.089	4.418	0.0949	5.845
	314.05	0.094	3.901	0.0935	3.953
	324.15	0.098	3.304	0.0922	5.343
	334.35	0.101	2.889	0.0909	6.680
	344.55	0.102	2.876	0.0895	8.462
[C_4-mim][NTf_2]	303.85	0.077	4.934	0.0847	11.678
	314.05	0.080	6.920	0.0848	10.143
	324.15	0.081	7.140	0.0848	9.668
	334.35	0.083	6.173	0.0849	8.365
	344.55	0.087	5.012	0.0850	6.945
[C_6-mim][NTf_2]	303.85	0.089	8.233	0.0745	9.676
	314.05	0.092	6.714	0.0760	8.629

	308	0.114	9.191	0.1220	10.534
	313	0.117	8.403	0.1223	9.411
	318	0.118	8.205	0.1227	8.986
	323	0.122	7.575	0.1230	7.714
	328	0.123	7.401	0.1234	7.480
[C6-mim][PF6]	303	0.115	7.150	0.1114	7.610
	308	0.116	9.348	0.1124	9.518
	313	0.117	6.700	0.1134	7.402
	318	0.119	7.081	0.1145	7.926
	323	0.121	6.712	0.1155	7.705
	328	0.122	6.151	0.1165	7.141
	333	0.123	6.018	0.1176	7.564
	338	0.125	4.290	0.1186	6.105
	324.15	0.095	5.573	0.0775	8.070
	334.35	0.097	4.282	0.0790	7.706
	344.55	0.097	3.553	0.0805	7.185
[C8-mim][NTf2]	303.85	0.062	8.056	0.0643	11.895
	314.05	0.063	9.171	0.0672	12.153
	324.15	0.064	8.744	0.0701	12.262
	334.35	0.065	8.638	0.0730	12.032
	344.55	0.071	8.036	0.0759	10.718
[C4-mim][CF3SO3]	303.20	0.115	13.726	0.1072	14.825
	313.30	0.141	8.667	0.1151	9.765
	323.30	0.147	4.107	0.1230	8.510
	333.30	0.147	0.898	0.1309	8.439
	343.20	0.154	6.384	0.1388	10.705

[a]k_{ij} fitted on experimental VLE data. [b]k_{ij} estimated by equation 25. [c]Average absolute deviation on CO_2 mole fraction.

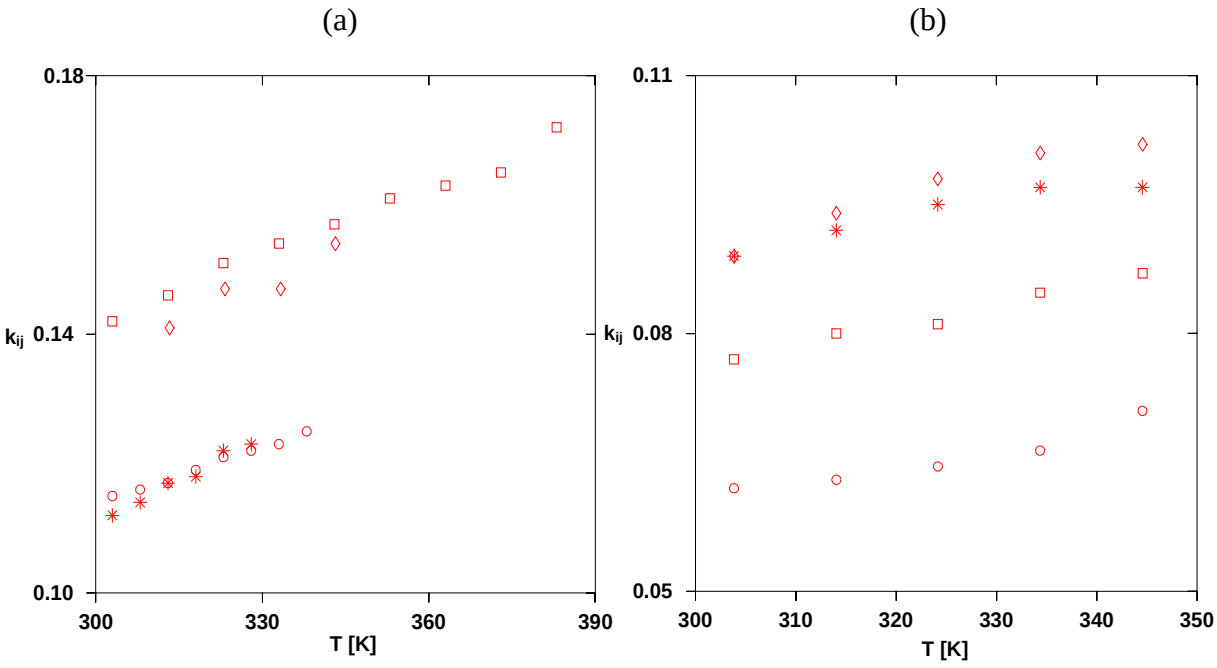

Figure II-7: Dependence on temperature of the binary interaction parameter for different ILs mixed with CO_2. (**a) :** [C4-mim][BF4] (□), [C4-mim][PF6] (*), [C6-mim][PF6] (○) and [C4-mim] [CF3SO3] (◊). (**b) :** [C2-mim][NTf2] (◊), [C4-mim][NTf2] (□), [C6-mim][NTf2] (*) and [C8-mim][NTf2] (○).

TABLE II-6: Parameters to be used in equation 25 in order to predict the binary interaction parameter, k_{ij}, for binary systems containing CO_2 and an imidazolium based IL.

Group	a_i	b_i
$[BF_4]$	-9.47E-05	1.98E-01
$[PF_6]$	-2.09E-04	2.06E-01
$[NTf_2]$	-2.66E-04	1.87E-01
$[CF_3SO_3]$	5.14E-04	-2.82E-02
$[C_2SO_4]$	1.98E-04	8.59E-02
$[C_1SO_4]$	-4.32E-05	1.84E-01
[DCA]	2.55E-04	1.11E-01
[SCN]	-1.62E-04	2.42E-01
CH_3/CH_2	6.93E-05	-2.61E-02

We now present and discuss calculations performed with the PC-SAFT EoS to correlate VLE data on systems containing CO_2 and a IL. Interaction parameter k_{ij} was obtained by fitting on experimental VLE data. Firstly, we studied the mixture {$[C_2$-mim$][BF_4]$+CO_2} at two different temperatures: T=298.20K and T=313.20K. Figure II-8 depicts the solubility isotherms obtained for these mixtures as compared to available experimental data.[35] It's striking to see the accuracy of these calculations at low pressures as compared to the experimental data. Within the same family, we studied $[C_4$-mim$][BF_4]$+CO_2 at different temperatures: T=303K, 323K, 343K, 363K and 383K. As shown in Figure II-9, a good agreement between experimental data[36] and the calculated values is observed at low pressure. However, a small deviation is observed at high pressure for T=343 K and T=363 K.

Fig. II-8 : CO_2 + [C_2-mim][BF_4]

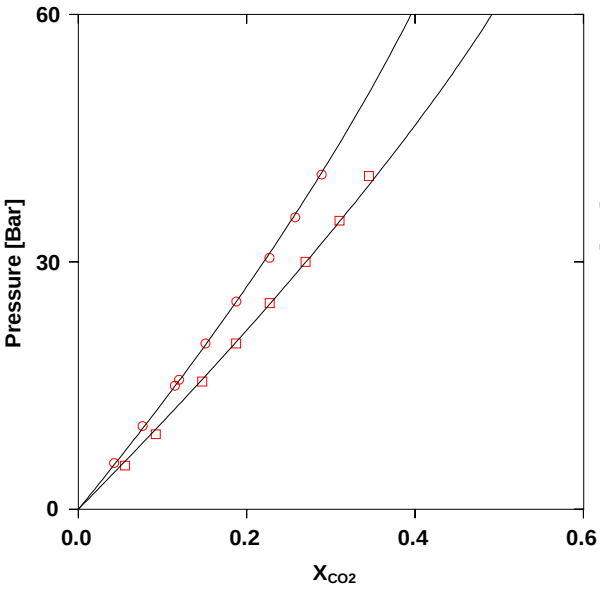

Fig. II-9 : CO_2 + [C_4-mim][BF_4]

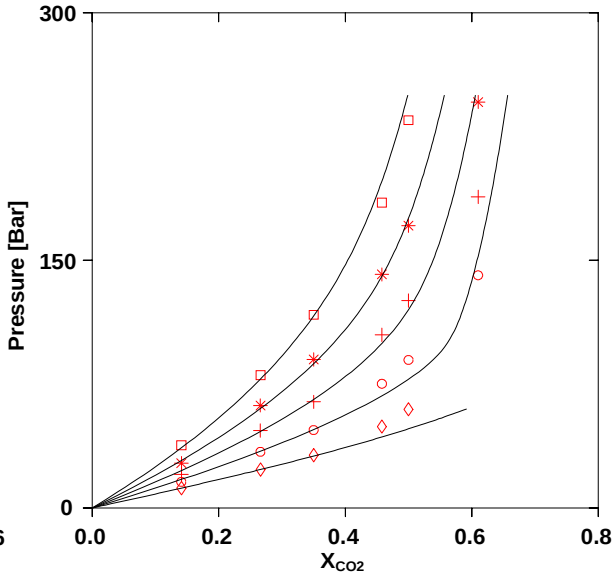

Figure II-8. Solubility of CO_2 in the [C_2-mim][BF_4] at different temperatures: T=298.20K (□) and T=313.20 K (○) with a temperature-dependent k_{ij} parameter. Solid lines are the PC-SAFT calculations.

Figure II-9. Solubility of CO_2 in the [C_4-mim][BF_4] at different temperatures: T=303K (◊), T=323K (○), T=343K (+), T=363K (∗) and T=383K (□) with a temperature-dependent k_{ij} parameter. Solid lines are the PC-SAFT calculations.

Phase diagrams of binary systems {[C_6-mim][PF_6] + CO_2}, {[C_2-mim][Tf_2N] + CO_2} and {[C_6-mim][Tf_2N] + CO_2} are represented with an absolute average deviations on CO_2 mole fraction of 7.00%, 3.48% and 5.67% respectively. Results presented in figures II 10-12 show that the PC-SAFT model may be used to predict with high accuracy the phase diagrams of these ionic liquids with carbon dioxide.

Finaly, figure II-13 shows that the model has a difficulty to represent with high accuracy the binary system {CO_2 + [C_4-mim][CF_3SO_3]}[37] at 303.20 K and 343.20 K while intermediate temperatures are well represented. Phase diagrams of binary systems {[C_4-mim][CF_3SO_3] + CO_2} are represented with an absolute average deviations on CO_2 mole fraction of 6.76%.

Fig. II-10 : CO_2 + [C_6-mim][PF_6]

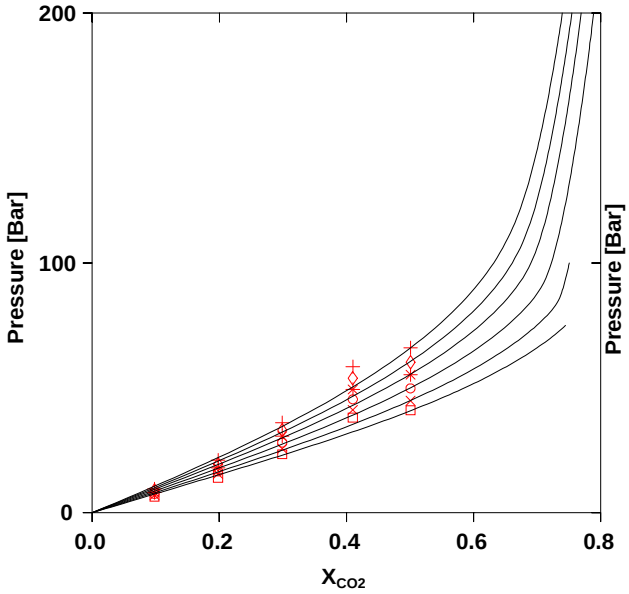

Fig. II-11 : CO_2 + [C_2-mim][NTf_2]

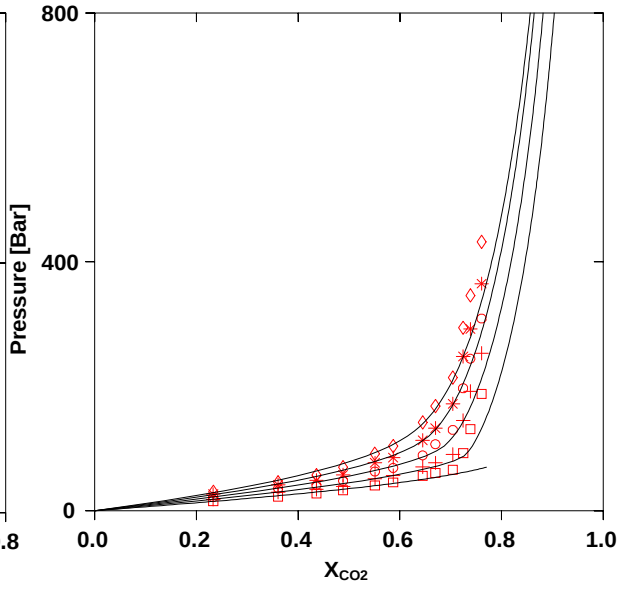

Fig. II-12 : CO_2 + [C_6-mim][NTf_2]

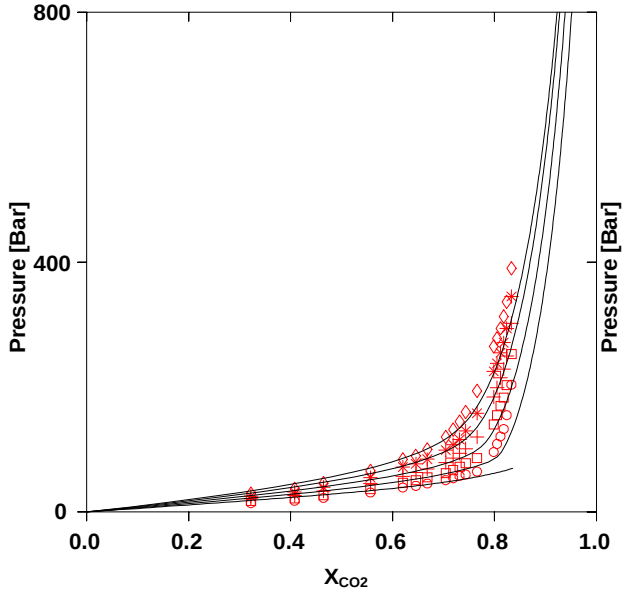

Fig. II-13: CO_2 + [C_4-mim][CF_3SO_3]

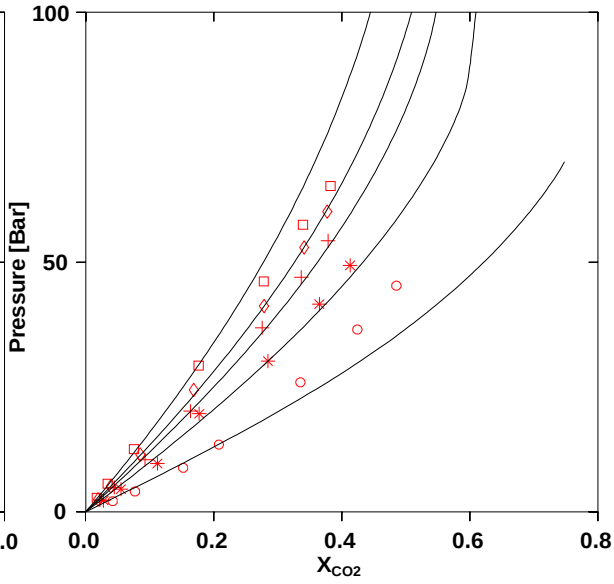

Figure II-10. Solubility of CO_2 in the [C_6-mim][PF_6] at different temperatures: T=308K (□), T=313K (×), T=318K (○), T=323K (∗), T=328K (◊) and T=333K (+) with a temperature-dependent k_{ij} parameter. Solid lines are the PC-SAFT calculations.

Figure II-11. Solubility CO_2 in the [C_2-mim][NTf_2] at different temperatures: T=303.85K (□), T=314.05K (+), T=324.15K (○), T=334.35K (∗) and T=344.55K (◊) with a temperature-dependent k_{ij} parameter. Solid lines are the PC-SAFT calculations.

Figure II-12. Solubility of CO_2 in the [C_6-mim][NTf_2] at different temperatures: T=303.85K (○), T=314.05K (□), T=324.15K (+), T=334.35K (∗) and T=344.55K (◊) with a temperature-dependent k_{ij} parameter. Solid lines are the PC-SAFT calculations.

Figure II-13. Solubility of CO_2 in the [C_4-mim][CF_3SO_3] at different temperatures: T=303.20K (○), T= 313.20K (∗), T=323.20K (+), T=333.20K (◊) and T=343.20K (□) with a temperature-dependent k_{ij} parameter. Solid lines are the PC-SAFT calculations.

In general, we notice a higher accuracy at low pressure than at high pressure. As a consequence, the simple model presented here is able to capture the solubility of these mixtures in quantitative agreement with available experimental data. It is also noticeable that the well-known pitfalls of the PC-SAFT EoS[38,39] were not evidenced in this work.

II.5 Conclusions

PC-SAFT parameters of pure ILs were estimated from component density data. In a second step, such parameters were simply correlated to the IL molar weight. It's thus possible to estimate m, σ and ε/k_B for ILs for which no experimental data are available. The interaction parameter k_{ij} is highly temperature-dependent and increases linearly with temperature. The contributions of the anion and the cation to the value of this parameter have been investigated. We have shown that PC-SAFT EoS was able to reproduce the solubility of CO_2 in imidazolium-based ILs in a wide range of temperatures and pressures.

References

(1) Pennline, H. W.; Luebke, D. R.; Jones, K. L.; Myers, C. R.; Morsi, B. I.; Heintz, Y. J.; Ilconich, J. B. *Fuel Process. Technol.* **2008**, *89*, 897-907.

(2) da Silva, E. F.; Svendsen, H. F. *Ind. Eng. Chem. Res.* **2006**, *45*, 2497-2504.

(3) Bello, A.; Idem, R. O. *Ind. Eng. Chem. Res.* **2005**, *44*, 945-969.

(4) Aionicesei, E.; Škerget, M.; Knez, Ž. *J. Chem. Eng. Data* **2008**, *53*, 185-188.

(5) Revelli, A. L.; Mutelet, F.; Jaubert, J. N. *Ind. Eng. Chem. Res.* **2010**, *49*, 3883-3892.

(6) Mutelet, F.; Revelli, A. L.; Jaubert, J. N.; Sprunger, L. M.; Acree, W. E.; Baker, G. A. *J. Chem. Eng. Data* **2010**, *55*, 234-242.

(7) Mutelet, F.; Jaubert, J. N.; Rogalski, M.; Harmand, J.; Sindt, M.; Mieloszynski, J. L. *J. Phys. Chem. B* **2008**, *112*, 3773-3785.

(8) Revelli, A. L.; Mutelet, F.; Turmine, M.; Solimando, R.; Jaubert, J. N. *J. Chem. Eng. Data* **2009**, *54*, 90-101.

(9) Wertheim, M. S. *J.Stat.Phys.* **1984**, *35*, 19-34.

(10) Wertheim, M. S. *J.Stat.Phys.* **1984**, *35*, 35-47.

(11) Wertheim, M. S. *J.Stat.Phys.* **1986**, *42*, 459-476.

(12) Wertheim, M. S. *J.Stat.Phys.* **1986**, *42*, 477-492.

(13) Chapman, W. G.; Jackson, G.; Gubbins, K. E. *Mol. Phys.* **1988**, *65*, 1057-1079.

(14) Chapman, W. G.; Gubbins, K. E.; Jackson, G.; Radosz, M. *Ind. Eng. Chem. Res.* **1990**, *29*, 1709-1721.

(15) Huang, S. H.; Radosz, M. *Ind. Eng. Chem. Res.* **1990**, *29*, 2284-2294.

(16) Fu, Y. H.; Sandler, S. I. *Ind. Eng. Chem. Res.* **1995**, *34*, 1897-1909.

(17) Garcia-Lisbona, M. N.; Galindo, A.; Jackson, G.; Burgess, A. N. *J. Am. Chem. Soc.* **1998**, *120*, 4191-4199.

(18) GilVillegas, A.; Galindo, A.; Whitehead, P. J.; Mills, S. J.; Jackson, G.; Burgess, A. N. *J. Chem. Phys.* **1997**, *106*, 4168-4186.

(19) Pamies, J. C.; Vega, L. F. *Ind. Eng. Chem. Res.* **2001**, *40*, 2532-2543.

(20) Blas, F. J.; Vega, L. F. *Mol. Phys.* **1997**, *92*, 135-150.

(21) Gross, J.; Sadowski, G. *Ind. Eng. Chem. Res.* **2001**, *40*, 1244-1260.

(22) Llovell, F.; Valente, E.; Vilaseca, O.; Vega, L. F. *J. Phys. Chem. B* **2011**, *115*, 4387-4398.

(23) Karakatsani, E. K.; Economou, I. G. *J. Phys. Chem. B* **2006**, *110*, 9252-9261.

(24) Karakatsani, E. K.; Kontogeorgis, G. M.; Economou, I. G. *Ind. Eng. Chem. Res.* **2006**, *45*, 6063-6074.

(25) Kroon, M. C.; Karakatsani, E. K.; Economou, I. G.; Witkamp, G.-J.; Peters, C. J. *J. Phys. Chem. B* **2006**, *110*, 9262-9269.

(26) Karakatsani, E. K.; Economou, L. G.; Kroon, M. C.; Peters, C. J.; Witkamp, G. J. *J. Phys. Chem. C* **2007**, *111*, 15487-15492.

(27) Paduszynski, K.; Domanska, U. *J. Phys. Chem. B* **2011**, *115*, 12537-12548.

(28) Baker, J. A.; Henderson, D. *J. Chem. Phys.* **1967**, *47*, 2856-2861.

(29) Baker, J. A.; Henderson, D. *J.Chem. Phys.* **1967**, *47*, 4714-4721.

(30) Huang, S. H.; Radosz, M. *Ind. Eng. Chem. Res.* **1991**, *30,* 1994-2005.

(31) Wolbach, J. P.; Sandler, S. I. *Ind. Eng. Chem. Res.* **1998**, *37*, 2917-2928.

(32) Pamies, J. C. *Ph.D.Thesis, Universitat Rovira i Virgili, Tarragona, Spain* **2003**.

(33) Andreu, J. S.; Vega, L. F. *J. Phys. Chem. C* **2007**, *111*,16028-16034.

(34) Sanmamed, Y. A.; Gonzalez-Salgado, D.; Troncoso, J.; Cerdeirina, C. A.; Romani, L. *Fluid Phase Equilib.* **2007**, *252*, 96-102.

(35) Lei, Z.; Yuan, J.; Zhu, J. *J. Chem. Eng. Data* **2010**, *55*, 4190-4194.

(36) Revelli, A.-L.; Mutelet, F.; Jaubert, J.-N. *J. Phys. Chem. B* **2010**, *114*, 12908-12913.

(37) Soriano, A. N.; Doma Jr., B. T.; Li, M.-H. *J. Taiwan Inst. Chem. Eng.* **2009**, *40*, 387-393.

(38) Privat, R.; Gani, R.; Jaubert, J.-N. *Fluid Phase Equilib.* **2010**, *295*, 76-92.

(39) Privat, R.; Conte, E.; Jaubert, J. N.; Gani, R. *Fluid Phase Equilib.* **2012**, *318*, 61-76.

(40) Klomfar, J.; Součková, M.; Pátek, J. *Fluid Phase Equilib.* **2009**, *282*, 31-37.

(41) Stoppa, A.; Zech, O.; Kunz, W.; Buchner, R. *J. Chem. Eng. Data* **2010**, *55*, 1768-1773.

(42) Seddon, K. R.; Stark, A.; Torres, M.-J. *ACS Symp. Ser.* **2002**, *819*, 34-49.

(43) Navia, P.; Troncoso, J.; Romani, L. *J. Chem. Eng. Data* **2007**, *52*, 1369-1374.

(44) Shiflett, M. B.; Yokozeki, A. *J. Chem. Eng. Data* **2007**, *52*, 1302-1306.

(45) Schreiner, C.; Zugmann, S.; Hartl, R.; Gores, H. J. *J. Chem. Eng. Data* **2010**, *55*, 1784-1788.

(46) Stoppa, A.; Hunger, J.; Buchner, R. *J. Chem. Eng. Data* **2009**, *54*, 472-479.

(47) Nishida, T.; Tashiro, Y.; Yamamoto, M. *J. Fluorine Chem.* **2003**, *120*, 135-141.

(48) Huo, Y.; Xia, S.; Ma, P. *J. Chem. Eng. Data* **2008**, *53*, 2535-2539.

(49) Huo, Y.; Xia, S. Q.; Ma, P. S. *J. Chem. Eng. Data* **2007**, *52*, 2077-2082.

(50) Vakili-Nezhaad, G.; Vatani, M.; Asghari, M.; Ashour, I. *J. Chem. Thermodyn.* **2012**, *54*, 148-154.

(51) Fredlake, C. P.; Crosthwaite, J. M.; Hert, D. G.; Aki, S. N. V. K.; Brennecke, J. F. *J. Chem. Eng. Data* **2004**, *49*, 954-964.

(52) Zhou, Q.; Wang, L. S.; Chen, H. P. *J. Chem. Eng. Data* **2006**, *51*, 905-908.

(53) Jacquemin, J.; Husson, P.; Padua, A. A. H.; Majer, V. *Green Chem.* **2006**, *8*, 172-180.

(54) Tokuda, H.; Tsuzuki, S.; Susan, M. A. B. H.; Hayamizu, K.; Watanabe, M. *J. Phys. Chem. B* **2006**, *110*, 19593-19600.

(55) Iglesias-Otero, M. A.; Troncoso, J.; Carballo, E.; Romani, L. *J. Solution Chem.* **2007**, *36*, 1219-1230.

(56) Harris, K. R.; Kanakubo, M.; Woolf, L. A. *J. Chem. Eng. Data* **2007**, *52*, 2425-2430.

(57) Kumar, A. *J. Solution Chem.* **2008**, *37*, 203-214.

(58) Garcia-Miaja, G.; Troncoso, J.; Romani, L. *Fluid Phase Equilib.* **2008**, *274*, 59-67.

(59) Qi, F.; Wang, H. J. *J. Chem. Thermodyn.***2009**, *41*, 265-272.

(60) Gao, H. Y.; Qi, F.; Wang, H. J. *J. Chem. Thermodyn.* **2009**, *41*, 888-892.

(61) Sanchez, L. G.; Espel, J. R.; Onink, F.; Meindersma, G. W.; de Haan, A. B. *J. Chem. Eng. Data* **2009**, *54*, 2803-2812.

(62) Garcia-Miaja, G.; Troncoso, J.; Romani, L. *J. Chem. Thermodyn.***2009**, *41*, 334-341.

(63) Soriano, A. N.; Doma Jr., B. T.; Li, M.-H. *J. Chem. Thermodyn.* **2009**, *41*, 301-307.

(64) Li, Y.; Ye, H.; Zeng, P. L.; Qi, F. *J. Solution Chem.* **2010**, *39*, 219-230.

(65) Harris, K. R.; Kanakubo, M.; Woolf, L. A. *J. Chem. Eng. Data* **2006**, *51*, 1161-1167.

(66) Gardas, R. L.; Freire, M. G.; Caryalho, P. J.; Marrucho, I. M.; Fonseca, I. M. A.; Ferreira, A. G. M.; Coutinho, J. A. P. *J. Chem. Eng. Data* **2007**, *52*, 80-88.

(67) Gu, Z. Y.; Brennecke, J. F. *J. Chem. Eng. Data* **2002**, *47*, 339-345.

(68) Kabo, G. J.; Blokhin, A. V.; Paulechka, Y. U.; Kabo, A. G.; Shymanovich, M. P.; Magee, J. W. *J. Chem. Eng. Data* **2004**, *49*, 453-461.

(69) Kumelan, J.; Kamps, A. P. S.; Tuma, D.; Maurer, G. *Fluid Phase Equilib.* **2005**, *228*, 207-211.

(70) Harris, K. R.; Woolf, L. A.; Kanakubo, M. *J. Chem. Eng. Data* **2005**, *50*, 1777-1782.

(71) Zafarani-Moattar, M. T.; Shekaari, H. *J. Chem. Eng. Data* **2005**, *50*, 1694-1699.

(72) Jacquemin, J.; Husson, P.; Majer, V.; Gomes, M. F. C. *Fluid Phase Equilib.* **2006**, *240*, 87-95.

(73) Troncoso, J.; Cerdeirina, C. A.; Sanmamed, Y. A.; Romani, L.; Rebelo, L. P. N. *J. Chem. Eng. Data* **2006**, *51*, 1856-1859.

(74) Jacquemin, J.; Husson, P.; Mayer, V.; Cibulka, I. b. *J. Chem. Eng. Data* **2007**, *52*, 2204-2211.

(75) Pereiro, A. B.; Legido, J. L.; Rodriguez, A. *J. Chem. Thermodyn.* **2007**, *39*, 1168-1175.

(76) Pereiro, A. B.; Rodriguez, A. *J. Chem. Thermodyn.* **2007**, *39*, 978-989.

(77) Pereiro, A. B.; Rodriguez, A. *J. Chem. Eng. Data* **2007**, *52*, 600-608.

(78) Kumar, A.; Singh, T.; Gardas, R. L.; Coutinho, J. A. P. *J. Chem. Thermodyn.* **2008**, *40*, 32-39.

(79) Fan, W.; Zhou, Q.; Sun, J.; Zhang, S. J. *J. Chem. Eng. Data* **2009**, *54*, 2307-2311.

(80) Zech, O.; Stoppa, A.; Buchner, R.; Kunz, W. *J. Chem. Eng. Data* **2010**, *55*, 1774-1778.

(81) Singh, T.; Kumar, A. *J. Mol. Liq.* **2010**, *153*, 117-123.

(82) Muhammad, A.; Mutalib, M. I. A.; Wilfred, C. D.; Murugesan, T.; Shafeeq, A. *J. Chem. Thermodyn.* **2008**, *40*, 1433-1438.

(83) Pereiro, A. B.; Tojo, E.; Rodriguez, A.; Canosa, J.; Tojo, J. *J. Chem. Thermodyn.* **2006**, *38*, 651-661.

(84) Harris, K. R.; Kanakubo, M.; Woolf, L. A. *J. Chem. Eng. Data* **2007**, *52*, 1080-1085.

(85) Tomida, D.; Kenmochi, S.; Tsukada, T.; Qiao, K.; Yokoyama, C. *Int. J. Thermophys.* **2007**, *28*, 1147-1160.

(86) Taguchi, R.; Machida, H.; Sato, Y.; Smith, R. L. *J. Chem. Eng. Data* **2009**, *54*, 22-27.

(87) Tomida, D.; Kumagai, A.; Kenmochi, S.; Qiao, K.; Yokoyama, C. *J. Chem. Eng. Data* **2007**, *52*, 577-579.

(88) Tariq, M.; Serro, A. P.; Mata, J. L.; Saramago, B.; Esperança, J. M. S. S.; Lopes, J. N. C.; Rebelo, L. P. N. *Fluid Phase Equilib.* **2010**, *294*, 131-138.

(89) Krummen, M.; Wasserscheid, P.; Gmehling, J. *J. Chem. Eng. Data* **2002**, *47*, 1411-1417.

(90) Tokuda, H.; Hayamizu, K.; Ishii, K.; Susan, M.; Watanabe, M. *J. Phys. Chem. B* **2005**, *109*, 6103-6110.

(91) Jacquemin, J.; Husson, P.; Majer, V.; Gomes, M. F. C. *J. Solution Chem.* **2007**, *36*, 967-979.

(92) Gardas, R. L.; Freire, M. G.; Carvalho, P. J.; Marrucho, I. M.; Fonseca, I. M. A.; Ferreira, A. G. M.; Coutinho, J. A. P. *J. Chem. Eng. Data* **2007**, *52*, 1881-1888.

(93) Wandschneider, A.; Lehmann, J. K.; Heintz, A. *J. Chem. Eng. Data* **2008**, *53*, 596-599.

(94) Esperanca, J.; Visak, Z. P.; Plechkova, N. V.; Seddon, K. R.; Guedes, H. J. R.; Rebelo, L. P. N. *J. Chem. Eng. Data* **2006**, *51*, 2009-2015.

(95) de Azevedo, R. G.; Esperanca, J.; Szydlowski, J.; Visak, Z. P.; Pires, P. F.; Guedes, H. J. R.; Rebelo, L. P. N. *J. Chem. Thermodyn.* **2005**, *37*, 888-899.

(96) Palgunadi, J.; Kang, J. E.; Nguyen, D. Q.; Kim, J. H.; Min, B. K.; Lee, S. D.; Kim, H.; Kim, H. S. *Thermochimica Acta* **2009**, *494*, 94-98.

(97) Kato, R.; Gmehling, J. *J. Chem. Thermodyn.* **2005**, *37*, 603-619.

(98) Kumelan, J.; Kamps, I. P. S.; Tuma, D.; Maurer, G. *J. Chem. Thermodyn.* **2006**, *38*, 1396-1401.

(99) Widegren, J. A.; Magee, J. W. *J. Chem. Eng. Data* **2007**, *52*, 2331-2338.

(100) Kandil, M. E.; Marsh, K. N.; Goodwin, A. R. H. *J. Chem. Eng. Data* **2007**, *52*, 2382-2387.

(101) Ahosseini, A.; Sensenich, B.; Weatherley, L. R.; Scurto, A. M. *J. Chem. Eng. Data* **2010**, *55*, 1611-1617.

(102) Esperanca, J.; Guedes, H. J. R.; Lopes, J. N. C.; Rebelo, L. P. N. *J. Chem. Eng. Data* **2008**, *53*, 867-870.

(103) Zaitsau, D. H.; Kabo, G. J.; Strechan, A. A.; Paulechka, Y. U.; Tschersich, A.; Verevkin, S. P.; Heintz, A. *J. Phys. Chem. A* **2006**, *110*, 7303-7306.

(104) Alonso, L.; Arce, A.; Francisco, M.; Soto, A. *J. Chem. Thermodyn.* **2008**, *40*, 265-270.

(105) Freire, M. G.; Teles, A. R. R.; Rocha, M. A. A.; Schroder, B.; Neves, C.; Carvalho, P. J.; Evtuguin, D. V.; Santos, L.; Coutinho, J. A. P. *J. Chem. Eng. Data* **2011**, *56*, 4813-4822.

(106) Domańska, U.; Laskowska, M. *J. Chem. Eng. Data* **2009**, *54*, 2113-2119.

(107) Domańska, U.; Królikowska, M. *J. Chem. Eng. Data* **2010**, *55*, 2994-3004.

(108) Vercher, E.; Orchillés, A. V.; Miguel, P. J.; Martíhez-Andreu, A. *J. Chem. Eng. Data* **2007**, *52*, 1468-1482.

(109) García-Miaja, G.; Troncoso, J.; Romaní, L. *J. Chem. Thermodyn.* **2009**, *41*, 161-166.

(110) Gardas, R. L.; Costa, H. F.; Freire, M. G.; Carvalho, P. J.; Marrucho, I. M.; Fonseca, I. M. A.; Ferreira, A. G.; Coutinho, J. A. P. *J. Chem. Eng. Data* **2008**, *53*, 805-811.

(111) Wong, C.-L.; Soriano, A. N.; Li, M.-H. *Fluid Phase Equilib.* **2008**, *271*, 43-52.

(112) Rodríguez, H.; Brennecke, J. F. *J. Chem. Eng. Data* **2006**, *51*, 2145-2155.

(113) Ge, M. L.; Zhao, R. S.; Yi, Y. F.; Zhang, Q.; Wang, L. S. *J. Chem. Eng. Data* **2008**, *53*, 2408-2411.

(114) Ficke, L. E.; Novak, R. R.; Brennecke, J. F. *J. Chem. Eng. Data* **2010**, *55*, 4946-4950.

(115) Nebig, S.; Gmehling, J. *Fluid Phase Equilib.* **2010**, *294*, 206-212.

(116) Mokhtarani, B.; Sharifi, A.; Mortaheb, H. R.; Mirzaei, M.; Mafi, M.; Sadeghian, F. *J. Chem. Thermodyn.* **2009**, *41*, 1432-1438.

(117) Blanchard, L. A.; Gu, Z.; Brennecke, J. F. *J. Phys. Chem. B* **2001**, *105*, 2437-2444.

(118) Klomfar, J.; Souckova, M.; Patek, J. *J. Chem. Eng. Data* **2011**, *56*, 3454-3462.

(119) Carvalho, P. J.; Regueira, T.; Santos, L. M. N. B. F.; Fernandez, J.; Coutinho, J. A. P. *J. Chem. Eng. Data* **2010**, *55*, 645-652.

(120) Seoane, R. G.; Corderi, S.; Gomez, E.; Calvar, N.; Gonzalez, E. J.; Macedo, E. A.; Dominguez, A. *Ind. Eng. Chem. Res.* **2012**, *51*, 2492-2504.

(121) Singh, T.; Kumar, A. *J. Solution Chem.* **2009**, *38*, 1043-1053.

(122) Kumelan, J.; Kamps, A. P. S.; Tuma, D.; Maurer, G. *J. Chem. Eng. Data* **2006**, *51*, 1802-1807.

(123) Pereiro, A. B.; Verdia, P.; Tojo, E.; Rodriguez, A. *J. Chem. Eng. Data* **2007**, *52*, 377-380.

(124) Gonzalez, B.; Calvar, N.; Gomez, E.; Dominguez, A. *J. Chem. Thermodyn.* **2008**, *40*, 1274-1281.

(125) Fernandez, A.; Garcia, J.; Torrecilla, J. S.; Oliet, M.; Rodriguez, F. *J. Chem. Eng. Data* **2008**, *53*, 1518-.1522

(126) Gómez, E.; González, B.; Calvar, N.; Tojo, E.; Domínguez, Á. *J. Chem. Eng. Data* **2006**, *51*, 2096-2102.

(127) Yang, J. Z.; Lu, X. M.; Gui, J. S.; Xu, W. G. *Green Chem.* **2004**, *6*, 541-543.

(128) Yang, H. Z.; Lu, X. M.; Gui, J. S.; Xu, W. G.; Li, H. W. *J. Chem. Thermodyn.* **2005**, *37*, 1250-1255.

(129) Gonzalez, E. J.; Gonzalez, B.; Calvar, N.; Dominguez, A. *J. Chem. Eng. Data* **2007**, *52*, 1641-1648.

(130) Hofman, T.; Goldon, A.; Nevines, A.; Letcher, T. M. *J. Chem. Thermodyn.* **2008**, *40*, 580-591.

(131) Tome, L. I. N.; Carvalho, P. J.; Freire, M. G.; Marrucho, I. M.; Fonseca, I. M. A.; Ferreira, A. G. M.; Coutinho, J. A. P.; Gardas, R. L. *J. Chem. Eng. Data* **2008**, *53*, 1914-1921.

(132) Matkowska, D.; Goldon, A.; Hofman, T. *J. Chem. Eng. Data* **2010**, *55*, 685-693.

(133) Hiroshi Machida; Yoshiyuki Sato; Richard, L. S., Jr. *J. Chem. Eng. Data* **2011**, *56*, 923-928.

(134) Govinda, V.; Attri, P.; Venkatesu, P.; Venkateswarlu, P. *Fluid Phase Equilib.* **2011**, *304*, 35-43.

(135) Huddleston, J. G.; Visser, A. E.; Reichert, W. M.; Willauer, H. D.; Broker, G. A.; Rogers, R. D. *Green Chem.* **2001**, *3*, 156-164.

(136) Gomez, E.; Gonzalez, B.; Dominguez, A.; Tojo, E.; Tojo, J. *J. Chem. Eng. Data* **2006**, *51*, 696-701.

(137) Gonzalez, E. J.; Alonso, L.; Dominguez, A. *J. Chem. Eng. Data* **2006**, *51*, 1446-1452.

(138) David, W.; Letcher, T. M.; Ramjugernath, D.; Raal, J. D. *J. Chem. Thermodyn.* **2003**, *35*, 1335-1341.

(139) Fröba, A. P.; Rausch, M. H.; Krzeminski, K.; Assenbaum, D.; Wasserscheid, P.; Leipertz, A. *Int. J. Thermophys.* **2010**, *31*, 2059-2077.

(140) Quijada-Maldonado, E.; van der Boogaart, S.; Lijbers, J. H.; Meindersma, G. W.; de Haan, A. B. *J. Chem. Thermodyn.* **2012**, *51*, 51-58.

(141) Shiflett, M. B.; Kasprzak, D. J.; Junk, C. P.; Yokozeki, A. *J. Chem. Thermodyn.* **2008**, *40*, 25-31.

(142) Bogolitsyn, K. G.; Skrebets, T. E.; Makhova, T. A. *Russ. J. Gen. Chem.* **2009**, *79*, 125-128.

(143) Li, J.-G.; Hu, Y.-F.; Sun, S.-F.; Liu, Y.-S.; Liu, Z.-C. *J. Chem. Thermodyn.* **2010**, *42*, 904-908.

(144) Rocha, M. A. A.; Lima, C.; Gomes, L. R.; Schroder, B.; Coutinho, J. A. P.; Marrucho, I. M.; Esperanca, J.; Rebelo, L. P. N.; Shimizu, K.; Lopes, J. N. C.; Santos, L. *J. Phys. Chem. B* **2011**, *115*, 10919-10926.

(145) Paduszynski, K.; Domanska, U. *J. Phys. Chem. B* **2011**, *116*, 5002-5018.

Chapitre III. La solubilité du dioxyde de carbone dans [BMIM][MDEGSO$_4$] et [P$_{6,6,6,14}$][C$_{12}$H$_{25}$PhSO$_3$]

This chapter is focused on the possible capture of carbon dioxide using ionic liquids (ILs). Such solvents are gaining special attention since the efficiency of many processes can be enhanced by the judicious manipulation of their properties. In this chapter, the potential use of two ILs: 1-butyl-3-methylimidazolium diethylene-glycolmonomethylethersulfate [BMIM][MDEGSO$_4$] and trihexyl(tetradecyl)phosphonium dodecyl-benzenesulfonate [P$_{6,6,6,14}$][C$_{12}$H$_{25}$PhSO$_3$] is evaluated through the experimental measurement of the liquid–vapor equilibrium in mixture with CO_2 at temperatures up to 373 K and pressures up to 300 bar. Experimental data indicate that 95 g of CO_2 can be absorbed per kg of ionic liquid. For each IL, the parameters of the PC-SAFT EoS were estimated using experimental density data measured under atmospheric pressure in a wide range of temperatures. After fitting a binary interaction parameter k_{ij} on experimental liquid–vapor equilibria data, the model was able to describe accurately carbon dioxide solubility in these two ionic liquids.

III.1 Introduction

Recently, emissions of carbon dioxide from fossil fuel combustion, arguably the most significant anthropogenic greenhouse gas, have received worldwide attention because of the possible implications for climate change. Consequently, the development of reversible, efficient and economic capture technologies for CO_2 is becoming increasingly important [1,2]. Nowadays, different separation technologies can be applied to carbon dioxide capture including solvent, membrane and adsorbent based processes. One of the most popular technologies for the capture of CO_2 is liquid absorbents designed to selectively solvate CO_2 [3]. The alkanolamines are the most generally accepted and widely used of the various available solvents for removal of CO_2 from natural gas stream. CO_2 will chemically react with the alkanolamines. The reactivity and availability at low cost of this family of compounds, especially monoethanolamine and diethanolamine, have made the solvent achieve a pinnacle position in the gas processing industry. Although these aqueous alkanolamine solutions are industrially effective on CO_2 removal, this method presents several drawbacks such as the intensive energy consumption, cost increases, corrosion problems in the presence of high concentration acid gases [4,5] and important losses of alkanolamine within relatively high vapor pressure. An alternative method to alkanolamines is the use of chilled ammonia [6]. Reaction of CO_2 with NH_3 results in the formation of ammonium bicarbonate. Ammonia has several advantages over alkanolamine including lower cost, higher CO_2 capacity, lower decomposition temperature of the ammonium bicarbonate product, and a less corrosive environment [7]. However, the very low temperatures necessary to minimize evaporative losses of NH_3 result in an increased energy usage and unfavorable operating costs [7].

Within the last few years, another class of solvent named ionic liquids (ILs) have attracted significant attention for their potential as alternative media for the capture of CO_2 [8-15], due to their good thermal stability and negligible vapor pressure.

Furthermore, physical properties of ILs may be modified and adjusted by employing different cation-anion combinations [16-20], giving the opportunity to select among a vast range of different ILs. For all these reasons, a large number of experimental and theoretical studies on the solubility of CO_2 in ILs have been performed [21-25], with a focus on imidazolium-based ILs. The results have shown that imidazolium ILs have remarkable physical absorption capacities. Recently, Couthino's group found that phosphonium based ILs are the best performing ILs for the CO_2 capture [26,27]. A good knowledge of the phase behavior of {CO_2 + IL} systems is necessary in order to design optimal ILs for the greenhouse gases capture.

During the past years, numerous thermodynamic models have been tested to represent phase diagrams of mixtures containing ionic liquids. Llovell et al. [28] used the Soft-SAFT (statistical associating fluid theory) equation to check its capability in capturing the thermodynamic behavior of several complex associating mixtures such as the behavior of binary mixtures of ionic liquids with different cations and anions, the vapor–liquid equilibria of mixtures containing short-chain alcohols and dialkylimidazolium [Tf_2N] and liquid-liquid equilibria of binary systems {water + IL}. They showed that such phase equilibria could be represented with high accuracy using soft-SAFT. The truncated perturbed-chain polar statistical associating fluid theory (tPC-PSAFT) [29,30] was also evaluated for the prediction of CO_2 solubility in dialkylimidazolium ionic liquids. In their works, Kroon et al. [31] and Karakatsani et al.[32] calculated the parameters of pure ionic liquids by fitting them to experimental liquid density data. In the case of pure ILs, the association contribution was not taken into account but dipolar interactions of ILs molecules and quadrupolar interactions of CO_2 molecule were considered. In the case of ILs, they assumed that their polarity was comparable to the polarity of lower to medium alcohols. In the work of Ashrafmansouri et al. [33], a group contribution approach is used to predict the phase behavior of CO_2 + IL systems based on the statistical associating fluid theory (SAFT-γ). The IL molecule is divided into groups of CH_3, CH_2, cation head, and the anion. The SAFT-γ parameters are optimized to experimental data. The ability of the

model to describe the phase behavior of these systems is demonstrated within a temperature range of 313.15–353.15K and pressures up to 100 bars. Then, Paduszynski and Domanska [34][35] proposed to represent VLE and LLE of binary systems containing aliphatic hydrocarbons and ionic liquids using the PC-SAFT equation. Pure fluid parameters of the model were obtained from experimental liquid density and solubility parameter data at ambient pressure and tested against high pressure densities. The authors have shown that the PC-SAFT, NRHB (nonrandom hydrogen-bonding theory) models and UNIFAC (UNIquac Fonctional group Activity Coefficient) were both able to capture phase behavior in a qualitative manner. Moreover, PC-SAFT allows accurate and reliable calculations of phase properties in a totally predictive manner.Vega et al.[36] provided an overview of the different approaches that have been applied to describe the thermodynamic behavior of ionic liquids and the solubility of selected compounds in them, including carbon dioxide, hydrogen, water, BF_3 and other compounds. The paper deals with some of the most recent and refined approaches involving physical models developed to characterize the ionic liquids. It is seen that the great advance in the refined modeling tools allows not only quantitative agreement with known experimental data, but also a guide to some of the physics governing the behavior of these systems, a step forward into developing ad hoc ionic liquids for specific applications. Recently, we have shown that simple molecular weight based correlation could be established to determine the PC-SAFT parameters of pure ILs and the interaction parameter needed to describe with accuracy the phase diagram of binary mixtures {CO_2 + IL}.

In this work, two ILs 1-butyl-3-methylimidazolium diethylene-glycolmonomethylethersulfate [BMIM][$MDEGSO_4$] and trihexyl(tetradecyl)phosphonium dodecyl-benzenesulfonate [$P_{6,6,6,14}$][$C_{12}H_{25}PhSO_3$] are evaluated as solvents for the CO_2 capture. The PC-SAFT [37] EoS was choosen to model both the pure components and the binary system: {CO_2+IL}.

III.2 PC-SAFT modelling

The Perturbed Chain-Statistical Associating Fluid Theory (PC-SAFT) EoS has been developed in 2001 by Gross and Sadowski [37]. They derived a dispersion expression for chain molecules and used a hard-chain reference fluid, to compare with other classical SAFT EoS which use a hard-sphere reference meaning that the dispersion term accounts for attraction between spherical segments, not for attraction between hard chains.

The PC-SAFT equation is usually written in terms of the residual Helmholtz energy. Each term in the equation represents different microscopic contributions to the total free energy of the fluid. The equation writes:

$$\tilde{a}^{res} = \tilde{a}^{hc} + \tilde{a}^{disp} + \tilde{a}^{assoc} \qquad \text{(III-1)}$$

where $\tilde{a}^{res}$ is the residual Helmholtz free energy of the system. The superscripts hc, disp and assoc refer to a reference hard chain contribution, a dispersion contribution and an associating contribution, respectively. The use of these different terms depends on the particular system under study, according to its physical nature.

The hard chain terms come from Wertheim's theory, provided and defined by Gross and Sadowski:

$$\tilde{a}^{hc} = \bar{m}\tilde{a}^{hs} - \sum_{i=1}^{n_c} x_i \left(m_i - 1\right) \ln g_{ij}^{hs} \qquad \text{(III-2)}$$

It depends on the radial pair distribution function for segments in the hard-sphere system (g_{ij}^{hs}), on the hard-sphere contribution ($\tilde{a}^{hs}$) and on the mean segment number ($\bar{m}$).

The dispersion contribution to the Helmholtz free energy $\tilde{a}^{disp}$ accounts for Van der Waals forces. In this work, we use the dispersion expression defined by Gross and Sadowski:

$$\tilde{a}^{disp} = -2\pi\tilde{\rho}I_1\overline{m^2\varepsilon\sigma^3} - \pi\tilde{\rho}\overline{m}C_1I_2\overline{m^2\varepsilon^2\sigma^3} \qquad \text{(III-3)}$$

where $\tilde{\rho}$ is number density, the coefficient C_1 depends on the mean segment number ($\overline{m}$) and on the reduced density (η), I_1 and I_2 are power series which depend on η and m, σ, ε are the pure component PC-SAFT parameters.

For evaluating the VLE of non associative fluids, inclusion of $\tilde{a}^{hc}$ and $\tilde{a}^{disp}$ in the PC-SAFT approach is sufficient. Three parameters, the segment number (m), the segment energy parameter (ε/k_B), and the segment diameter (σ) are required to characterize each compound. However, in numerous substances such as alkanol, amine or acid solution, hydrogen bonding contributes dominantly to the nonideality of these solutions and its contribution should be taken into account. The Helmholtz free energy due to association $\tilde{a}^{assoc}$ is defined by: [38,39]

$$\tilde{a}^{assoc} = \sum_{i=1}^{nc} x_i \left[\sum_{A_i} \left(\ln X^{A_i} - \frac{X^{A_i}}{2} \right) + \frac{1}{2} M_i \right] \qquad \text{(III-4)}$$

where X^{A_i} is the mole fraction of molecules i not bonded at site A, M_i is the number of association sites on each molecule and $\sum_{A_i}$ represents a sum over all associating sites on each molecule. The parameter X^{A_i} is given by:

$$X^{A_i} = \left[1 + N_{AV} \sum_j \sum_{B_j} \rho_j X^{B_j} \Delta^{A_i B_j} \right]^{-1} \qquad \text{(III-5)}$$

where ρ_j is the molar density of component j, $\Delta^{A_iB_j}$ is the association strength which depends on the association energy $\varepsilon^{A_iB_j}$ and the association volume $k^{A_iB_j}$ between associating substances i and j.

Hence, if one of the substances in a mixture is non-associating, $k^{A_iB_j}$ and $\Delta^{A_iB_j}$ will vanish consequently. More details about PC-SAFT have been described in our previous publication [40].

III.3 Experimental section

III.3.1 Materials

Carbon dioxide was purchased from Messer with a purity of 0.999999 in mass fraction. The ILs studied in this work: 1-butyl-3-methylimidazolium diethylene-glycolmonomethylethersulfate [BMIM][MDEGSO$_4$] (purity >0.98 mass fraction) and trihexy(tetradecy)phosphonium dodecyl-benzenesulfonate [THTDP][$C_{12}H_{25}PhSO_3$] (purity >0.98 mass fraction) were supplied by STREM Chemicals Inc.. n-Dodecane (purity >0.99 mass fraction, supplied by Sigma-Aldrich) and tetrachloroethylene (purity >0.99 mass fraction, supplied by Acros Organics) were used as reference fluids for mesuring the density of ILs. All these materials with suppliers and purities were listed in table III-1. Before each measurement, the ionic liquids were purified by subjecting the liquid under vacuum for approximately 12 h to remove possible traces of solvents and moisture. Analysis for the water content of the ionic liquids using the Karl Fischer technique showed that water contents were from 300 to 700 ppm.

Table III-1: Materials used in experiments with supplier and purity

Materials	Suppliers	Purity%
CO_2	Messer	99.99
[BMIM][MDEGSO$_4$]	STREM Chemicals Inc	98
[THTDP][$C_{12}H_{25}PhSO_3$]	STREM Chemicals Inc	98
n-dodecane	Sigma-Aldrich	99
Tetrachloroethylene	Acros Organics	99

III.3.2 Apparatus and procedure

III.3.2.1 Density measurement

Experimental densities of ILs were measured using an Anton Paar DMA 60 digital vibrating-tube densimeter, with a DMA 512P measuring cell in the temperature range (293.75–335.75) K at atmospheric pressure. The temperature in the vibrating-tube cell was measured by a platinum resistance thermometer Pt-100 with an accuracy of ±0.1 K. A thermostatic bath with oil as circulating fluid was used in the thermostat circuit of the measuring cell, which was held constant to ±0.1 K. n-Dodecane and tetrachloroethylene were used as reference fluids for the calibration of the vibrating-tube densimeter in order to determine the IL densities.

III.3.2.2 Measurement of carbon dioxide solubility

Bubble point pressures of the systems {CO_2 + IL} were measured using a high-pressure variable-volume visual cell (Top Industry, S.A.) as shown in Figure III-1. The technique used to carry out phase equilibrium measurement was based on a synthetic method which avoids sampling and analyses of the phases. The high-pressure cell was equipped with a moving piston and a sapphire window allowing a visual observation of the equilibrium cell. The window allows following the phase transition of the binary mixture with pressure and temperature using a video camera and a monitor. The mixture was permanently homogenized using a small magnetic bar and an external magnetic stirrer. The temperature inside the cell is kept constant using a thermostatic bath and is measured by a platinum resistance thermometer Pt-100 with an accuracy of ±0.1 K. The pressure is measured by a piezoresistive calibrated pressure sensor (KULITE HEM 375, working in the full scale range of 1–340 bar) directly placed inside the cell to minimize dead volumes with an accuracy of 0.1bar.

First, the equilibrium cell is loaded with a fixed amount of IL and its exact mass is determined using an analytical balance (SARTORIUS) with a resolution of ±0.001g.

Then, CO_2 is introduced under pressure from an aluminum reservoir tank. Its mass was measured with precision balance by weighting the reservoir tank before and after the gas introduction. After these filling operations, precise mole fractions of the compounds contained in the cell (i.e., CO_2 + synthetic mixture) and molar fractions of each compound could be calculated with an accuracy of 0.0001 mol.

When the desired cell temperature is reached, the pressure was slowly increased until the system becomes a one-phase system. The pressure at which the last bubble disappears represents the equilibrium pressure for the fixed temperature.

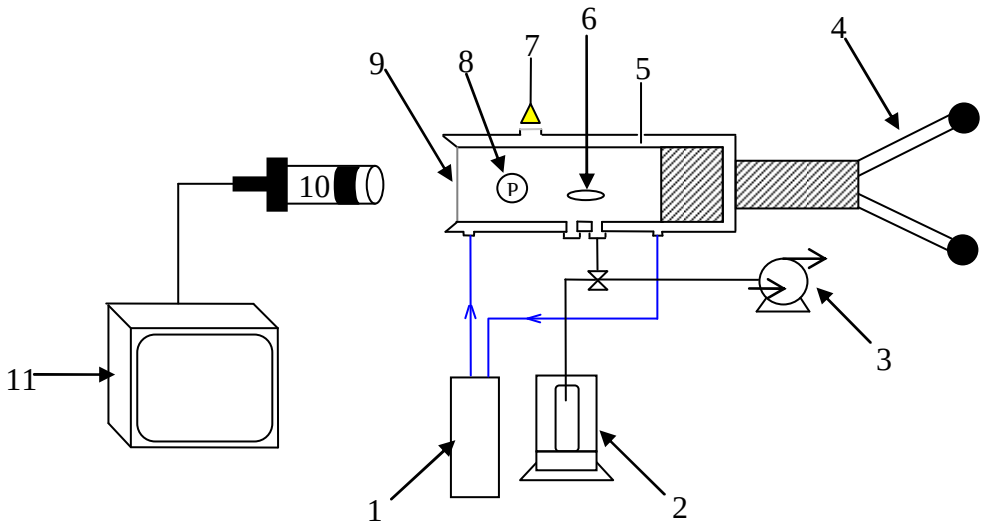

Figure III-1: Schema of the VLE apparatus: **(1)** Thermostated Bath; **(2)** Analytical Balance; **(3)** Vacuum Pump; **(4)** Piston; **(5)** Temperature Probe (Pt100); **(6)** Magnetic stirrer; **(7)** Light source; **(8)** Calibrated pressure sensor (0 < P < 340 bar); **(9)** Sapphire window; **(10)** Video camera; and **(11)** Monitor.

III.4 Results and discussion

III.4.1 Experimental vapour-liquid equilibrium data

The (vapor + liquid) equilibrium data of carbon dioxide in the two ILs were measured for mole fractions ranging from 0.097 to 0.743 in the temperature range 303–363 K and pressures from 4 to 265 bar. For systems with a fixed overall composition of carbon dioxide and ionic liquid, bubble point pressures were measured as a function of temperature. All results are listed in Tables III-2 and III-3.

The isotherms above the critical point of pure CO_2 present (vapor + liquid) equilibrium (VLE) throughout the pressure range measured. For temperature below the critical point of CO_2, a region of VLE exists at low pressures followed by a pressure at which (vapor + liquid + liquid) is observed.

Table III-2: Experimental bubble point data for various molar fractions of CO_2 in the {CO_2 + [C_4-mim][$MDEGSO_4$]} system. The standard uncertainties u are u(T)[a], u(P)[a], u(x_{CO2}) [a]<0.00005.

x_{co2}	T [K]	P [Bar]	x_{co2}	T [K]	P [Bar]
0.2309	313.15	22.6	0.5227	313.15	63.3
	323.15	27.5		323.15	80.0
	333.15	31.6		333.15	93.4
	343.15	35.8		343.15	110.1
	353.15	40.7		353.15	124.7
	363.15	45.0		363.15	141.9
0.2530	313.15	24.1	0.5802	313.15	76.7
	323.15	30.1		323.15	98.9
	333.15	34.2		333.15	129.2
	343.15	39.4		343.15	157.3
	353.15	43.4		353.15	181.3
	363.15	47.6		363.15	208.1
0.3017	313.15	24.8	0.6316	313.15	90.7
	323.15	31.3		323.15	123.5
	333.15	37.8		333.15	151.3
	343.15	43.2		343.15	189.2
	353.15	48.7		353.15	222.7
	363.15	55.1	0.6420	313.15	91.9
0.4127	313.15	39.8		323.15	128.0
	323.15	49.8		333.15	154.7
	333.15	60.8		343.15	191.9
	343.15	73.1		353.15	233.8
	353.15	84.9	0.6556	313.15	99.9
	363.15	98.2		323.15	169.8
0.4486	313.15	48.3		333.15	216.0
	323.15	56.0		343.15	264.8
	333.15	64.1	0.6638	313.15	117.8
	343.15	76.5		323.15	205.3
	353.15	97.7	0.6835	313.15	174.0
	363.15	109.0			
0.4775	313.15	54.4			
	323.15	62.5			
	333.15	72.6			
	343.15	83.0			
	353.15	102.0			

	363.15	118.0			

[a] Standard uncertainties u: $u_{[C4\text{-}mim][MDEGESO4]}$ (P)=0.1 Bar, $u_{[C4\text{-}mim][MDEGESO4]}$ (T)=0.01 K

Table III-3: Experimental bubble point data for various molar fractions of CO_2 in the {CO_2 + [THTDP][$C_{12}H_{25}PhSO_3$]} system. The standard uncertainties u are u(T)[a], u(P)[a], u (x_{CO2})[a]<0.00005.

x_{co2}	T [K]	P [Bar]	x_{co2}	T [K]	P [Bar]
	303.15	3.9		303.15	26.4
	313.15	4.6		313.15	28.6
	323.15	5.7		323.15	32.5
0.0971	333.15	6.1	0.4744	333.15	36.1
	343.15	6.4		343.15	38.5
	353.15	6.7		353.15	41.3
	363.15	7.1		363.15	43.9
	303.15	7.6		303.15	32
	313.15	9.7		313.15	35
	323.15	9.2		323.15	40
0.1954	333.15	11.7	0.5513	333.15	43.5
	343.15	12		343.15	48
	353.15	15.1		353.15	52.7
	363.15	16.2		363.15	56.4
	303.15	9.3		303.15	35.1
	313.15	11.3		313.15	37.9
	323.15	11.5		323.15	43.9
0.2220	333.15	13.3	0.5883	333.15	50.2
	343.15	14.2		343.15	55.3
	353.15	16.4		353.15	59.6
	363.15	18.1		363.15	64
	303.15	11.9		303.15	42.5
	313.15	13.3		313.15	49.2
	323.15	15		323.15	60.4
0.2716	333.15	16.7	0.6702	333.15	66.5
	343.15	18.1		343.15	72.9
	353.15	19.4		353.15	80.3
	363.15	21.2		363.15	87.6
0.3217	303.15	14.9	0.7051	303.15	46.2
	313.15	15.5		313.15	55.7
	323.15	19		323.15	66.2
	333.15	22		333.15	74.7
	343.15	22.9		343.15	83.2
	353.15	24		353.15	91.8

	363.15	25.2		363.15	100.7
0.3644	303.15	18.4	0.7134	303.15	47.5
	313.15	20.1		313.15	58.4
	323.15	22.8		323.15	68.5
	333.15	25.3		333.15	76
	343.15	27.3		343.15	85.1
	353.15	27.6		353.15	94
	363.15	31.4		363.15	102.9
0.4064	303.15	20.5	0.7329	303.15	50.6
	313.15	22.6		313.15	61
	323.15	25.7		323.15	71.5
	333.15	28.5		333.15	82
	343.15	30.7		343.15	91.2
	353.15	32		353.15	100.8
	363.15	35.4		363.15	110.4
0.4440	303.15	23.5	0.7435	303.15	54.3
	313.15	26.1		313.15	63.6
	323.15	29.8		323.15	74.9
	333.15	32.3		333.15	84.1
	343.15	34.4		343.15	93.5
	353.15	36.9		353.15	103.4
	363.15	39.5		363.15	113.7

[a] Standard uncertainties u: $u_{[THTDP][C12H25PhSO3]}(P)$=0.1 Bar, $u_{[THTDP][C12H25PhSO3]}(T)$=0.01 K.

The solubility in terms of molality (moles of CO_2 absorbed per kilogram of ionic liquid) at 313 K and 40 bar are presented in Table III-4. According to the results, it is possible to solubilize 101 g of carbon dioxide per kilogram of [THTDP][$C_{12}H_{25}PhSO_3$] studied in this work. The solubility of CO_2 in trihexyltetradecylphosphonium based ILs were measured by Neves et al. [41] and Song et al. [42]. Results presented in Table III-4 show the influence of the anion on the solubility of the carbon dioxide. The most performant IL for the CO_2 capture is the [THTDP][Tf_2N] able to solubilize 3.05 mol per kilogram of IL. The solubility of CO_2 decreases in [THTDP] when [Tf_2N] anion is replaced by [Cl], [Br] or [$C_{12}H_{25}PhSO_3$]. Brennecke et al. have reported that an increase of number of fluorine atoms on the anion increases the CO_2 solubility [21,43]. In table III-4, the solubility of CO_2 in a physical solvent well known for its

strong affinity, the poly (ethylene glycol) dimethyl ether, is also given. It is clear that poly (ethylene glycol) dimethyl ether is a better solvent than ionic liquids for the capture of gases. Nevertheless, poly (ethylene glycol) dimethyl ether has the main drawback that heavy hydrocarbons are dissolved in it.

Table III-4: Solubility of CO_2 in physical solvent and different ILs at 313 K and 40 bar

Solvents	x_{CO_2}	$mol_{CO_2} \cdot kg_{IL}^{-1}$	References
Poly(ethylene glycol) dimethyl ether	0.53	4.51	[47]
[BMIM][BF_4]	0.35	2.38	[47]
[BMIM][SCN]	0.25	1.69	[47]
[DMIM][MP]	0.25	1.53	[47]
[BMIM][Tf_2N]	0.50	2.39	[48]
[BMIM][PF_6]	0.40	2.27	[49]
[$(ETO)_2$IM][Tf_2N]	0.55	2.79	[47]
[BMIM][$MDEGSO_4$]	0.413	2.10	This work
[THTDP] [$C_{12}H_{25}PhSO_3$]	0.65	2.30	This work
[THTDP][Cl]	0.58	2.66	[41, 42]
[THTDP][Tf_2N]	0.88	3.05	[41, 42]

III.4.2 Modelling the solubility of carbon dioxide in ionic liquids

The experimental densities of pure ILs obtained are reported in Table III-5. The densities of the two ILs are measured for the first time in this study. The values of density at atmospheric pressure (necessary for the PC-SAFT parameters of pure ILs) were adjusted to linear

$$\rho_{[CYPHOS]} / g \cdot cm^{-3} = 1.4325 - 0.0009 \times (T/K) \quad \text{(III-6)}$$

$$\rho_{[C4mim][MDEGSO4]} / g \cdot cm^{-3} = 1.1231 - 0.0006 \times (T/K)$$

The parameters of PC-SAFT for pure ILs were determined using these experimetal densities in order to minimize the following objective function (OF):

$$OF = \sum_{i=1}^{npts} \left(\frac{\rho_i^{sat,\exp} - \rho_i^{sat,cal}}{\rho_i^{sat,\exp}} \right)^2 \quad \text{(III-7)}$$

The carbon dioxide molecule was modeled as a non-associating substance according to the paper of Huang and Radoz [38]. In this work, the CO_2 molecule was thus represented by three molecular parameters: m, the segment number; σ, the segment diameter; ε/k_B, the segment energy parameter. The values of these three parameters are taken from the paper of Gross and Sadowski [37]. The PC-SAFT parameters of pure ILs were determined considering ILs as self-associating compounds. The three non-associating parameters (m, σ, ε/k_B) were obtained by a fitting procedure on pure-component data. In order to keep a minimum number of parameters to be fitted, the two self-associating parameters ($\varepsilon^{A_iB_j}$ and $k^{A_iB_j}$) were transferred from those of 1-alkanols [44], i.e., $\varepsilon^{A_iB_j}$ =3450 K and $k^{A_iB_j}$ =0.00225. Both associating parameters were assumed constant because the alkyl chain length of the cation has a negligible effect on the strength of the associating bonds. Results for molecular parameters of carbon dioxide and pure ILs with absolute average deviation (AAD%) on density are provided in Table III-6.

Then, the PC-SAFT equation was evaluated in the representation of the thermodynamic properties of pure ILs such as temperature-dependent density. The resulting density-temperature diagrams are shown in Figure III-2. We can thus conclude that the density is well represented by the PC-SAFT equation of state.

Table III-5: Experimental densities of pure [C_4-mim][$MDEGSO_4$] and [THTDP][$C_{12}H_{25}PhSO_3$] in the (298.75 to 335.75) K range at atmospheric pressure with standard uncertainty u(ρ)[a].

ILs	T [K]	Density [g/cm³]	ILs	T [K]	Density [g/cm³]
[C_4-mim][$MDEGESO_4$]	298.75	1.1754	[THTDP][$C_{12}H_{25}PhSO_3$]	313.95	0.9258
	301.75	1.1722		316.05	0.9243
	302.65	1.1716		317.95	0.9235
	304.55	1.1697		319.75	0.9223
	306.25	1.1679		321.75	0.9213

308.45	1.1667	323.65	0.9202
310.35	1.1653	325.55	0.9189
312.35	1.1637	327.35	0.9175
313.95	1.1626	329.95	0.9159
316.05	1.1603	331.95	0.9146
317.95	1.1584	333.85	0.9131
319.75	1.1569	335.75	0.9123
321.75	1.1547		

[a] The standard uncertainty u is u(ρ)=0.0001 g/cm^3

Table III-6: Optimized PC-SAFT parameters of pure ILs: [C$_4$-mim][MDEGSO$_4$] and [THTDP] [C$_{12}$H$_{25}$PhSO$_3$].

ILs	M_w (g·mol^{-1})	σ (Å)	ε/k$_B$ (K)	m	K$_{HB}$ (-)	ε$_{HB}$/k$_B$ (K)	AAD%
[C$_4$-mim][MDEGSO$_4$]	338.45	4.2800	319.60	5.4800	0.00225	3450	0.0751
[THTDP][C$_{12}$H$_{25}$PhSO$_3$]	809.34	4.5100	342.80	14.6000	0.00225	3450	0.1088
CO$_2$	44.01	2.7852	169.21	2.0729	0	0	–

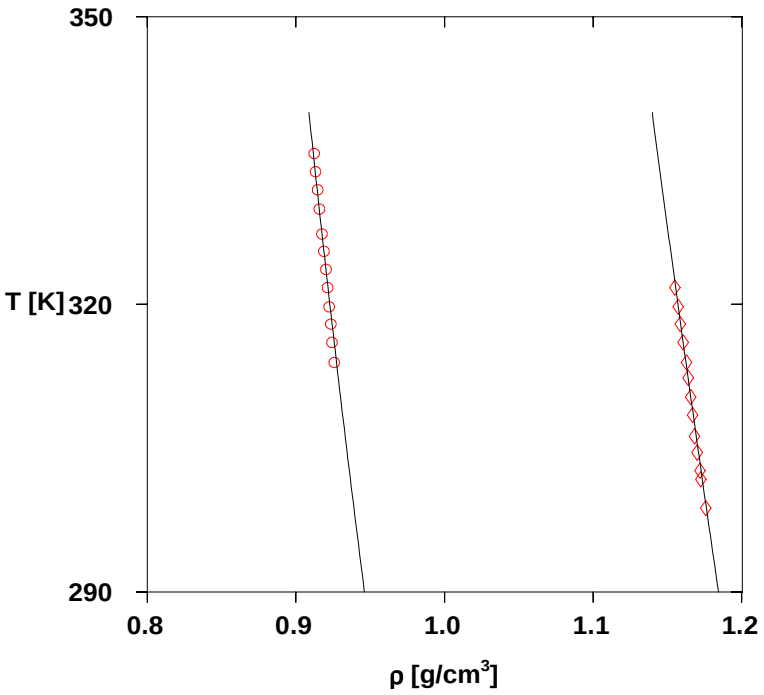

Figure III-2: Temperature-density diagrams for ILs: [C_4-mim][$MDEGSO_4$] (◊) and [THTDP][$C_{12}H_{25}PhSO_3$] (○). Symbols: experimental data obtained in this work. Solid lines: PC-SAFT estimations

In our approach, the use of PC-SAFT equation of state for mixtures requires the knowledge of a binary interaction parameter k_{ij}, which is generally fitted on experimental VLE data. The k_{ij} parameters of various binary mixtures containing IL and carbon dioxide were determined in order to minimize the deviations between calculated and experimental VLE data. Values of interaction parameters k_{ij} at different temperatures are shown in Table III-7 with absolute average deviations on CO_2 molar fraction. Figure III-3 highlights that interaction parameter k_{ij} is a temperature-dependent parameter and increases linearly with temperature.

We now present and discuss calculations performed with the PC-SAFT EoS to correlate VLE data on systems containing CO_2 and an IL. Interaction parameter k_{ij} was fitted on experimental VLE data. Firstly, we studied the mixture {[C_4-mim][$MDEGSO_4$] + CO_2} at different temperatures: T=313.15K, T=323.15K, T=333.15K, T=343.15K, T=353.15K and T=363.15K. Figure III-4 depicts the solubility isotherms obtained for these mixtures as compared to experimental VLE data. It's striking to see the accuracy of these calculations as compared to the experimental data. Results obtained on the binary mixture {CO_2 + [THTDP][$C_{12}H_{25}PhSO_3$]} are presented in Figure III-5. A good agreement between experimental VLE data and the calculated values is observed.

Table III-7: k_{ij} interaction parameters at different temperatures for CO_2+ IL binary mixtures.

ILs	T [K]	k_{ij}	AAD%
[THTDP][$C_{12}H_{25}PhSO_3$]	303.15	0.143	3.7633
	313.15	0.146	2.4264
	323.15	0.148	3.6804
	333.15	0.150	2.0047
	343.15	0.151	1.9037
	353.15	0.152	2.9867
	363.15	0.155	3.1642

	Total average deviation		2.8471
[C4-mim][MDEGSO4]	293.15	0.129	6.9555
	303.15	0.135	7.0485
	313.15	0.141	3.1290
	323.15	0.146	3.1766
	333.15	0.152	3.3550
	343.15	0.156	3.5255
	353.15	0.162	3.3274
	363.15	0.168	2.7022
	Total average deviation		4.1525

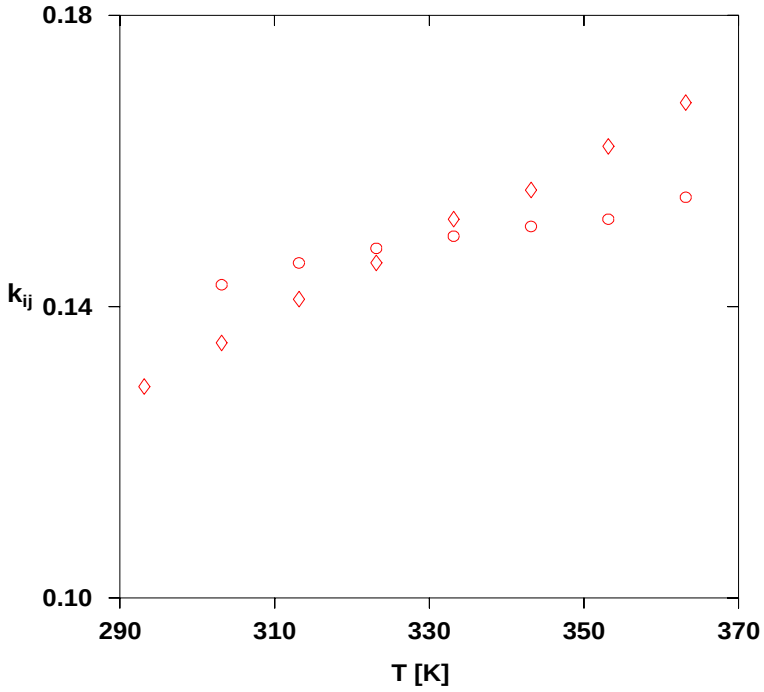

Figure III-3: Dependence on temperature of the binary interaction parameter for different ILs mixed with CO_2. [C_4-mim][$MDEGSO_4$] (◊) and [THTDP][$C_{12}H_{25}PhSO_3$] (○).

Fig.III-4: CO_2 + [C_4-mim][$MDEGSO_4$]

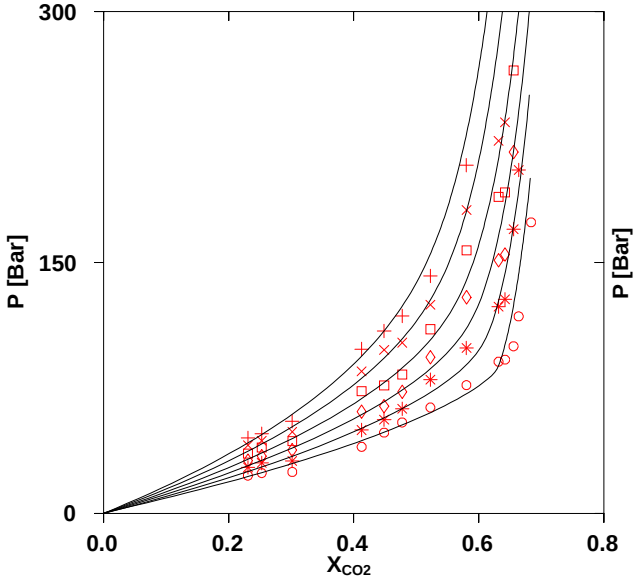

Fig.III-5: CO_2 + [THTDP][$C_{12}H_{25}PhSO_3$]

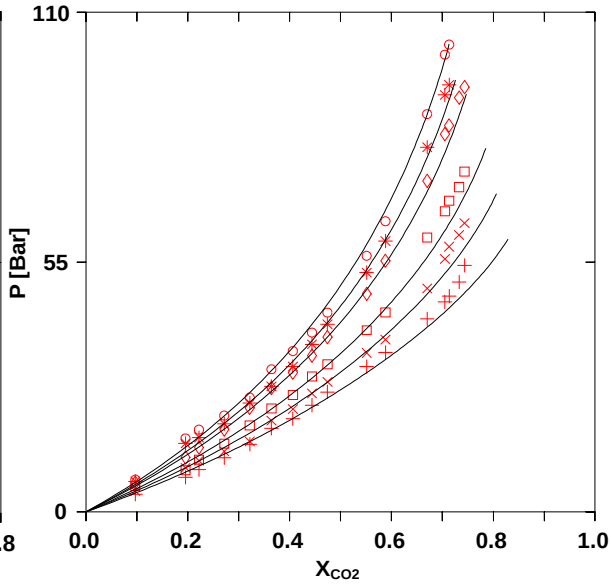

Figure III-4: Solubility of CO_2 in the [C_4-mim][$MDEGSO_4$] at different temperatures: T=313K (○), T=323K (*), T=333K (◊), T=343K (□), T=353K (×) and T=363K (+) with a temperature-dependent k_{ij} parameter. Solid lines are the PC-SAFT calculations.

Figure III-5: Solubility of CO_2 in the [THTDP][$C_{12}H_{25}PhSO_3$] at different temperatures: T=303.15K (+), T=313.15K (×), T=323.15K (□), T=343.15K (◊), T=353.15K (*) and T=363.15K (○) with a temperature-dependent k_{ij} parameter. Solid lines are the PC-SAFT calculations.

III.5 Conclusions

The solubility of CO_2 in 1-butyl-3-methylimidazolium diethylene-glycolmonomethylethersulfate and trihexyl(tetradecyl)phosphonium dodecyl-benzenesulfonate was studied in a wide range of temperatures and pressures. It is shown that phosphonium ionic liquids can dissolve even larger amounts of CO_2 (on a molar fraction basis) than the imidazolium based ILs with the same anion. The solubilities here reported are the largest observed for ionic liquids in absence of chemical interactions. Moreover, an interesting increase of the CO_2 solubility with temperature was observed for these ILs at very high pressures. A thermodynamic model based on the PC-SAFT EoS was used with success in the correlation of the measured data. The model provides a good description of the experimental data and the well-know pitfalls of the PC-SAFT EoS [45,46] were not evidenced in this work.

References

[1] J.D. Figueroa, T. Fout, S. Plasynski, H. McIlvried, R.D. Srivastava, Int. J. Greenh. Gas Con. 2 (2008) 9-20.

[2] X.Q. Xu, C.M. Wang, H.R. Li, Y. Wang, W.L. Sun, Z.Q. Shen, Polym. J. 48 (2007) 3921-3924.

[3] H.W. Pennline, D.R. Luebke, K.L. Jones, C.R. Myers, B.I. Morsi, Y.J. Heintz, J.B. Ilconich, Fuel Process. Technol. 89 (2008) 897-907.

[4] E.F. da Silva, H.F. Svendsen, Ind. Eng. Chem. Res. 45 (2006) 2497-2504.

[5] A. Bello, R.O. Idem, Ind. Eng. Chem. Res. 44 (2005) 945-969.

[6] F. Mani, M. Peruzzini, P. Stoppioni, Green Chem. 8 (2006) 995-1000.

[7] J.K. You, H. Park, S.H. Yang, W.H. Hong, W. Shin, J.K. Kang, K.B. Yi, J.N. Kim, J. Phys. Chem. B 112 (2008) 4323-4328.

[8] J.E. Bara, T.K. Carlisle, C.J. Gabriel, D. Camper, A. Finotello, D.L. Gin, R.D. Noble, Ind. Eng. Chem. Res. 48 (2009) 2739-2751.

[9] J.E. Bara, C.J. Gabriel, S. Lessmann, T.K. Carlisle, A. Finotello, D.L. Gin, R.D. Noble, Ind. Eng. Chem. Res. 46 (2007) 5380-5386.

[10] J.E. Bara, S. Lessmann, C.J. Gabriel, E.S. Hatakeyama, R.D. Noble, D.L. Gin, Ind. Eng. Chem. Res. 46 (2007) 5397-5404.

[11] A. Finotello, J.E. Bara, S. Narayan, D. Camper, R.D. Noble, J. Phys. Chem. B, 112 (2008) 2335-2339.

[12] T.K. Carlisle, J.E. Bara, C.J. Gabriel, R.D. Noble, D.L. Gin, Ind. Eng. Chem. Res. 47 (2008) 7005-7012.

[13] J.E. Bara, C.J. Gabriel, T.K. Carlisle, D.E. Camper, A. Finotello, D.L. Gin, R.D. Noble, Chem. Eng. J. 147 (2009) 43-50.

[14] B.A. Voss, J.E. Bara, D.L. Gin, R.D. Noble, Chem. Mater. 21 (2009) 3027-3029.

[15] M. Ramdin, T.W. de Loos, T.J.H Vlugt, Ind. Eng. Chem. Res. 51 (2012) 8149-8177.

[16] A.L. Revelli, F. Mutelet, J.-N. Jaubert, Ind. Eng. Chem. Res. 49 (2010) 3883-3892.

[17] F. Mutelet, A.L. Revelli, J.-N. Jaubert, L.M. Sprunger, W.E. Acree, G.A. Baker, J. Chem. Eng. Data 55 (2010) 234-242.

[18] F. Mutelet, J.-N. Jaubert, M. Rogalski, J. Harmand, M. Sindt, J.L. Mieloszynski, J. Phys. Chem. B 112 (2008) 3773-3785.

[19] A.L. Revelli, F. Mutelet, M. Turmine, R. Solimando, J.-N. Jaubert, J. Chem. Eng. Data 54 (2009) 90-101.

[20] A.L. Revelli, F. Mutelet, J.-N. Jaubert, J. Chromatogr. A 1216 (2009) 4775-4786.

[21] C. Cadena, J.L. Anthony, J.K. Shah, T.I. Morrow, J.F. Brennecke, E.J. Maginn, J. Am. Chem. Soc.126 (2004) 5300-5308.

[22] M.J. Muldoon, S. Aki, J.L. Anderson, J.K. Dixon, J.F. Brennecke, J. Phys. Chem. B 111 (2007) 9001-9009.

[23] S. Aki, B.R. Mellein, E.M. Saurer, J.F. Brennecke, J. Phys. Chem. B 108 (2004) 20355-20365.

[24] A. Shariati, C.J. Peters, J. Supercrit. Fluids 34 (2005) 171-176.

[25] M.B. Shiflett, A. Yokozeki, Ind. Eng. Chem. Res. 44 (2005) 4453-4464.

[26] P.J. Carvalho, V.H. Alvarez, I.M. Marrucho, M. Aznar, J.A.P. Coutinho, J. Supercrit Fluids 52 (2010) 258-265.

[27] S.P.M. Ventura, J. Pauly, J.L. Daridon, J.A.L. da Silva, I.M. Marrucho, A.M.A. Dias, J.A.P. Coutinho, J. Chem. Thermodyn. 40 (2008) 1187-1192.

[28] F. Llovell, E. Valente, O. Vilaseca, L.F. Vega, J. Phys. Chem. B 115 (2011) 4387-4398.

[29] E.K. Karakatsani, G.M. Kontogeorgis, I.G. Economou, Ind. Eng. Chem. Res. 45 (2006) 6063-6074.

[30] E.K. Karakatsani, I.G. Economou, J. Phys. Chem. B 110 (2006) 9252-9261.

[31] M.C. Kroon, E.K. Karakatsani, I.G. Economou, G.J. Witkamp, C.J. Peters, J. Phys. Chem. B 110 (2006) 9262-9269.

[32] E.K. Karakatsani, L.G. Economou, M.C. Kroon, C.J. Peters, G.J. Witkamp, J. Phys. Chem. C 111 (2007) 15487-15492.

[33] S. Ashrafmansouri, S. Raeissi, J. Supercrit Fluids 63 (2012) 81-91.

[34] K. Paduszynski, U. Domanska, J. Phys. Chem. B 115 (2011) 12537-12548.

[35] K. Paduszynski, U. Domanska, J. Phys. Chem. B 116 (2012) 5002-5018.

[36] L.F. Vega, O. Vilasecaa, F. Llovell, J.S. Andreua, Fluid Phase Equilib. 294 (2010) 15- 30.

[37] J. Gross, G. Sadowski, Ind. Eng. Chem. Res. 40 (2001) 1244-1260.

[38] S.H. Huang, M. Radosz, Ind. Eng. Chem. Res. 29 (1990) 2284-2294.

[39] S.H. Huang, M. Radosz, Ind. Eng. Chem. Res. 30 (1991) 1994-2005.

[40] Y.S. Chen, F. Mutelet, J.-N, Jaubert, J. Phys. Chem. B 116 (2012) 14375-14388.

[41] C. Neves, P.J. Carvalho, M.G. Freire, J.A.P. Coutinho, J. Chem. Thermodyn. 43 (2011) 948-957.

[42] H.N. Song, B.C. Lee, J.S. Lim, J. Chem. Eng. Data 55 (2010) 891-896.

[43] J.L. Anderson, J.K. Dixon, J.F. Brennecke, Acc. Chem. Res. 40 (2007) 1208-1216.

[44] J.C. Pamies, Ph.D.Thesis, Universitat Rovira i Virgili, Tarragona, Spain 2003.

[45] R. Privat, R. Gani, J.-N. Jaubert, Fluid Phase Equilib. 295 (2010) 76-92.

[46] R. Privat, E. Conte, J.-N. Jaubert, R. Gani, Fluid Phase Equilib. 318 (2012) 61-76.

[47] A.L. Revelli, F. Mutelet, J.-N. Jaubert, J. Phys. Chem. B 114 (2010) 12908-12913.

[48] E.-K. Shin, B.-C. Lee, J.S. Lim, J. Supercrit Fluids 45 (2008) 282-292.

[49] L.A. Blanchard, Z. Gu, J.F. Brennecke, J. Phys. Chem. B 105 (2001) 2437-2444.

Chapitre IV. La solubilité du CO_2, du N_2O et du CH_4 dans différents liquides ioniques à proximité de la pression atmosphérique

The purpose of this chapter is to determine the solubility of greenhouse gases in different ionic liquids (ILs). Experimental values for the solubility of carbon dioxide, methane and nitrous oxide in ionic liquids are measured at different temperatures and at pressures close to atmospheric. Carbon dioxide is the most soluble gas studied with mole fraction solubility of the order of 10^{-2} and nitrous oxide is one order of magnitude less soluble than carbon dioxide, whereas methane is the least soluble gas. From the variation of mole fraction solubility, expressed as Henry's law constant, with temperature, a smaller Henry's law constant corresponding to a higher solubility in ionic liquid was observed. Finally, we strove to develop a group contribution method in order to determine the Henry's law constant of CO_2 as a function of temperature. We can thus establish a general expression of Henry's law constant of CO_2 which may be used to predict the CO_2 solubility in ionic liquids when experimental data are unavailable.

IV.1 Introduction

The main greenhouse gases in the earth's atmosphere are water vapor, carbon dioxide (CO_2), methane (CH_4), and nitrous oxide (N_2O). These gases are considered the major source responsible for global warming which is the greatest environmental challenge in the world. Currently, a number of technologies have been developed in order to reduce and capture these gases.

Since CO_2 is one of the most important greenhouse gases, the research and development in the CO_2 emission reduction have long been the focus of many academic and industrial studies. Among a number of separation technologies that can be applied to CO_2 capture, one approach being considered for capturing CO_2 is the use of liquid absorbents designed to selectively solvate CO_2.[1] The alkanolamines such as monoethanolamine (MEA) are the most generally accepted and widely used liquid absorbents for removal of CO_2 from natural gas stream due to their reactivity and availability at low cost. Although these aqueous alkanolamine solutions are industrially effective on CO_2 removal, this family presents several drawbacks such as intensive energy consumption, cost increases, and corrosion problems.[2,3] In this regard, it is necessary to find new alternatives for absorption solvents.

Another class of solvent named ionic liquids (ILs)[4] seems to be a good candidate for capturing greenhouse gases due to their advantages in comparison to other solvents. Indeed, these liquids have good thermal stability and negligible vapor pressure. Physical properties of ILs may be modified and adjusted by using different cation-anion combinations.[5-7] For all these reasons, a wide range of studies on the solubility of CO_2 in ILs have been performed.[8-14] Recently, a few research groups have published measurements of solubility of other gases in ILs like CH_4 [15], H_2S[16] and SO_2.[17] However, until now, only one study presented N_2O solubility in ILs at relatively low pressure.[11] Nevertheless, N_2O is a potent greenhouse gas with a global warming potential approximately 310 times greater than CO_2 when normalized over 100 years.[18] Moreover, N_2O is the major source of NO_x in the stratosphere and

therefore an important natural regulator of stratospheric ozone.[19] N_2O is produced by both natural and anthropogenic sources. The main N_2O emission source is from agriculture activities and represents approximately 62 % of total emissions. The industrial sources of N_2O include nylon production, nitric acid production, fossil fuel fired power plants, and vehicular emissions. Technological options for emission reduction of N_2O may be categorized into three groups: reduced emissions from fluidized bed combustion, use of selective catalytic reduction, and fuel shift and reduction in fossil fuel consumption.[20,21] However, all these processes aimed at reducing N_2O emissions require large energy consumption and may increase the carbon dioxide emission.

Methane is another important greenhouse gas with a global warming potential. Atmospheric CH_4 is primarily emitted from biological sources and this accounts for more than 70% of the global total.[22] CH_4 is consumed primarily through oxidation by way of OH within the troposphere.[22,23] Moreover, CH_4 exerts strong influence over the chemistry of the troposphere and the stratosphere[24]. Therefore, CH_4 has a considerable impact on the earth's climate system, second anthropogenic greenhouse gas after CO_2.

In this chapter, we propose to check the ability of ionic liquids as greenhouse gases absorption solvents. The solubilities of CO_2, N_2O and CH_4 in 13 ionic liquids were measured in an equilibrium cell with a constant volume at pressures close to atmospheric. The solubility determination was based on the measurement of saturation pressure for a mixture of greenhouse gas and ionic liquid with a known composition at different temperatures. The influence of the nature of cation / anion in gas solubility was also investigated. A group contribution method was carried out in order to determinate the Henry's law constant of CO_2 in different ionic liquids and a general expression of Henry's law constant of CO_2 was obtained.

IV.2 Experimental section

IV.2.1 Materials

Carbon dioxide, methane and nitrous oxide were obtained from Messer with a purity of 0.99999, 0.99995 and 0.99997 respectively in mass fraction. The ILs studied in this work were listed in table IV-1 with the purity and suppliers.

Table IV-1: Ionic liquids used in this work with suppliers and purities

ILs	Suppliers	Purity%
[bmim][BF_4]	Solvionic	≥99
[bmpy][BF_4]	Sigma Aldrich	≥97
[1-ethanol mim][BF_4]	Solvionic	≥98
[1-ethanol mim][PF_6]	Solvionic	≥98
[1-ethanol mim][Tf_2N]	Solvionic	99.5
[$CH_3O(CH_2)_2$mim][Tf_2N]	Solvionic	≥98
[$N_{(6)111}$][Tf_2N]	Solvionic	99.5
[$P_{(14)666}$][Tf_2N]	Solvionic	99.5
[emim][Tf_2N]	Sigma Aldrich	≥97
[bmim][beti]	Solvionic	≥98
[bmim][CF_3SO_3]	Solvionic	99.5
[dmim][$MePO_3$]	Solvionic	≥98
[bmim][octysulfate]	Sigma Aldrich	≥95

IV.2.2 Apparatus and procedure

The experimental apparatus based on an isochoric saturation technique is applied to measure the gas solubility in different ILs at pressures close to atmospheric. It has been presented in other publications.[25,26] In this technique, a known quantity of gaseous solute is put in contact with a determined quantity of IL at a constant temperature with an accurately known volume. When thermodynamic equilibrium is attained, the pressure above the liquid solution is constant and is directly related to the solubility of the gas in the IL.

The experimental apparatus is schematically represented in figure IV-1. The equilibrium section of the apparatus is constituted with an equilibrium cell EC together with the precision manometer PM and glass bulbs limited by valves V4 and V5. The simple designed equilibrium cell is able to appropriately study relatively viscous liquid solvents like ILs presented in this work. Moreover, it allows handling volumes of liquid solvent varying from 5 ml to 15 ml and an appropriate contact between gas and liquid can be achieved by means of good agitation using a magnetic bar. The gas solubility measurement begins with the introduction of a known quantity of gas solute in the calibrated glass bulbs limited by valves V4 and V5. The exact amount of gas solute is obtained by measuring its pressure with the precision manometer PM (Druck DPI 282 series 0007, precision of 0.0001 bar) at constant temperature. The volume of the various sections of the apparatus given below: the volume of the equilibrium cell delimited by V3, V4, V5 and PM has a total volume of:

$$V_{EC} = 61.29\ cm^3 \tag{IV-1}$$

The two bulbs were calibrated at 303 K by argon. After considering corrections due to thermal expansion, the volume of each bulb is

$$\begin{aligned} V_{bulb,V_4} &= 58.15\ cm^3 \pm 0.02\ cm^3 \\ V_{bulb,V_5} &= 31.95\ cm^3 \pm 0.02\ cm^3 \end{aligned} \tag{IV-2}$$

The vacuum gauge (ACS 2000, ALCATEL model) which allows controlling the pressure of the upper part of the apparatus, and which is delimited by V1, V2, and V3 has a volume:

$$V_{VG} = 17.04\ cm^3 \tag{IV-3}$$

The solubility of the gaseous solute in the ionic liquid can be expressed in mole fraction by

$$x_2 = n_2^{liq} \Big/ \left(n_1^{liq} + n_2^{liq} \right) \tag{IV-4}$$

where n_2^{liq} is the quantity of gaseous solute dissolved in the ionic liquid and $n_1^{liq} = n_1^{total}$ is the total quantity of ionic liquid. The amount of solute in liquid solution is determined by the difference between two PVT measurements. The gas solute is initially introduced into the equilibrium cell and after thermodynamic equilibrium is attained:

$$n_2^{liq} = p_{ini} V_{GB} \Big/ \left[Z_2 \left(p_{ini}, T_{ini} \right) RT_{ini} \right] - p_{eq} \left(V_{total} - V_{liq} \right) \Big/ \left[Z_2 \left(p_{eq}, T_{eq} \right) RT_{eq} \right] \tag{IV-5}$$

where V_{GB} is the volume of glass bulb initially filled with gas solute at initial temperature T_{ini} and initial pressure p_{ini} equaled to V_{bulb,V_4}. V_{total} is the total volume of the equilibrium section. Z_2 is the compressibility factor of pure gas. V_{liq} represents the volume occupied by liquid solution at equilibrium temperature T_{eq} and equilibrium pressure p_{eq}, it can be calculated in the following manner:

$$V_{liq} = \frac{m_{ini}}{\rho} (IL) + V_{mb} \tag{IV-6}$$

where V_{mb} is the volume of magnetic bar equaled to 0.5 cm^3 in this work. m_{ini} represents the initial amount of an IL. ρ is the density of an IL and was measured in our laboratory using an Anton Paar densitometer (DMA 512 P) with a precision of 0.01%.

The procedure of gas solubility measurements in ILs is now presented. The first step is to make the entire apparatus vacuum using a vane pump, by opening valves

except the gas supply valve. Then, a known quantity of gas is introduced into one of two calibrated glass bulbs (valve V4 and V5). In our experiments, only the bigger bulb connected to the valve V4 will be used to introduce the solute gas. Thirdly, an ionic liquid is put into the equilibrium cell using a pasteur pipette through the connection C2. The mass of ionic liquid, varied from 4 to 6 g, is determined by a balance (Sartorius Analytic model A200S-F1) with an accuracy of 0.0001g. Before using ILs, they are dried in vacuum at a temperature around 80 °C and a pressure about 10 Pa for at least 8 hours. Finally, the entire equilibrium cell is maintained in an oven, with a precision of ±0.1 K, at a fixed temperature. The determination of solubility in ionic liquid at different temperatures is simply effected by changing the temperature of the oven and wait for a new thermal equilibrium. Each pressure and temperature of the equilibrium state is then recorded. Thus, only a single operation is required for measuring the solubility of gases in a wide range of temperatures.

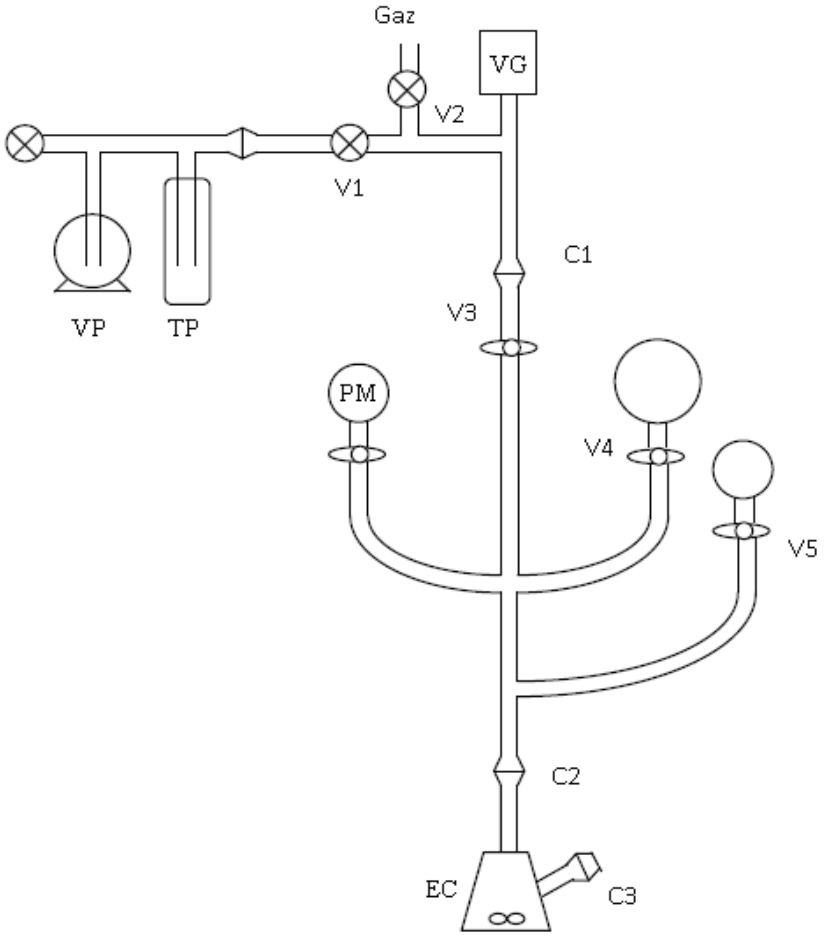

Figure IV-1: Schema of the solubility apparatus: VP, vacuum pump; TP, cold trap; VG, vacuum gauge; PM, precision manometer; EC, equilibrium cell; V3, V4, V5, constant volume glass valves; C1, C2, vacuum O'ring connections.

IV.3 Results and discussion

Values of experimental solubilities in the temperature range 293.15 K – 313.15 K of CO_2, CH_4 and N_2O in 13 ILs are reported in table IV-2. The solubility results are expressed in terms of mole fraction and Henry's law constant for each equilibrium pressure.

Table IV-2: Experimental values of gas solubility in different ionic liquids, expressed as Henry's law constant- K_H and as mole fraction-x, P is the experimental equilibrium pressure.

CO_2+ ILs	T[K]	P [Bar]	K_H [Bar]	x (10^4)	N_2O+ ILs	T[K]	P [Bar]	K_H [Bar]	x (10^4)
$N_{6,111}$ Tf_2N	296.45	0.4800	30.19	159.00	$N_{6,111}$ Tf_2N	302.15	0.5057	33.85	149.39
	303.30	0.4933	33.08	149.13		306.35	0.5152	36.69	140.42
	308.15	0.5030	35.63	141.17		307.85	0.5190	38.22	135.78
	313.65	0.5142	39.07	131.59		312.15	0.5290	41.94	126.14
$P_{14,666}$ Tf_2N	298.40	0.4846	31.39	154.38		314.15	0.5332	43.26	123.27
	305.40	0.4981	36.75	135.56	$P_{14,666}$ Tf_2N	293.95	0.4836	20.20	239.41
	309.25	0.5054	39.82	126.93		298.05	0.4925	22.36	220.22
	315.50	0.5170	44.87	115.23		302.35	0.5021	25.33	198.21
bmim beti	298.25	0.4624	32.26	143.34		307.35	0.5126	28.54	179.60
	303.15	0.4724	34.71	136.09		314.25	0.5268	33.62	156.71
	305.15	0.4781	37.28	128.23	bmim beti	298.95	0.4797	22.02	217.89
	313.65	0.4950	41.96	117.97		299.65	0.4809	22.10	217.63
emim Tf_2N	298.65	0.4764	31.43	151.56		302.85	0.4874	22.91	212.73
	305.15	0.4895	34.56	141.63		309.95	0.5023	25.03	200.67
	309.65	0.4992	37.62	132.69		314.25	0.5096	25.52	199.65
	315.00	0.5098	40.55	125.72	emim Tf_2N	298.95	0.4816	40.77	118.13
bmim TfO	294.85	0.4835	41.92	115.34		302.55	0.4896	44.82	109.23
	301.55	0.4990	48.01	103.94		308.05	0.5019	52.33	95.90
	307.65	0.5133	54.89	93.52		313.15	0.5138	62.81	81.80
	312.05	0.5223	58.39	89.46	bmim TfO	299.15	0.3825	59.15	64.67
bmpy BF_4	296.90	0.5104	43.40	117.61		303.15	0.3889	63.84	60.92
	303.30	0.5238	48.50	108.00		308.75	0.3977	70.63	56.31
	308.35	0.5336	51.44	103.74		313.25	0.4058	81.55	49.76
	313.40	0.5437	55.23	98.44	bmpy BF_4	298.45	0.4935	79.37	62.18

bmim BF_4	299.35	0.4751	57.81	82.18
	303.65	0.4850	63.21	76.72
	308.85	0.4965	69.77	71.17
	313.85	0.5072	76.13	66.62
dmim $MePO_3$	299.55	0.484	64.37	75.19
	303.03	0.492	69.56	70.73
	308.91	0.5048	77.99	64.73
	314.21	0.5165	87.23	59.21
1-ethanolmim BF_4	298.15	0.4373	107.78	40.57
	302.65	0.4440	111.28	39.90
	308.95	0.4535	118.90	38.14
	312.35	0.4585	120.30	38.11
CH_4+ ILs	**T[K]**	**P [Bar]**	**K_H [Bar]**	**x (10^4)**
$N_{6,111}$ Tf_2N	298.95	0.5107	306.21	16.68
	304.45	0.5208	365.59	14.25
	308.05	0.5277	445.04	11.86
	313.15	0.5378	750.41	7.17
emim Tf_2N	299.65	0.5021	258.95	19.39
	300.65	0.5048	347.27	14.54
	304.35	0.5118	469.66	10.90
	310.15	0.5229	1041.37	5.02
	312.35	0.5268	1259.16	4.18
bmim CF_3SO_3	294.15	0.5132	458.40	11.20
	297.85	0.5198	478.50	10.86
	303.05	0.5296	591.89	8.95
	307.75	0.5384	736.46	7.31
	312.75	0.5482	1273.32	4.31
bmim BF_4	297.95	0.5334	769.30	6.93
	304.15	0.5458	1214.25	4.49
	307.45	0.5521	1407.55	3.92
	312.95	0.5630	2781.63	2.02
dmim $MePO_3$	298.15	0.5102	581.69	8.77
	303.25	0.5199	724.34	7.18
	307.65	0.5287	1035.37	5.11
	312.95	0.5394	2063.12	2.61
1-ethanolmim BF_4	298.65	0.5098	547.27	9.32
	302.95	0.5191	906.18	5.73
	308.05	0.5288	1275.19	4.15
	312.65	0.5377	2232.05	2.41
1-ethanolmim PF_6	298.45	0.5079	435.33	11.67
	300.85	0.5126	499.50	10.26
	303.95	0.5184	568.68	9.12
	308.15	0.5261	650.42	8.09
	312.95	0.5350	811.91	6.59
	304.05	0.5044	96.78	52.12
	308.15	0.5130	113.86	45.06
	313.05	0.5227	134.27	38.93
bmim BF_4	303.15	0.5306	77.88	68.13
	308.15	0.5420	86.38	62.75
	313.15	0.5535	96.73	57.22
1-ethanolmim BF_4	295.35	0.5140	127.93	40.18
	298.05	0.5196	134.86	38.53
	304.05	0.5328	158.67	33.58
	308.35	0.5427	184.28	29.45
	313.95	0.5553	225.37	24.64
bmim octysulfate	298.15	0.4985	53.36	93.43
	302.75	0.5077	57.56	88.20
	308.15	0.5192	64.91	79.99
	313.75	0.5314	75.22	70.65
$CH_3O(CH_2)_2$mim Tf_2N	302.25	0.4827	35.24	136.99
	306.75	0.4927	38.71	127.27
	308.45	0.4963	39.87	124.47
	313.45	0.5073	44.32	114.47
1-ethanolmim Tf_2N	296.45	0.4834	39.34	122.87
	301.65	0.4942	43.13	114.58
	301.85	0.4948	43.56	113.60
	308.45	0.5092	50.31	101.20
	315.25	0.5241	59.18	88.56
1-ethanolmim PF_6	294.65	0.4943	69.45	71.18
	297.35	0.5007	75.10	66.67
	302.65	0.5122	84.52	60.60
	307.65	0.5232	95.41	54.84
	312.45	0.5333	105.75	50.43
CH_4+ ILs	**T[K]**	**P [Bar]**	**K_H [Bar]**	**x (10^4)**
bmim octysulfate	300.85	0.5093	423.12	12.04
	303.55	0.5143	486.76	10.57
	308.15	0.5230	682.97	7.66
	313.25	0.5329	1551.69	3.43
1-ethanolmim Tf_2N	300.05	0.5039	192.79	26.14
	301.25	0.5062	204.22	24.79
	303.95	0.5113	230.80	22.15
	308.15	0.5189	259.40	20.00
	313.15	0.5286	373.62	14.15

IV.3.1 Results obtained with carbon dioxide

We now present and discuss solubility results of each gaseous solute in ILs. Figure IV-2 outlines values of the Henry's law constant of CO_2 in various ILs at different temperatures. We observe that the Henry's law constant of CO_2 increases linearly with temperature. This confirms that the solubility of CO_2 in ILs is larger at low temperature which corresponds to a smaller Henry's law constant than at high temperature.

The highest solubility of CO_2 is obtained in trimethyl(hexyl)ammonium bis(trifluoromethylsulfonyl)imide, where, it is three times greater than in 1-ethanol-3-methylimidazolium tetrafluoroborate which presents the lowest solubility. On the other hand, ILs with anions such as $[Tf_2N]^-$ and $[Beti]^-$ have a stronger absorption rate for CO_2. These two anions exhibit the same property in the field of CO_2 absorption due to their significant number of fluoroalkyl groups (or fluorine atom). It had already been indicated in previous publications[27,28] that the solubility of CO_2 increases with the number of fluoroalkyl groups contained in anion. This may be explained by the fact that there is a favorable interaction between the negative charge of fluorine atom and the positive charge of carbon in CO_2. The effect of anion and cation on the solubility of CO_2 was then studied. Solubilities in ILs based on anion $[Tf_2N]^-$ and cation $[bmim]^+$ were compared respectively. Results show that the change of cation has little influence on the solubility of CO_2 as compared to the change of anion.

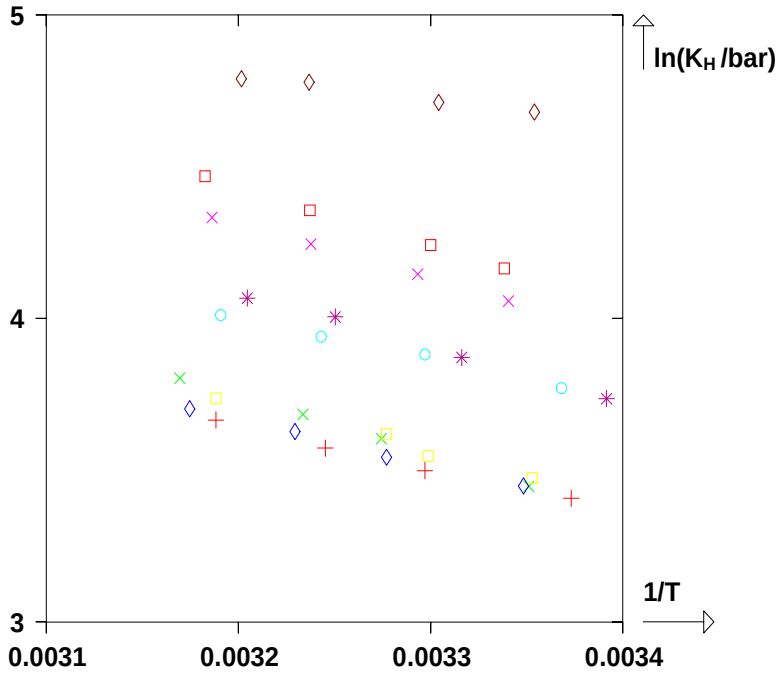

Figure IV-2: Henry's law constant of CO_2 in $[N_{6,111}][Tf_2N]$(+), $[P_{14,666}][Tf_2N]$(×), [emim][Tf_2N](◊), [bmim][beti](□), [bmim][TfO](*), [bmim][BF_4](×), [bmpy][BF_4](○), [dmim][$MePO_3$](□) and [1-ethanolmim][BF_4](◊).

IV.3.2 Results obtained with nitrous oxide

A relationship between $\ln K_H$ and $1/T$ of each ionic liquid was depicted in Figure IV-3. We observe that the Henry's law constant of N_2O in an ionic liquid varies linearly with temperature. The most effective solubility of N_2O is obtained in 1-butyl-3-methylimidazolium bis(perfluoromethylsulfonyl)imide and Henry's law constant is from 6 to 9 times , depending on temperature, lower than in 1-ethanol-3-methylimidazolium tetrafluoroborate where N_2O has the lowest solubility. An IL with the anion: $[Tf_2N]^-$ or $[Beti]^-$ has a greater absorption of N_2O as compared to other anions. We can thus confirm that the solubility of N_2O increases with the number of fluoroalkyl groups contained by the anion.

Then, we studied the effect of anion and cation on the solubility of N_2O in different ILs. Results of $[Tf_2N]^-$ with different cations and $[bmim]^+$ with different anions were

compared respectively. As the same case with CO_2, the change of cation has a minor effect on the solubility of N_2O and ILs with fluoroalkyl groups present a higher solubility. Furthermore, the solubility of N_2O is improved in an IL whose cation contains an oxygen atom as compared to cations contained alkyl groups only. This may be explained by the fact that ILs containing the cation such as [1-ethanolmim] or [$CH_3O(CH_2)_2$mim] present a smaller volumetric mass, thus providing a greater compactness and free volume. Therefore, the solubility of N_2O increases due to their favorable interactions between ILs and N_2O.

Finally, previous findings for N_2O can be explained by the same reason for CO_2. There is a favorable interaction between the negative charge of fluorine atoms in anion and the positive charge in N_2O. However, this interaction is less significant for N_2O, because the positive charge is distributed between two nitrogen atoms. Thus, CO_2 has a greater solubility than N_2O in a majority of ILs.

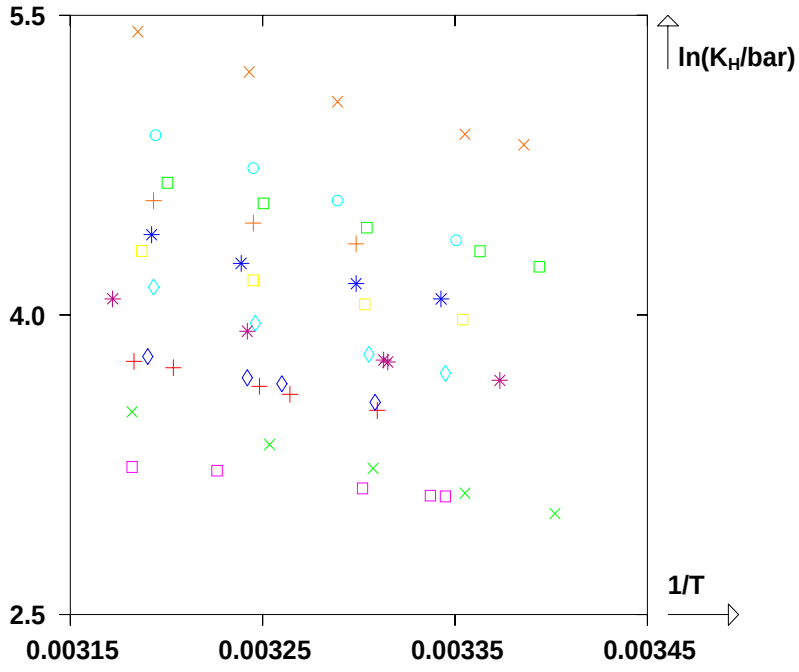

Figure IV-3: Henry's law constant of N_2O in [$P_{14,666}$][Tf_2N](×), [$N_{6,111}$][Tf_2N](+), [1-methoxyethanemim][Tf_2N](◊), [1-ethanolmim][Tf_2N](*), [emim][Tf_2N](◊), [bmim][octysulfate](□), [bmim][TfO](*), [bmim][BF_4](+), [bmim][beti](□), [1-ethanolmim][PF_6](□), [bmpy][BF_4](○) and [1-ethanolmim][BF_4](×).

IV.3.3 Results obtained with methane

The same study for the solubility of methane in ILs was performed in this chapter. The relationship of $\ln(K_H) = f(1/T)$ for each IL was reported in Figure IV-4. We observe that the Henry's law constant of CH_4 in an IL was depicted in a linear trend varied with temperature, but this trend is less marked than in the case of CO_2 and N_2O. The solubility of CH_4 in 1-ethanol-3-methylimidazolium bis(terfluoromethylsulfonyl)imide is the highest and Henry's law constant is from 3 to 9 times lower than in 1-butyl-3-methylimidazolium tetrafluoroborate where CH_4 presents the lowest solubility. On the other hand, an IL with the anion $[Tf_2N]^-$ presents a greater solubility of CH_4, which confirms that the solubility of CH_4 increases with the number of fluoroalkyl groups in the anion.

Furthermore, the effect of cation and anion on the CH_4 solubility in ILs was then studied. The solubility of CH_4 in $[Tf_2N]^-$ -based ILs and $[bmim]^+$ -based ILs were reported respectively. Results indicated the change of cation has much influence on the solubility of CH_4 as compared to the change of anion, contrary to what was observed for CO_2 and N_2O. The figure IV-4, illustrating the influence of the anion, shows a similar solubility of CH_4 in [bmim][octysulfate] and [bmim][CF_3SO_3], although the [bmim][CF_3SO_3] contains three fluorine atoms in anion. For the influence of cation, the best solubility is obtained with the cation containing the alcohol group. Because the cation substituted by –OH group which presents a smaller volumetric mass improves the solubility of CH_4 in ILs.

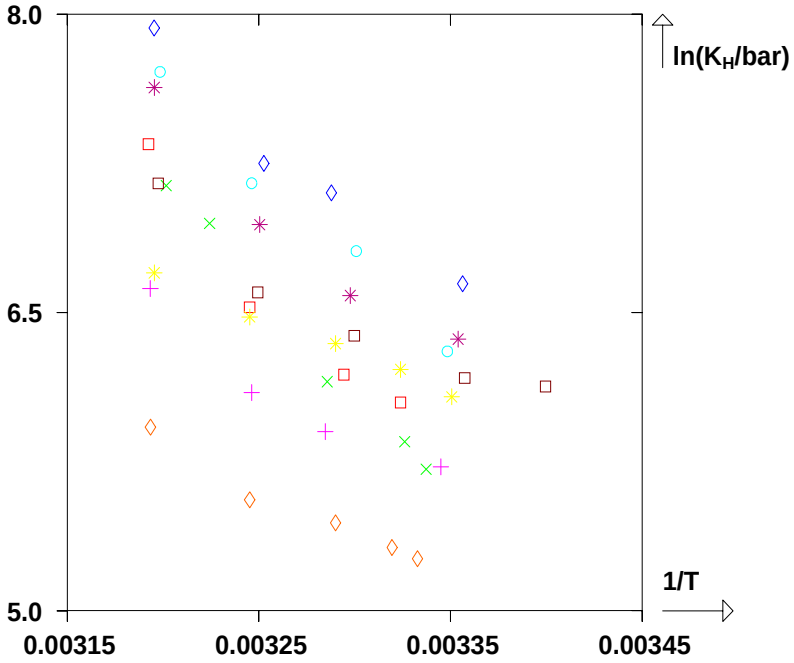

Figure IV-4: Henry's law constant of CH_4 in [1-ethanolmim][Tf_2N](◊), [$N_{6,111}$][Tf_2N](+), [emim][Tf_2N](×), [bmim][octysulfate](□), [bmim][CF_3SO_3](□), [bmim][BF_4](◊), [1-ethanolmim][PF_6] (*), [1-ethanolmim][BF_4] (○) and [dmim][$MePO_3$] (*).

IV.3.4 Results obtained with three gases

Finally, it is interesting to compare the solubility of CO_2, N_2O and CH_4 in the same ionic liquids. Figure IV-5 depicts the solubility of 3 gaseous solutes in four different ILs which are [$N_{6,111}$][Tf_2N], [emim][Tf_2N], [bmim][BF_4] and [1-ethanolmim][BF_4]. CO_2 is the most soluble gas in these ILs. N_2O has a solubility similar to CO_2 in [$N_{6,111}$][Tf_2N] and slightly lower in [emim][Tf_2N], [bmim][BF_4] and [1-ethanolmim][BF_4]. However, CH_4 is hardly soluble in these ILs. Furthermore, we observed that the Henry law's constant of CH_4 is 100 to 200 times higher than that of CO_2 and N_2O. Therefore, other solubilisation techniques must be considered and developed to achieve CH_4 capture.

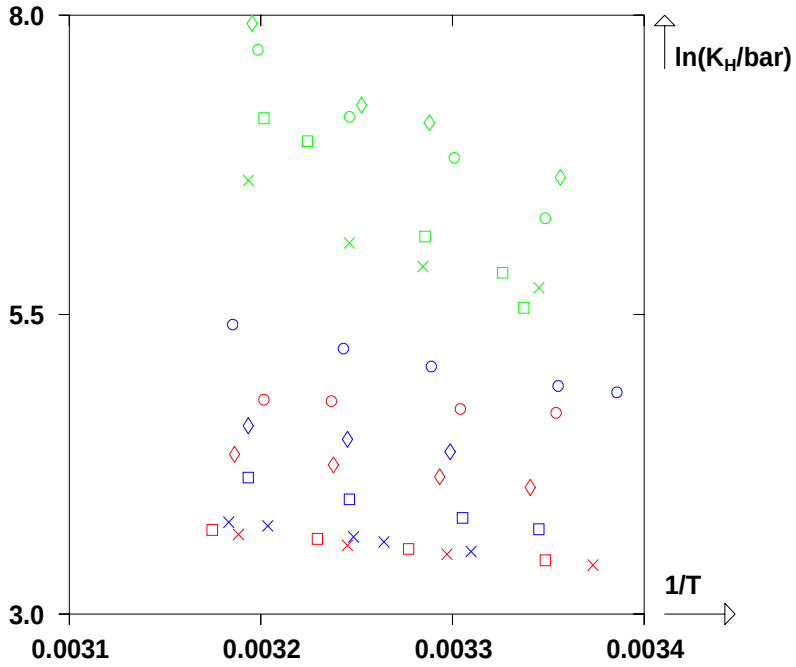

Figure V-5: Henry's law constants for CO_2, N_2O and CH_4 in four different ILs, CO_2: $[N_{6,111}][Tf_2N]$(×), [emim][Tf_2N](□), [bmim][BF_4](◊) and [1-ethanolmim][BF_4](○); N_2O: $[N_{6,111}][Tf_2N]$(×), [emim][Tf_2N](□), [bmim][BF_4](◊) and [1-ethanolmim][BF_4](○) and CH_4: $[N_{6,111}][Tf_2N]$(×), [emim][Tf_2N](□), [bmim][BF_4](◊) and [1-ethanolmim][BF_4](○).

IV.3.5 Group contribution method to determine the Henry's law constant of carbon dioxide

The Henry's law constant of component 2 dissolved in component 1 ($K_{H_{2,1}}$) which depends on the equilibrium pressure and temperature is defined by the relation:

$$K_{H_{2,1}} = \lim_{x_2 \to \phi} f_2(T,P,x_2)/x_2 = f_{2,\,pure\ liquid}(T,P) \times \gamma_2^{\infty} \qquad \text{(IV-7)}$$

Under moderate pressure $f_{2,\,pure\ liquid}(T,P) = P_2^{sat}(T)$ and $\gamma_2^{\infty} = \dfrac{P_{eq} \cdot y_2}{P_2^{sat} \cdot x_2} = \dfrac{P_{eq}}{P_2^{sat} \cdot x_2}$

with $y_2 = 1$. So that $K_{H_{2,1}}$ is equal to P_{eq}/x_2. f_2 is the fugacity of component 2, γ_2^{∞} is

the activity coefficient at infinite dilution. P_{eq} is equilibrium pressure, P^{sat} is saturation pressure and x_2, y_2 present the mole fraction of component 2.

We now propose to apply the group contribution concept to estimate the Henry's law constant of CO_2 in various ILs. To get representative values of the solubility, the Henry's law constant can be correlated as a function of temperature by an equation as follows:

$$\ln\left\{K_H(T)/(10^5 Pa)\right\} = \sum_{i=0}^{n} A_i (T/K)^{-i} \quad \text{(IV-8)}$$

In our study, we took n=1. Therefore, the Henry's law constant was expressed in the following manner:

$$\ln\left\{K_H(T)/(10^5 Pa)\right\} = A_0 + \frac{A_1}{T} \quad \text{(IV-9)}$$

$$A_0 = \sum_i n_i G_i \quad \text{(IV-10)}$$

$$A_1 = \sum_i n_i G_i' \quad \text{(IV-11)}$$

where n_i is the number of group i in an IL, G_i is the coefficient associated with the group i to estimate A_0 and G_i' is used to estimate A_1.

In our approach, each ionic liquid is characterized by different basic groups: (i) anion or cation is considered as one basic group, (ii) alkyl groups in cation and/or anion are divided into $-CH_3$ and $-CH_2-$. For example, the molecule of 1-butyl-3 methylimidazolium tetrafluoroborate [bmim][BF_4] consists of 3 ($-CH_2-$) groups, 2 ($-CH_3$) groups , 1 imidazolium 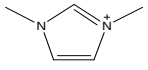 group and 1 tetrafluoroborate $\left[BF_4\right]^-$ group. With sufficient experimental data of Henry's law constant of CO_2 in various ILs and

reasonable basic groups constituting these ILs, we can thus obtain optimal coefficients A_0 and A_1 to express the Henry's law constant of CO_2. This method allows us to predict the solubility of CO_2 in ILs the physicochemical properties of which are little known.

27 ILs with 206 experimental Henry's law constants were gathered in this work in order to define 19 basic groups. Experimental Henry's law constant from literature and values of parameters G_i and $G_i^{'}$ for each group were reported in table IV-3 and table IV-4 respectively. The Henry's law constant of CO_2 for different ILs were then calculated using coefficients: G_i and $G_i^{'}$ issued from equation 9, 10 and 11, expressed as $\ln K_{H,GC}$. The difference between $\ln K_{H,GC}$ and $\ln K_{H,\exp}$ was presented in figure IV-6 which obviously visualizes the experimental values deviating from those obtained by the group contribution method. This Figure clearly highlights that the proposed equation is very accurate to determinate the Henry's law constant of CO_2 with AAD% ≤4%.

Table IV-3: Experimental Henry's law constant of CO_2 in different ionic liquids obtained from literature.

ILs	Temperature (K)	ln(K_H)	N° points	References
[bmim][BF_4]	303.38-344.27	4 .121-4.815	11	29
	303.72-344.49	4.094-4.474	4	25
	283.15-323.15	3.735-4.431	6	30
[hmim][BF_4]	299.35-313.85	4.028-4.296	4	31
	303.15-353.15	2.380-2.986	6	32
[bmpy][BF_4]	289.9-313.4	3.697-4.008	5	31
[bmim][PF_6]	283.15-343.04	3.633-4.697	14	33
	298.15	3.978	1	34
	303	4.078	1	35
	303.15	4.250	1	36
[C_3-mim][PF_6]	298.15	3.951	1	28
[emim][Et_2PO_4]	313.15-333.15	1.944-2.268	3	27
[mmim][$MeSO_4$]	298.15-343.15	4.868-5.561	4	37
[dmim][$MePO_3$]	299.55-314.21	4.171-4.472	4	31
[bmim][CF_3SO_3]	284.85-312.05	3.528-4.064	6	31
[emim][CF_3SO_3]	303.15	4.230	1	36
[desmim][CF_3SO_3]	303.15	4.038	1	36

[bmim][Beti]	292.65-303.15	3.326-3.547	5	31
	303.15	3.837	1	36
	298.15-343.15	3.664-4.357	4	37
	303	3.664	1	33
[emim][Tf_2N]	283.43-343.07	3.214-4.290	5	14
	303.63-344.23	3.640-4.289	14	38
	291.65-315	3.473-3.703	9	31
[C_1C_4-pyrr][Tf_2N]	303.78-344.15	3.601-4.217	11	38
[N_{1132}-OH][Tf_2N]	304.16-344.84	3.732-4.403	7	38
	283.15-323.15	3.332-3.932	6	30
[bmim][Tf_2N]	283.36-343.79	3.174-4.205	14	14
	298.15	3.611	1	28
[pmmim][Tf_2N]	283.15-323.15	3.388-3.970	6	30
[bmpy][Tf_2N]	283.15-323.15	3.258-3.829	6	30
[perfluoro-hmim][Tf_2N]	283.15-323.15	3.239-3.738	6	30
	298.15-343.15	3.526-4.159	4	37
[hmim][Tf_2N]	288.48-343.2	3.203-4.063	11	39
	298.15	3.555	1	28
[$N_{(4)111}$][Tf_2N]	282.94-343.07	3.169-4.249	10	14
[$P_{(14)666}$][Tf_2N]	303.15	3.497	1	40
	291.85-315.5	3.321-3.804	5	31
[$N_{(6)111}$][Tf_2N]	296.45-313.65	3.407-3.665	1	31
[$N_{(1)888}$][Tf_2N]	303.15	3.367	1	36
[C_3-mim][Tf_2N]	298.15	3.611	1	36
[C_8F_{13}-mim][Tf_2N]	298.15	1.504	1	37
[C_8-mim][Tf_2N]	298.15	3.401	1	37

Table IV-4: Coefficients G_i and $G_i^{'}$ obtained by group contribution method for each group of ILs.

Group	G_i	G'_i
CH_2	1.695	-488.423
CH_3	-0.145	35.661
Imidazolium	1.925	-512.809
Pyrilium	0.671	-168.551
Pyrridilium	1.491	-368.296
Ammonium	-0.697	232.171
Phosphonium	0.917	-57.890
Tetrafluoroborate	5.115	-403.870
Texafluorophosphate	4.648	-274.631
Phosphonate	0.900	91.800
Phosphate	4.107	98.388
Sulfonate	3.586	22.398
Sulfate	3.945	-136.707
Bis(perfluoromethylsulfonyl)imide	3.619	-110.162
Bis((trifluoromethyl)sulfonyl)imide	3.807	-160.684
Methoxy	-2.412	157.887
Hydroxy	1.041	-229.363
Trifluoromethane	-0.589	50.367
Bisfluoromethane	0.079	13.715

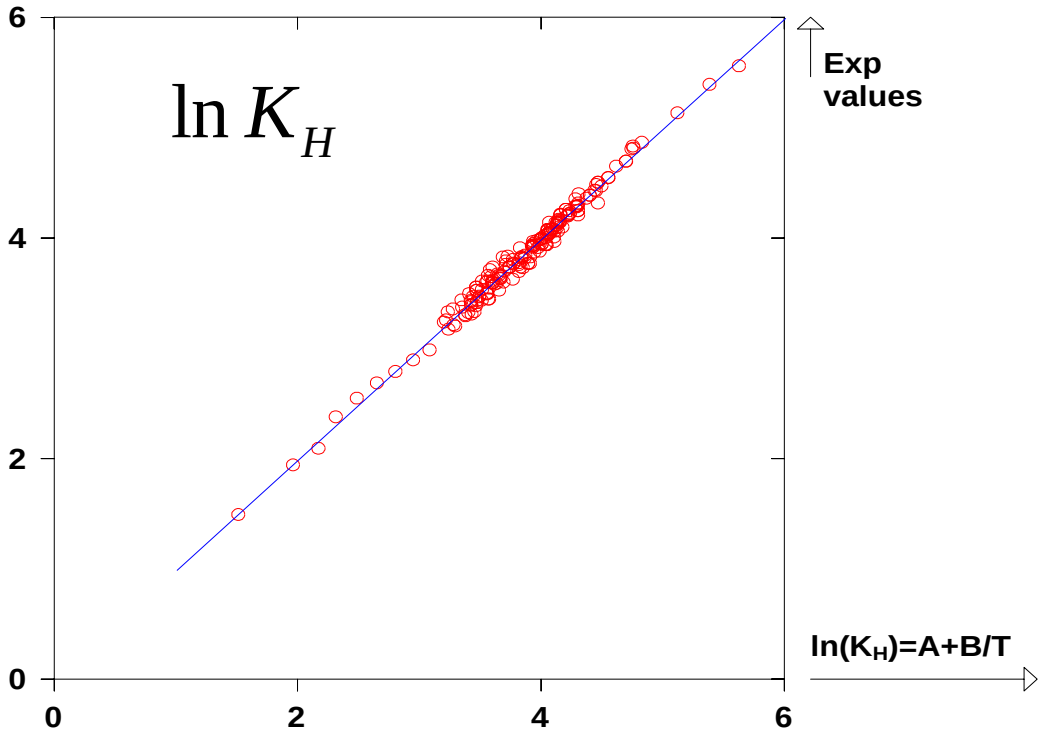

Figure IV-6: Comparison the values of $\ln K_H$ obtained by group contribution method and experimental values.

IV.4 Conclusions

In this chapter, we have determined the solubility of three gaseous solutes in different ionic liquids using low-pressure experimental apparatus based on isochoric and isothermal solubilization measurement. Carbon dioxide is the most soluble in ILs, whereas methane is the least soluble gas. We observed that the solubility of gas solute increases with the number of fluoroalkyl groups contained by anion or cation. Furthermore, the change of cation has little effect on the gas solubility as compared to the change of anion except in the case of methane. Finally, a group contribution method allowed us to obtain a general expression of the Henry's law constant of CO_2 in ILs. This approach is able to describe accurately the Henry's law constant of CO_2 but also predict the CO_2 solubility in ILs whose physicochemical properties are even unknown.

References

(1) Pennline, H. W.; Luebke, D. R.; Jones, K. L.; Myers, C. R.; Morsi, B. I.; Heintz, Y. J.; Ilconich, J. B. *Fuel Process. Technol.* **2008**, *89*, 897-907.

(2) Da Silva, E. F.; Svendsen, H. F. *Ind. Eng. Chem. Res.* **2006**, *45*, 2497-2504.

(3) Bello, A.; Idem, R. O. *Ind. Eng. Chem. Res.* **2005**, *44*, 945-969.

(4) Aionicesei, E.; Škerget, M.; Knez, Ž. *J. Chem. Eng. Data* **2008**, *53*, 185-188.

(5) Revelli, A. L.; Mutelet, F.; Jaubert, J. N. *Ind. Eng. Chem. Res.* **2010**, *49*, 3883-3892.

(6) Mutelet, F.; Revelli, A. L.; Jaubert, J. N.; Sprunger, L. M.; Acree, W. E.; Baker, G. A. *J. Chem. Eng. Data* **2010**, *55*, 234-242.

(7) Mutelet, F.; Jaubert, J. N.; Rogalski, M.; Harmand, J.; Sindt, M.; Mieloszynski, J. L. *J. Phys. Chem. B* **2008**, *112*, 3773-3785.

(8) Wappel, D.; Gronald, G.; Kalb, R.; Draxler, J. *Int. J. Greenhouse Gas Control* **2010**, *4*, 486-494.

(9) Cadena, C.; Anthony, J. L.; Shah, J. K.; Morrow, T. I.; Brennecke, J. F.; Maginn, E. J. *J. Am. Chem. Soc.* **2004**, *126*, 5300-5308.

(10) Aki, S.; Mellein, B. R.; Saurer, E. M.; Brennecke, J. F. *J. Phys. Chem. B* **2004**, *108*, 20355-20365.

(11) Anthony, J. L.; Anderson, J. L.; Maginn, E. J.; Brennecke, J. F. *J. Phys. Chem. B* **2005**, *109*, 6366-6374.

(12) Shariati, A.; Peters, C. J. *J. Supercrit. Fluids* **2005**, *34*, 171-176.

(13) Shiflett, M. B.; Yokozeki, A. *Ind. Eng. Chem. Res.* **2005**, *44*, 4453-4464.

(14) Jacquemin, J.; Husson, P.; Majer, V.; Gomes, M. F. C. *J. Sol. Chem.* **2007**, *36*, 967-979.

(15) Anderson, J. L.; Dixon, J. K.; Brennecke, J. F. *Acc. Chem. Res* **2007**, *40*, 1208-1216.

(16) Rahmati-Rostami, M.; Ghotbi, C.; Hosseini-Jenab, M.; Ahmadi, A. N.; Jalili, A. H. *J. Chem. Thermodyn.* **2009**, *41*, 1052-1055.

(17) Anderson, J. L.; Dixon, J. K.; Maginn, E. J.; Brennecke, J. F. *J. Phys. Chem. B* **2006**, *110*, 15059-15062.

(18) Ramanathan, V. *Ambio* **1998**, *27*, 187-197.

(19) Pérez-Ramírez, J.; Kapteijn, F.; Schöffel, K.; Moulijn, J.A. *Appl. Catal., B: Environ.* **2003**, *44*, 117-151.

(20) Blok, K.; Dejager, D. *Environ. Monit. Assess.* **1994**, *31*, 17-40.

(21) De Soate, G. (1993) "Nitrous Oxide from Combustion and Industry: Chemistry, emissions, and Control", in *Proc. of International Workshop Methane and Nitrous Oxide: Methods in National Emissions Inventories and Options for Control*, Amersfoort, the Netherlands, February 3-5.

(22) Denman, K.L.; Brasseur, G.; Chidthaisong, A. (2007) Couplings between changes in the climate system and biogeochemistry. In: *Climate Change 2007: The Physical Science Basis. Contribution of Working Group I to the Fourth Assessment Report of the Intergovernmental Panel on Climate Change*, pp. 501–587. Cambridge University Press, Cambridge, UK and New York, NY.

(23) Le Mer, J.; Roger, P. *Eur. J. Soil. Biol.* **2001**, *37*, 25-50.

(24) Cicerone, R.L.; Oremland, R.S. *Global Biogeochem. Cycles* **1988**, 2, 299–327.

(25) Husson-Borg, P.; Majer, V.; Gomes, M. F. C. *J. Chem. Eng. Data* **2003**, *48*, 480-485.

(26) Gomes, M.F.C; Husson, P.; Jacquemin, J.; Majer, V. Interactions of gases with ionic liquids: experimental approach, in: Rogers, R.D.; Seddon, K.R. (Eds.), *ACS Symposium Series Ionic Liquids III: Fundamentals, Progress, Challenges, and Opportunities,* American Chemical Society Publications, Washigton DC, **2005** (Chapter 16).

(27) Palgunadi, J.; Kang, J. E.; Nguyen, D. Q.; Kim, J. H.; Min, B. K.; Lee, S. D.; Kim, H.; Kim, H. S. *Thermochim. Acta* **2009**, *494*, 94-98.

(28) Jacquemin, J.; Gomes, M. F. C.; Husson, P.; Majer, V. *J. Phys. Chem. B* **2004**, *108*, 721-727.

(29) Jacquemin, J.; Gomes, M. F. C.; Husson, P.; Majer, V. *J. Chem. Thermodyn.* **2006**, 38, 490-502.

(30) Hou, Y.; Baltus, R.E. *Ind. Eng. Chem. Res.* **2007**, 46, 8166-8175.

(31) Andrew, M. *Master Thesis*, Ecole Nationale Supérieure des Industries Chimiques, France, **2010**.

(32) Shokouhi, M.; Abidi, M.; Jalili, A.H.; Hosseini-Jenab, M.; Mehdizadeh, A. *J. Chem. Eng. Data* **2010**, 55, 1663-1668.

(33) Jacquemin, J.; Gomes, M.F.C.; Husson, P.; Majer, V. *Fluid Phase Equilib.* **2006**, 240, 87-95.

(34) Moutiers, G.; Billard, I.; Labet, A. *Inorg. Chem.* **2003**, 42, 1726-1733.

(35) Camper, D.; Scovazzo, P.; Koval, C.; Noble, R. *Ind. Eng. Chem. Res.* **2004**, 43, 3049-3054.

(36) Kilaru, P.K.; Scovazzo, P. *Ind. Eng. Chem. Res.* **2008**, 47, 910-919.

(37) Finotello, A.; Bara, J. E.; Camper, D.; Noble, R. D. *Ind. Eng. Chem. Res.* **2008**, 47, 3453-3459.

(38) Hong, G.; Jacquemin, J.; Deetlefs, M.; Husson, P.; Gomes M.F.C. *Fluid Phase Equilibra.* **2007**, 257, 27-34.

(39) Gomes, M.F.C; *J. Chem. Eng. Data* **2007**, 52, 472-475.

(40) Ferguson, L.; Scovazzo, P. *Ind. Eng. chem. Res.* **2007**, *46*, 1369-1374.

Chapitre V. Étude thermodynamique des systèmes binaires rencontrés dans la désulfurisation des essences à l'aide des liquides ioniques

The aim of this chapter is to investigate vapor-liquid equilibrium of binary systems encountered in the extractive desulfurization of gasoline and diesel using ionic liquids. This work is focused on two ionic liquids: 1, 3-dimethylimidazolium methylphosponate [DMIM][Ph] and 1-ethyl-3-methylimidazolium thiocynate [EMIM][SCN]. Vapor-liquid equilibrium (VLE) measurements on binary mixtures of ionic liquids with various solutes including thiophene, pyridine, toluene and water at pressures close to the atmospheric pressure were performed and correlated with the PC-SAFT EoS. The pure ILs parameters were estimated from experimental density data whereas binary interaction parameters k_{ij} were fitted on experimental VLE data. The eight binary systems: {thiophene+ILs}, {pyridine+ILs}, {toluene+ILs} and {water+ILs} studied in this chapter were accurately described by the PC-SAFT EoS.

V.1 Introduction

Recently, the environmental protection strategies have led to drastic restrictions by the European Community on sulfur and nitrogen contents in produced fuels because their combustion gives birth to sulfur and nitrogen oxides which are responsible for acid rain, global warming effects and air pollution. Therefore, a considerable attention has been attracted to the desulfurization of fuels and many countries including Europe and Japan, were striving to reduce the sulfur content in gasoline to less than 10 ppm by 2010[1].

Until now, the most widely used desulfurization process in industry is hydrodesulfurization (HDS), by which most of the sulfur compounds (thiols, sulfides and disulfides) are converted to H_2S under the catalysis of $Co/Mo/Al_2O_3$ or $Ni/Mo/Al_2O_3$ at high temperature and high pressure. Such a method however suffers of several drawbacks: (i) it is operated at very high temperatures and pressures, (ii) octane and cetane numbers are reduced due to hydrogenation side reactions, (iii) it is efficient for the removal of thiols, sulfides and thiophenes, but less effective for removing refractory sulfur compounds such as benzothiophene, dibenzothiophene, and their alkyl derivatives[2,3] due to their extremely low hydrogenation activity[4]. For these reasons, deep desulfurization is still a challenging task for the conventional HDS process and it is necessary to develop alternative approaches for the production of low or even ultralow sulfur content diesel oils by some other sulfur removal mechanisms.

An alternative process: extractive desulfurization using ionic liquids (ILs) is regarded as a promising process: it has a high sulfur removal efficiency and a high selectivity under mild operating conditions, moreover, it is simple, safe and reproducible. The use of ILs for extractive desulfurization shows a great potential in comparison with conventional organic solvents, due to their physical-chemical properties (negligible vapor pressure, high chemical and thermal stabilities, recyclability). Moreover, they are able to dissolve a wide range of organic or inorganic substances, and it is possible

to adjust some of their properties such as polarity or miscibility for certain system requirements. These properties make ILs very good solvents for liquid-liquid extractions but also for a number of applications e.g. catalysis, synthesis and gas separations[5-7]. The extractive desulfurization of diesel oil using a series of ILs was reported by Jess et al.[8] in 2001. Then, extractive desulfuration[9-18] and denitrogenation[19] processes of gasoline employing ILs have been extensively investigated. Such studies highlight that the ILs have higher liquid-liquid extraction ratios and greater selectivity in comparison with the conventional organic solvents. Among many types of studied ionic liquids, those based on imidazolium cations and $[BF_4]^-$ or $[PF_6]^-$ anions showed high efficiency for organic sulfur as well as organic nitrogen compounds extraction[20,21]. However, several liquid-liquid equilibrium data show that unwanted effect of aromatic hydrocarbons extraction proceeds parallel to desulfurization and diminishes the fuel octane number[10]. Due to the stability and corrosion problems as well as the total costs of deep fuel desulfurization, the choice of the most suitable ionic liquid is still a challenging task for researchers. As an example, it was found that the imidazolium thiocyanate ILs, e.g. [C_n-mim][SCN] could selectivity separate[22-24] hydrocarbons from sulfur compounds.

Since sulfur compounds are partially miscible with ILs, phase equilibrium measurements were mainly focused on liquid-liquid equilibrium (LLE). It is however obvious that binary mixtures encountered in the desulfurization process present not only liquid-liquid equilibrium but also vapor-liquid equilibrium (VLE) regions[25]. Vapor-liquid equilibrium data for IL-containing binary systems are extremely scarce but essential for the development of thermodynamic model and for the calculation of phase diagrams in multi-component systems. For these reasons, it was decided to measure the vapor-liquid equilibrium of various systems involved in the extractive desulfurization of fuels from ILs. VLE data of binary systems containing either: 1,3-dimethylimidazolium methylphosphonate [DMIM][Ph] or 1-ethyl-3-methylimidazolium thiocynate [EMIM][SCN] and one of the following solutes: thiophene, pyridine, toluene and water are determined in this work. A total of eight

binary systems: {thiophene + ILs}, {pyridine + ILs}, {toluene + ILs} and {water+ ILs} were thus studied. The PC-SAFT (Perturbed-Chain SAFT) EoS was choosen to correlate the acquired data. The pure ILs parameters were determined from density measurement also performed in this chapter.

V.2 PC-SAFT modelling

The Pertubed Chain-Statistical Associating Fluid Theory (PC-SAFT) EoS has been developed in 2001 by Gross and Sadowski[26] who derived a dispersion expression for chain molecules and used a hard-chain reference fluid.

The PC-SAFT equation is usually written in terms of the residual Helmholtz energy. Each term in the equation represents different microscopic contributions to the total free energy of the fluid. The equation writes:

$$\tilde{a}^{res} = \tilde{a}^{hc} + \tilde{a}^{disp} + \tilde{a}^{assoc} \qquad \text{(V-1)}$$

where $\tilde{a}^{res}$ is the residual Helmholtz free energy of the system. The superscripts hc, disp and assoc refer to a reference hard chain contribution, a dispersion contribution and an associating contribution, respectively. The use of these different terms depends on the particular system under study, according to its physical nature.

The hard chain term which comes from Wertheim's theory is provided and defined by Gross and Sadowski as :

$$\tilde{a}^{hc} = \bar{m}\tilde{a}^{hs} - \sum_{i=1}^{n_c} x_i \left(m_i - 1\right) \ln g_{ij}^{hs} \qquad \text{(V-2)}$$

It depends on the radial pair distribution function for segments in the hard-sphere system (g_{ij}^{hs}), on the hard-sphere contribution ($\tilde{a}^{hs}$) and on the mean segment number ($\bar{m}$).

The dispersion contribution to the Helmholtz free energy $\tilde{a}^{disp}$ accounts for Van der Waals forces. In this work, the dispersion expression defined by Gross and Sadowski was used:

$$\tilde{a}^{disp} = -2\pi\tilde{\rho}I_1\overline{m^2\varepsilon\sigma^3} - \pi\tilde{\rho}\overline{m}C_1I_2\overline{m^2\varepsilon^2\sigma^3} \quad \text{(V-3)}$$

where $\tilde{\rho}$ is the number density, the coefficient C_1 depends on the mean segment number ($\overline{m}$) and on the reduced density (η), I_1 and I_2 are power series which depend on η and m, σ, ε are the pure component PC-SAFT parameters.

For evaluating the VLE of non associative fluids, inclusion of $\tilde{a}^{hc}$ and $\tilde{a}^{disp}$ in the PC-SAFT approach is sufficient. Three parameters, the segment number (m), the segment energy parameter (ε/k_B), and the segment diameter (σ) are required to characterize each compound. However, the Helmholtz free energy due to association $\tilde{a}^{assoc}$, absolutely necessary to model mixtures containing associating molecules, is defined by:[27,28]

$$\tilde{a}^{assoc} = \sum_{i=1}^{nc} x_i \left[\sum_{A_i} \left(\ln X^{A_i} - \frac{X^{A_i}}{2} \right) + \frac{1}{2} M_i \right] \quad \text{(V-4)}$$

where X^{A_i} is the mole fraction of molecules i not bonded at site A, M_i is the number of association sites on each molecule and $\sum_{A_i}$ represents a sum over all associating sites on each molecule. The parameter X^{A_i} is given by:

$$X^{A_i} = \left[1 + N_{AV} \sum_j \sum_{B_j} \rho_j X^{B_j} \Delta^{A_i B_j} \right]^{-1} \quad \text{(V-5)}$$

where ρ_j is the molar density of component j, $\Delta^{A_iB_j}$ is the association strength which depends on the association energy $\varepsilon^{A_iB_j}$ and the association volume $k^{A_iB_j}$ between associating substances i and j. Hence, if one of the substances in a mixture is non-associating, $k^{A_iB_j}$ and $\Delta^{A_iB_j}$ will vanish consequently.

V.3 Experimental section

V.3.1 Materials

1, 3-dimethylimidazolium methylphosponate [DMIM][Ph] (purity > 98%) was obtained from Solvionic and 1-ethyl-3-methylimidazolium thiocynate [EMIM][SCN] was supplied by Fluka with a purity > 95%. Pyridine, thiophene and toluene were supplied by Sigma-aldrich with a quoted purity of 99.8%, 99.8% and 99% respectively. n-Dodecane (purity > 99%) and tetrachloroethylene (purity > 99%) were used as reference fluids for measuring the density of ILs. All these materials with suppliers and purities were listed in table V-1.

Table V-1: Materials used in experiments with suppliers and purities.

Materials	Suppliers	Purity%
[DMIM][Ph]	Solvionic	>98
[EMIM][SCN]	Fluka	>95
Pyridine	Sigma-Aldrich	99.8
Thiophene	Sigma-Aldrich	99.8
Toluene	Sigma-Aldrich	99
n-dodecane	Sigma-Aldrich	>99
Tetrachloroethylene	Acros Organics	>99

V.3.2 Apparatus and procedure

V.3.2.1 Density measurement

Experimental densities of ILs were measured using an Anton Paar DMA 60 digital vibrating-tube densimeter, with a DMA 512P measuring cell in the temperature

range (298.15 to 318.75) K at atmospheric pressure. The temperature in the vibrating-tube cell was measured by a platinum resistance thermometer Pt-100 with an accuracy of ±0.1 K. A thermostatic bath with oil as circulating fluid was used in the thermostat circuit of the measuring cell, which was held constant to ±0.1 K. n-Dodecane and tetrachloroethylene were used as reference fluids for the calibration of the vibrating-tube densimeter in order to guarantee an extrapolation of the IL densities.

V.3.2.2 Vapour-liquid equilibrium measurement

The VLE measurements of binary mixtures have been performed in a glass cell by using a static method. The apparatus is shown schematically in Figure V-1. This apparatus can be applied for the measurement of reliable isothermal P-x data up to 298 K and 40 kPa. The experimental set up consists of a cell with an internal volume of about 15 cm^3 kept at constant temperature using a thermostated bath. The temperature inside the cell is measured by a platinum resistance thermometer PT-100 with an accuracy of ±0.1 K. The binary mixtures are weighted before introduction using an analytical balance with a resolution of ±0.00001g. The homogeneity of the composition of each phase is attained with a teflon coated magnet. The vapor phase is exclusively composed of the solvent. The equilibrium in the cell is a rapid process. The pressure is monitored using a calibrated pressure sensor. The method was checked by measuring the vapor-liquid equilibrium of the binary mixture {acetonitrile + methanol} where reliable VLE data exist in the literature. The experiences were carried out in the temperature range T = (283.15 to 303.15) K. In order to avoid corrections on the liquid phase composition, the liquid volume of the binary mixture was much larger than the volume of the vapor phase. The experimental pressure is assessed to be reliable to within ±1% according to the test measurements.

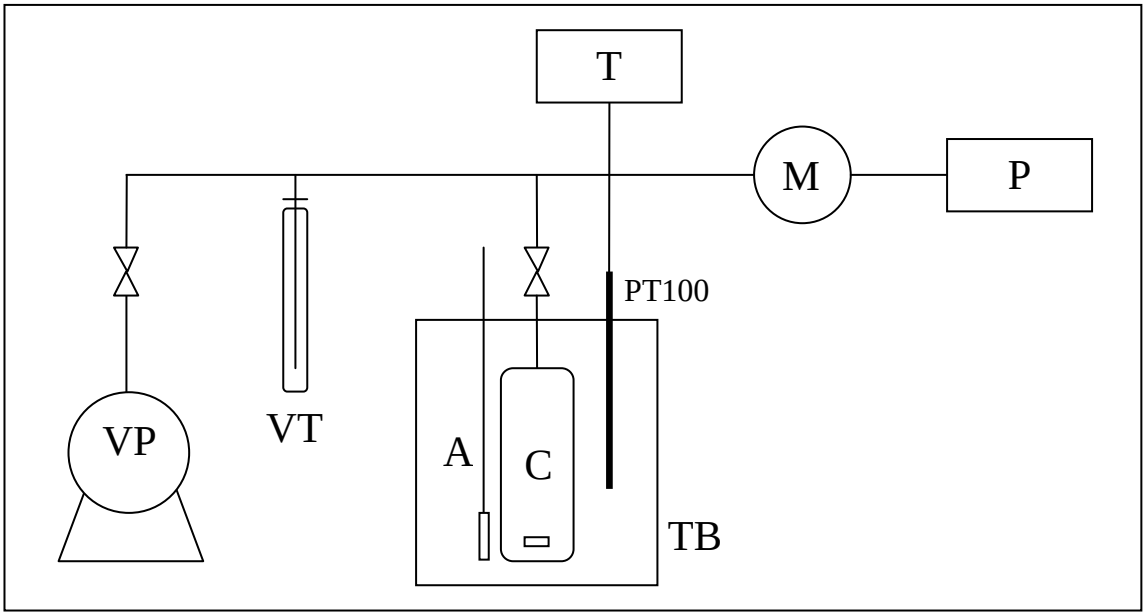

Figure V-1: Schema of the VLE apparatus: **VP**, vacuum pump; **VT**, vacuum trap; **A**, magnetic stirrer; **C**, equilibrium cell; **PT-100**, platinum resistance thermometer; **T**, temperature indicator; **M**, calibrated pressure sensor; **P**, digital pressure indicator; **TB**, thermostated bath.

V.4 Results and discussion

V.4.1 Pure components

The PC-SAFT equation was evaluated in the representation of the thermodynamic properties of pure ILs such as temperature-dependent density. Density measurements for 1,3-dimethylimidazolium methylphosponate [DMIM][Ph] were carried out at temperatures ranging from (298.15 to 318.75) K at atmospheric pressure. The experimental densities of [DMIM][Ph] measured in this work are reported in Table V-2, while the densities of [EMIM][SCN] were taken from literature[29]. The parameters of PC-SAFT for pure ILs were determined using experimental densities and by minimizing the following objective function (OF):

$$OF = \sum_{i=1}^{npts} \left(\frac{\rho_i^{sat,\exp} - \rho_i^{sat,cal}}{\rho_i^{sat,\exp}} \right)^2 \qquad \text{(V-6)}$$

which takes into account the deviations between calculated and experimental liquid densities. In this work, thiophene and toluene were modeled as non-associating substance and they were thus represented by three molecular parameters: m, the segment number; σ, the segment diameter; ε/k_B, the segment energy parameter. On the other hand, water and pyridine were considered as self-associating compounds and were presented by three non-assoicating parameters (m, σ, ε/k_B) but also two self-associating parameters (association energy -$\varepsilon^{A_iB_j}$ and the association volume-$k^{A_iB_j}$). The set of PC-SAFT parameters for pyridine, thiophene, toluene and water were taken from literature[26,30-32] and are recalled in Table V-3.

Table V-2: Experimental densities of pure [DMIM][Ph] in the range of the temperature form 298.15 K to 318.75 K.

ILs	T [K]	Density [g/cm³]
[DMIM][Ph]	298.15	1.2306
	299.45	1.2298
	300.75	1.2293
	302.15	1.2286
	303.45	1.2279
	304.75	1.2273
	305.85	1.2266
	307.15	1.2258
	308.65	1.2249
	310.35	1.2239
	311.75	1.2231
	313.05	1.2224
	314.45	1.2215
	315.85	1.2207
	317.25	1.2199
	318.75	1.2192

[a] The standard uncertainty u is u(ρ)=0.0001 g/cm³

Table V-3: Optimized PC-SAFT parameters of pure ILs: [EMIS][SCN], [DMIM][Ph] and PC-SAFT parameters of pyridine, thiophene, toluene and water.

ILs	M_w g·mol^{-1}	σ (Å)	ε/k_B (K)	m	k^{AB} (-)	ε^{AB} (K)	AAD% on density
[EMIM][SCN]	169.2500	4.2200	383.80	3.0500	0.002250	3450.00	0.32
[DMIM][Ph]	192.1500	4.1300	411.40	3.4200	0.002250	3450.00	0.12
H_2O	18.0150	3.0007	366.51	1.0656	0.034868	2500.70	–
Thiophene	84.1420	3.5655	301.73	2.3644	–	–	–
Pyridine	79.1014	3.8066	250.65	2.0352	0.189332	1890.30	–
Toluene	92.1410	3.7169	285.69	2.8149	–	–	–

The PC-SAFT parameters of pure ILs were determined considering ILs as self-associating compounds. The three non-associating parameters (m, σ, ε/k_B) were obtained by a fitting procedure on pure-component data. In order to keep a minimum number of parameters to be fitted, the two self-associating parameters ($\varepsilon^{A_iB_j}$ and $k^{A_iB_j}$) were transferred from those of 1-alkanols[33], i.e., $\varepsilon^{A_iB_j}$ =3450 K and $k^{A_iB_j}$ =0.00225. Both associating parameters were assumed constant because the alkyl chain length of the cation has a negligible effect on the strength of the associating bonds. Results obtained after optimization for the ILs studied in this paper and absolute average deviation (AAD%) on density are provided in Table V-3. Moreover, the resulting density-temperature diagrams are shown in Figure V-2. These results highlight that the density of pure ILs is well correlated by PC-SAFT EoS.

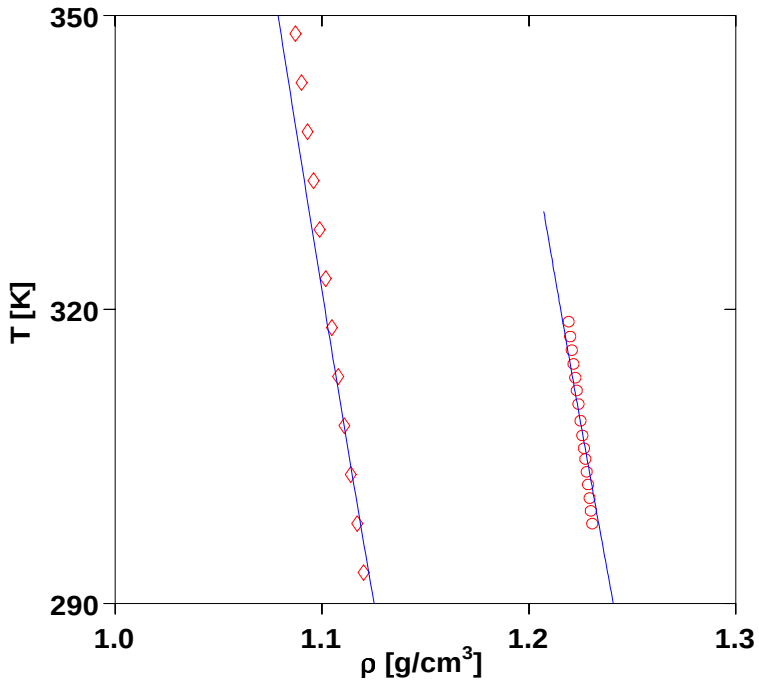

Figure V-2: Temperature-density diagrams for ILs: [EMIM][SCN] (◊) and [DMIM] [Ph] (○). Symbols: experimental densities data. Solid lines: PC-SAFT estimations.

V.4.2 Binary systems

Results of experimental VLE data obtained in this work are presented in Table V-4 and were correlated with the PC-SAFT EoS. In this study, mixtures are classically described with Berthelot-Lorentz combining rules where a binary interaction parameter, k_{ij}, is introduced to correct the cross-dispersive energy parameter according to $\varepsilon_{ij} = \sqrt{\varepsilon_i \varepsilon_j}(1-k_{ij})$. The interaction parameters k_{ij} of various binary mixtures were determined in order to minimize the deviations on mole fraction between calculated and experimental VLE data. The corresponding values with absolute average deviations on molar fraction are shown in Table V-5.

Table V-4: Experimental VLE and VLLE data for various molar fractions of different compounds in binary systems containing ILs.

ILs	T [K]	x_1	P [kPa]	State	T [K]	x_1	P [kPa]	State
[EMIM][SCN] +H_2O (1)	283.15	1.0000	1.27	VLE	288.15	1.0000	1.73	VLE
		0.8971	1.20			0.8971	1.62	
		0.8016	0.97			0.8016	1.37	
		0.7061	0.79			0.7061	1.09	
		0.6183	0.63			0.6183	0.84	
		0.5110	0.45			0.5110	0.65	
		0.4113	0.32			0.4113	0.46	
		0.3253	0.23			0.3253	0.36	
		0.2642	0.20			0.2642	0.30	
		0.1229	0.15			0.1229	0.21	
	293.15	1.0000	2.33	VLE	298.15	1.0000	3.20	VLE
		0.8971	2.19			0.8971	2.93	
		0.8016	1.78			0.8016	2.45	
		0.7061	1.48			0.7061	1.96	
		0.6183	1.19			0.6183	1.53	
		0.5110	0.85			0.5110	1.13	
		0.4113	0.62			0.4113	0.82	
		0.3253	0.46			0.3253	0.58	
		0.2642	0.37			0.2642	0.50	
		0.1229	0.25			0.1229	0.30	
[EMIM][SCN]+Toluene (1)	288.15	1.0000	2.42	LLE	293.15	1.0000	3.18	LLE
		0.8879	2.38			0.8879	3.10	
		0.7900	2.33			0.7900	3.04	
		0.6647	2.33			0.6647	3.04	
		0.5968	2.33			0.5968	3.04	
		0.4984	2.33			0.4984	3.04	
		0.3834	2.33			0.3834	3.04	
		0.3008	2.32			0.3008	3.04	
		0.1872	1.98	VLE		0.1872	2.68	VLE
		0.0957	1.28			0.0957	1.62	
		0.0438	0.63			0.0438	0.86	
	298.15	1.0000	3.81	LLE				
		0.8879	3.80					
		0.7900	3.76					
		0.6647	3.76					
		0.5968	3.76					
		0.4984	3.76					
		0.3834	3.76					
		0.3008	3.75					
		0.1872	3.20	VLE				
		0.0957	1.96					
		0.0438	1.15					
	288.15	1.0000	6.78	LLE	293.15	1.0000	8.70	LLE
		0.8953	6.67			0.8953	8.54	
		0.7889	6.68			0.7889	8.54	
		0.6954	6.64			0.6954	8.38	
		0.6009	5.83	VLE		0.6009	7.64	VLE
		0.4941	4.94			0.4941	6.33	

[EMIM][SCN]+Thiophene (1)		0.3985	4.01			0.3985	5.20	
		0.2999	3.11			0.2999	3.82	
		0.2028	2.28			0.2028	2.80	
		0.0980	1.15			0.0980	1.52	
		0.0526	0.68			0.0526	0.92	
		1.0000	10.37					
		0.8953	10.37	LLE				
		0.7889	10.36					
		0.6954	10.25					
		0.6009	9.73					
	298.15	0.4941	8.13					
		0.3985	6.70					
		0.2999	5.14	VLE				
		0.2028	3.63					
		0.0980	1.89					
		0.0526	1.18					
		1.0000	1.65			1.0000	2.20	
		0.9022	1.59			0.9022	2.13	
		0.8001	1.45			0.8001	1.95	
		0.7185	1.36			0.7185	1.84	
		0.5964	1.14			0.5964	1.53	
	288.15	0.4948	0.96	VLE	293.15	0.4948	1.30	VLE
		0.3971	0.80			0.3971	1.08	
		0.3050	0.59			0.3050	0.80	
		0.1956	0.44			0.1956	0.63	
[EMIM][SCN]+Pyridine (1)		0.1100	0.28			0.1100	0.38	
		1.0000	2.83					
		0.9022	2.71					
		0.8001	2.54					
		0.7185	2.38					
		0.5964	2.03					
	298.15	0.4948	1.70	VLE				
		0.3971	1.42					
		0.3050	1.12					
		0.1956	0.82					
		0.1100	0.57					
		1.0000	1.27			1.0000	1.73	
		0.8981	0.96			0.8981	1.37	
		0.8003	0.72			0.8003	0.93	
		0.7072	0.47			0.7072	0.67	
	283.15	0.6093	0.35	VLE	288.15	0.6093	0.50	VLE
		0.5232	0.26			0.5232	0.36	
		0.4160	0.17			0.4160	0.25	
		0.3274	0.13			0.3274	0.20	
[DMIM][Ph]+H_2O (1)		0.2154	0.10			0.2154	0.15	
		1.0000	2.33			1.0000	3.20	
		0.8981	1.86			0.8981	2.43	
		0.8003	1.28			0.8003	1.92	
		0.7072	0.89			0.7072	1.16	
		0.6093	0.62			0.6093	0.85	
	293.15	0.5232	0.49	VLE	298.15	0.5232	0.70	VLE
		0.4160	0.35			0.4160	0.47	
		0.3274	0.26			0.3274	0.35	
		0.2154	0.20			0.2154	0.25	

[DMIM][Ph]+Toluene (1)	288.15	1.0000	2.35	LLE	293.15	1.0000	3.05	LLE
		0.8916	2.30			0.9235	2.96	
		0.7910	2.27			0.8532	2.88	
		0.6859	2.21			0.7762	2.88	
		0.6014	2.25			0.6903	2.88	
		0.4946	2.27			0.7567	2.88	
		0.4007	2.27			0.4788	2.88	
		0.2999	2.27			0.3568	2.88	
		0.2037	2.27			0.2352	2.89	
		0.1004	2.17	VLE		0.1139	2.79	VLE
		0.0654	1.45			0.0651	1.86	
		0.0434	0.90			0.0414	1.23	
	298.15	1.0000	3.84	LLE	303.15	1.0000	4.73	LLE
		0.9235	3.82			0.9235	4.68	
		0.8532	3.77			0.8532	4.63	
		0.7762	3.76			0.7762	4.58	
		0.6903	3.76			0.6903	4.52	
		0.7567	3.76			0.7567	4.58	
		0.4788	3.76			0.4788	4.55	
		0.3568	3.76			0.3568	4.61	
		0.2352	3.77			0.2352	4.60	
		0.1139	3.68	ELV		0.1139	4.50	ELV
		0.0651	2.20			0.0651	2.90	
		0.0414	1.48			0.0414	1.88	
[DMIM][Ph]+Thiophene (1)	288.15	1.0000	6.75	LLE	293.15	1.0000	8.74	LLE
		0.9507	6.69			0.9497	8.69	
		0.9155	6.60			0.9115	8.52	
		0.8939	6.57			0.8891	8.49	
		0.8917	6.55			0.8635	8.53	
		0.8502	6.55			0.8945	8.47	
		0.6953	6.54			0.6953	8.40	
		0.6556	6.54			0.6556	8.43	
		0.4985	6.54			0.4985	8.48	
		0.3724	5.90	VLE		0.3646	7.58	VLE
		0.3001	5.18			0.2308	4.84	
		0.2353	4.16			0.1187	3.16	
		0.1071	2.54					
	298.15	1.0000	10.58	LLE	303.15	1.0000	12.98	LLE
		0.8945	10.38			0.8945	12.44	
		0.6953	10.36			0.6953	12.40	
		0.6556	10.38			0.6556	12.36	
		0.4985	10.24			0.4985	11.24	VLE
		0.3646	9.29	VLE		0.3646	10.57	
		0.2308	5.93			0.2308	7.20	
		0.1187	3.70			0.1187	4.29	
	288.15	1.0000	1.72	VLE	293.15	1.0000	2.25	VLE
		0.9013	1.66			0.9013	2.13	
		0.7794	1.58			0.7794	2.05	
		0.7066	1.58			0.7066	2.06	
		0.5934	1.57			0.5934	1.98	
		0.5061	1.48			0.5061	1.91	
		0.4364	1.38			0.4364	1.79	
		0.3010	1.08			0.3010	1.46	
		0.2201	0.84			0.2201	1.09	

[DMIM][Ph]+Pyridine (1)		0.1242	0.53			0.1242	0.69	
	298.15	1.0000	2.85	VLE	303.15	1.0000	3.45	VLE
		0.9013	2.76			0.9013	3.37	
		0.7794	2.57			0.7794	3.12	
		0.7066	2.56			0.7066	3.08	
		0.5934	2.43			0.5934	2.90	
		0.5061	2.32			0.5061	2.82	
		0.4364	2.26			0.4364	2.75	
		0.3010	1.86			0.3010	2.41	
		0.2201	1.40			0.2201	1.78	
		0.1242	0.91			0.1242	1.16	

[a] Standard uncertainties u: u(P)=0.05 kPa, u(T)=0.1 K and u(x_1)=0.0002

Table V-5: k_{ij} interaction parameters of binary mixtures at different temperatures

ILs	Compound	T [K]	k_{ij}	AAD% on mole fraction
[EMIM][SCN]	H_2O	283.15	-0.069	5.89
		288.15	-0.070	4.94
		293.15	-0.074	3.59
		298.15	-0.075	2.05
	Pyridine	288.15	0.059	7.86
		293.15	0.062	8.48
		298.15	0.061	8.83
	Toluene	288.15	0.070	3.43
		293.15	0.071	5.81
		298.15	0.070	4.37
	Thiophene	288.15	0.040	11.31
		293.15	0.043	14.10
		298.15	0.045	14.01
[DMIM][Ph]	H_2O	283.15	-0.154	7.35
		288.15	-0.153	6.28
		293.15	-0.154	4.94
		298.15	-0.156	4.80
	Pyridine	288.15	0.071	13.52
		293.15	0.068	9.04
		298.15	0.063	4.09
		303.15	0.060	5.46
	Toluene	288.15	0.045	16.90
		293.15	0.045	13.34
		298.15	0.044	14.81
		303.15	0.045	14.48
	Thiophene	288.15	0.036	10.16
		293.15	0.037	9.30
		298.15	0.034	8.61
		303.15	0.028	5.70

The VLE data of the 2 binary mixtures {H_2O + [EMIM][SCN]} and {H_2O + [DMIM][Ph]} at different temperatures: T = 283.15 K, T = 288.15 K, T =293.15 K and T = 298.15 K were first correlated and the corresponding isothermal phase diagrams are shown in Figures V-3 and V-4. In the experimental range of temperature, vapor-liquid equilibrium is observed in these systems for the overall range of composition. It is striking to see the high accuracy of the PC-SAFT EoS to correlate these data which highlight that the solubility of water in [EMIM][SCN] is much lower than in [DMIM][Ph].

Secondly, binary systems {Pyridine + ILs} were also studied at four temperatures: T = 283.15 K, T = 288.15 K, T = 293.15 K and T = 298.15 K. All experimental data along with their correlation by the PC-SAFT EoS are presented in Figure V-5 and V-6. As shown in Figure V-5, a good agreement between experimental VLE data and the calculated values is observed for the system {Pyridine + [EMIM][SCN]}. In the case of the binary system {Pyridine + [DMIM][Ph]} presented in Figure V-6, the PC-SAFT EoS predicts at 288.15 K a vapor-liquid-liquid line which is not observed experimentally. The flatness of the experimentally determined bubble curve however highlights that 288.15 K is very close to the upper critical solution temperature and it is thus not surprising that a 3-phase equilibrium was calculated with the PC-SAFT EoS. Futhermore, the VLE data evidences that for a given temperature, pyridine is more soluble in [EMIM][SCN] than in [DMIM][Ph].

Thirdly, phase diagrams of binary systems {Toluene + [EMIM][SCN]} and {Toluene + [DMIM][Ph]} are presented in Figures V-7, V-8. Vapor-liquid and vapor-liquid-liquid equilibrium are observed in both binary systems. For both systems, along the 3-phase line, temperature has a very small influence on the composition of the liquid phase rich in IL. Figure V-7 and Figure V-8 show that the PC-SAFT EoS may be used to predict with high accuracy the phase diagrams of these ionic liquids with toluene. Liquid-liquid equilibrium of the binary mixture {Toluene + [EMIM][SCN]} was reported by Marciniak[34], who concluded that the solubility of 15 hydrocarbons was the highest in ionic liquid with trifluoromethanesulfonate anion and the lowest in 1-

ethyl-3-methylimidazolium thiocyanate. In this work, we found that [DMIM][Ph] has a even poor efficiency for the absorption of toluene as compared to [EMIM][SCN].

Finally, systems {thiophene + ILs} have been studied and reported. Figure V-9 depicts the phase diagrams obtained for {thiophene + [DMIM][Ph]} as compared to experimental data. Vapor-liquid and vapor-liquid-liquid equilibrium are observed. Along the 3-phase line, the thiophene mole fraction in the liquid phase rich in IL changes from 0.52 to 0.66 when the temperature increases from 298.15 K to 303.15 K. A good agreement between experimental VLE data and the calculated values is demonstrated. However, the model has a difficulty to represent with high accuracy the binary system {thiophene + [EMIM][SCN]} which is presented in Figure V-10. Indeed the PC-SAFT EoS predicts VLE whereas LLE is experimentally determined. For a given temperature, thiophene is more soluble in [EMIM][SCN] than in [DMIM][Ph].

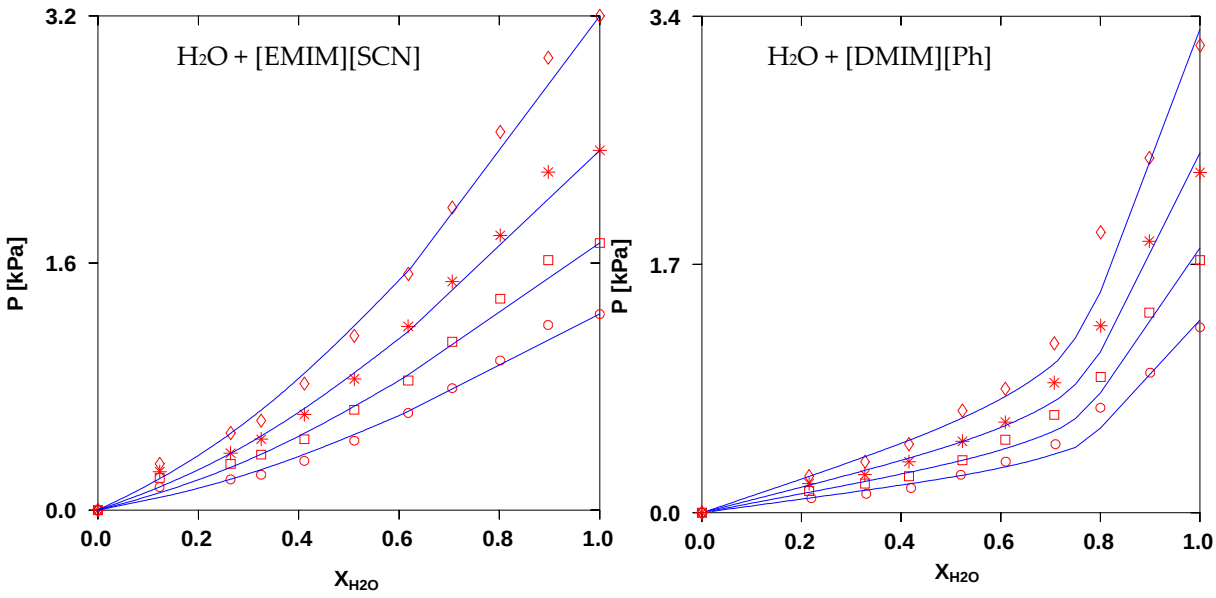

Figure V-3: Experimental VLE data for the investigated binary systems H_2O + [EMIM][SCN] at different temperatures: T = 283.15 K (○), T = 288.15 K (□) , T = 293.15 K (∗) and T = 298.15 (◊). Solid lines are the PC-SAFT calculations.

Figure V-4: Experimental VLE data for the investigated binary systems H_2O + [DMIM][Ph] at different temperatures: T = 283.15 K (○), T = 288.15 K (□) , T = 293.15 K (∗) and T = 298.15(◊). Solid lines are the PC-SAFT calculations.

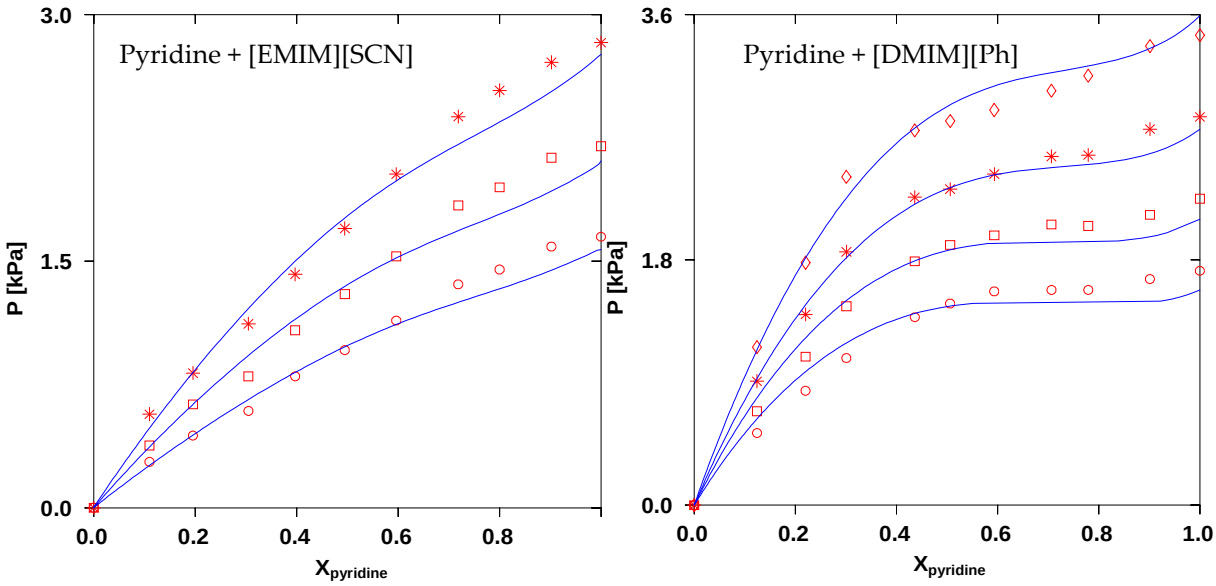

Figure V-5: Experimental VLE data for the investigated binary systems {Pyridine + [EMIM][SCN]} at different temperatures: T = 288.15 K (○) , T = 293.15 K (□) and T = 298.15(∗). Solid lines are the PC-SAFT calculations.

Figure V-6: Experimental VLE data for the investigated binary systems {Pyridine + [DMIM][Ph]} at different temperatures: T = 288.15 K (○) , T = 293.15 K (□), T = 298.15 K (∗) and T = 303.15 K (◊). Solid lines are the PC-SAFT calculations.

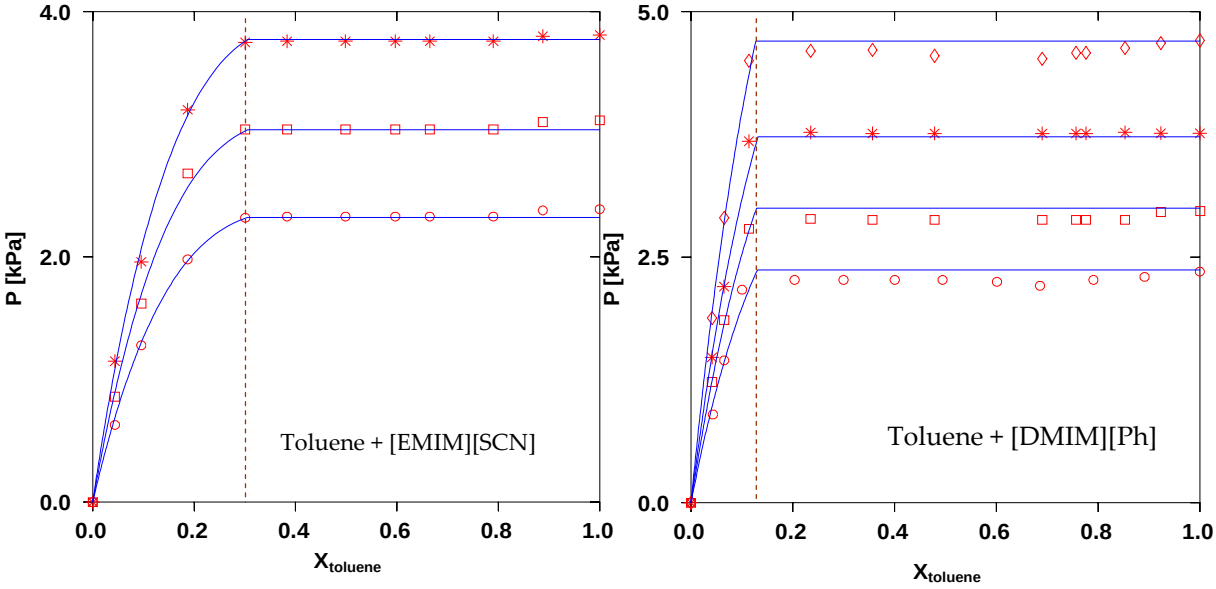

Figure V-7: Experimental VLE data for the investigated binary systems {Toluene + [EMIM][SCN]} at different temperatures: T = 288.15 K (○) , T = 293.15 K (□) and T = 298.15(∗). Solid lines are the PC-SAFT calculations.

Figure V-8: Experimental VLE data for the investigated binary systems {Toluene + [DMIM][Ph]} at different temperatures: T = 288.15 K (○) , T = 293.15 K (□), T = 298.15 K (∗) and T = 303.15 K (◊). Solid lines are the PC-SAFT calculations.

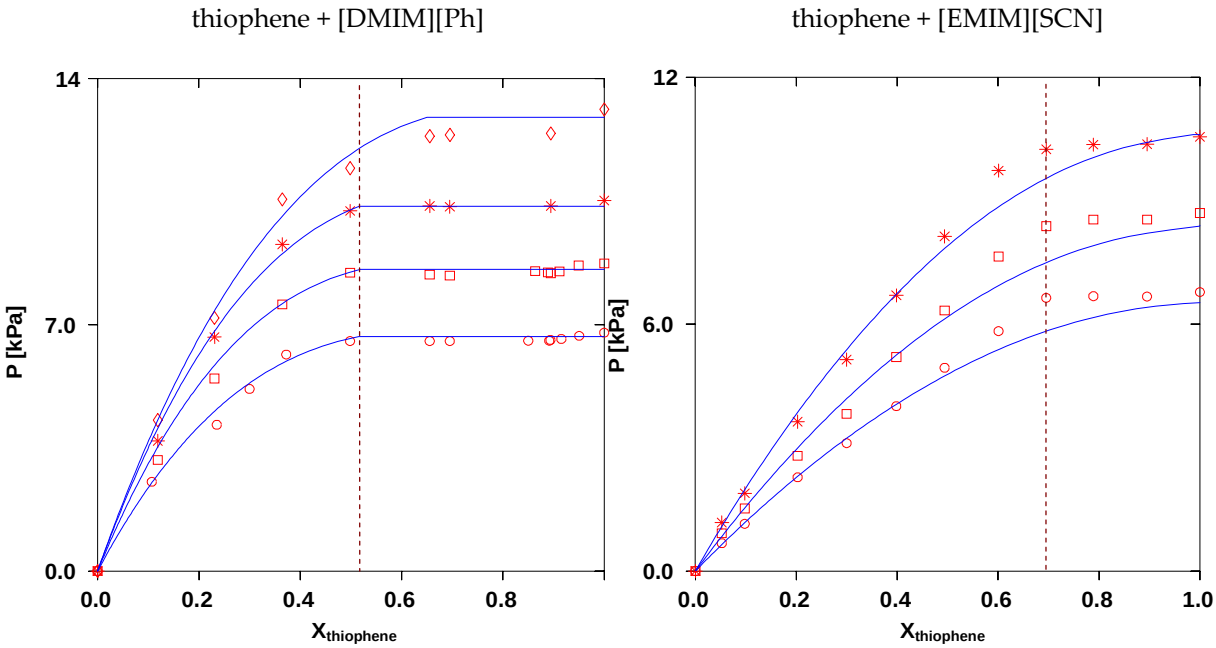

Figure V-9: Experimental VLE data for the investigated binary systems {thiophene + [DMIM][Ph]} at different temperatures: T = 288.15 K (○) , T = 293.15 K (□), T = 298.15 K (∗) and T = 303.15 K (◊). Solid lines are the PC-SAFT calculations.

Figure V-10: Experimental VLE data for the investigated binary systems {thiophene + [EMIM][SCN]} at different temperatures: T = 288.15 K (○) , T = 293.15 K (□) and T = 298.15(∗). Solid lines are the PC-SAFT calculations.

V.5 Conclusions

Eight binary systems encountered in the fuel desulfurization process using ILs were studied in this chapter. Attention was paid to a proper location of the 3-phase line. It was found that [EMIM][SCN] has a good capacity for fuels desulfurization as compared to [DMIM][Ph]. A thermodynamic model based on the PC-SAFT EoS was used with success in the correlation of the measured data and the well-known pitfalls of such an EoS[35,36] were not evidenced.

References

(1) Zhu, W. S.; Li, H. M.; Hang, X.; Yan, Y. S.; Lu, H. D.; Xia, J. X. Oxidative Desulfurization of Fuels Catalyzed by Peroxotungsten and Peroxomolybdenum Complexes in Ionic Liquids. *Energy Fuels* **2007**, *21*, 2514-2516.

(2) Baeza, P.; Aguila, G.; Gracia, F.; Araya, P. Desulfurization by Adsorption with Copper Supported on Zirconia. *Catal. Commun.* **2008**, *9*, 751-755.

(3) Rang, H.; Kann, J.; Oja, V. Advances in Desulfurization Research of Liquid Fuel. *Oil Shale* **2006**, *23*, 164-176.

(4) Shafi, R.; Hutchings, G. J. Hydrodesulfurization of Hindered Dibenzothiophenes: an Overview. *Catal. Today* **2000**, *59*, 423-442.

(5) Revelli, A. L.; Mutelet, F.; Turmine, M.; Solimando, R.; Jaubert, J. N. Activity Coefficients at Infinite Dilution of Organic Compounds in 1-Butyl-3-methylimidazolium Tetrafluoroborate Using Inverse Gas Chromatography. *J. Chem. Eng. Data* **2009**, *54*, 90-101.

(6) Revelli, A. L.; Mutelet, F.; Jaubert, J. N. Prediction of Partition Coefficients of Organic Compounds in Ionic Liquids: Use of a Linear Solvation Energy Relationship with Parameters Calculated through a Group Contribution Method. *Ind. Eng. Chem. Res.* **2010**, *49*, 3883-3892.

(7) Revelli, A. L.; Mutelet, F.; Jaubert, J. N. Partition Coefficients of Organic Compounds in New Imidazolium Based Ionic Liquids Using Inverse Gas Chromatography. *J. Chromatogr. A* **2009**, *1216*, 4775-4786.

(8) Bosmann, A.; Datsevich, L.; Jess, A.; Lauter, A.; Schmitz, C.; Wasserscheid, P. Deep Desulfurization of Diesel Fuel by Extraction with Ionic Liquids. *Chem. Commun.* **2001**, 2494-2495.

(9) Kedra-Krolik, K.; Fabrice, M.; Jaubert, J. N. Extraction of Thiophene or Pyridine from n-Heptane Using Ionic Liquids. *Ind. Eng. Chem. Res.* **2011**, *50*, 2296-2306.

(10) Mochizuki, Y.; Sugawara, K. Removal of Organic Sulfur from Hydrocarbon Resources Using Ionic Liquids. *Energy Fuels* **2008**, *22*, 3303-3307.

(11) Kulkarni, P. S.; Afonso, C. A. M. Deep Desulfurization of Diesel Fuel Using Ionic Liquids: Current Status and Future Challenges. *Green Chem.* **2010**, *12*, 1139-1149.

(12) Hansmeier, A. R.; Meindersma, G. W.; de Haan, A. B. Desulfurization and Denitrogenation of Gasoline and Diesel Fuels by Means of Ionic Liquids. *Green Chem.* **2011**, *13*, 1907-1913.

(13) Nefedieva, M.; Lebedeva, O.; Kultin, D.; Kustov, L.; Borisenkova, S.; Krasovskiy, V. Ionic Liquids Based on Imidazolium Tetrafluoroborate for the Removal of Aromatic Sulfur-Containing Compounds from Hydrocarbon Mixtures. *Green Chem.* **2010**, *12*, 346-349.

(14) Francisco, M.; Arce, A.; Soto, A. Ionic Liquids on Desulfurization of Fuel Oils. *Fluid Phase Equilib.* **2010**, *294*, 39-48.

(15) Zhang, S. G.; Zhang, Q. L.; Zhang, Z. C. Extractive Desulfurization and Denitrogenation of Fuels Using Ionic Liquids. *Ind. Eng. Chem. Res.* **2004**, *43*, 614-622.

(16) Ko, N. H.; Lee, J. S.; Huh, E. S.; Lee, H.; Jung, K. D.; Kim, H. S.; Cheong, M. Extractive Desulfurization Using Fe-Containing Ionic Liquids. *Energy Fuels* **2008**, *22*, 1687-1690.

(17) Huang, C. P.; Chen, B. H.; Zhang, J.; Liu, Z. C.; Li, Y. X. Desulfurization of Gasoline by Extraction with New Ionic Liquids. *Energy Fuels* **2004**, *18*, 1862-1864.

(18) Kedra-Krolik, K.; Mutelet, F.; Moise, J. C.; Jaubert, J. N. Deep Fuels Desulfurization and Denitrogenation Using 1-Butyl-3-methylimidazolium Trifluoromethanesulfonate. *Energy Fuels* **2011**, *25*, 1559-1565.

(19) Alonso, L.; Arce, A.; Francisco, M.; Soto, A. Extraction Ability of Nitrogen-Containing Compounds Involved in the Desulfurization of Fuels by Using Ionic Liquids. *J. Chem. Eng. Data* **2010**, *55*, 3262-3267.

(20) Zhang, S. G.; Zhang, Z. C. Novel Properties of Ionic Liquids in Selective Sulfur Removal from Fuels at Room Temperature. *Green Chem.* **2002**, *4*, 376-379.

(21) Alonso, L.; Arce, A.; Francisco, M.; Rodriguez, O.; Soto, A. Liquid-Liquid Equilibria for Systems Composed by 1-Methyl-3-octylimidazolium Tetrafluoroborate Ionic Liquid, Thiophene, and n-Hexane or Cyclohexane. *J. Chem. Eng. Data* **2007**, *52*, 1729-1732.

(22) Revelli, A. L.; Mutelet, F.; Jaubert, J. N. Extraction of Benzene or Thiophene from n-Heptane Using Ionic Liquids. *J. Phys. Chem. B* **2010**, *114*, 4600-4608.

(23) Domanska, U.; Marciniak, A. Measurements of Activity Coefficients at Infinite Dilution of Aromatic and Aliphatic Hydrocarbons, Alcohols, and Water in the New Ionic Liquid EMIM SCN Using GLC. *J. Chem. Thermodyn.* **2008**, *40*, 860-866.

(24) Domanska, U.; Laskowska, M. Measurements of Activity Coefficients at Infinite Dilution of Aliphatic and Aromatic Hydrocarbons, Alcohols, Thiophene, Tetrahydrofuran, MTBE, and Water in Ionic Liquid BMIM SCN Using GLC. *J. Chem. Thermodyn.* **2009**, *41*, 645-650.

(25) Domanska, U.; Zawadzki, M.; Paduszynski, K.; Krolikowski, M. Perturbed-Chain SAFT as a Versatile Tool for Thermodynamic Modeling of Binary Mixtures Containing Isoquinolinium Ionic Liquids. *J. Phy. Chem. B* **2012**, 116, 8191-8200.

(26) Gross, J.; Sadowski, G. Perturbed-Chain SAFT: An Equation of State Based on a Perturbation Theory for Chain Molecules. *Ind. Eng. Chem. Res.* **2001**, *40*, 1244-1260.

(27) Huang, S. H.; Radosz, M. Equation of State for Small, Large, Polydisperse, and Associating Molecules. *Ind. Eng. Chem. Res.* **1990**, *29*, 2284-2294.

(28) Huang, S. H.; Radosz, M. Equation of State for Small, Large, Polydisperse, and Associating Molecules: Extension to Fluid Mixtures. *Ind. Eng. Chem. Res.***1991**, *30*,, 1994-2005.

(29) Freire, M. G.; Teles, A. R. R.; Rocha, M. A. A.; Schroder, B.; Neves, C.; Carvalho, P. J.; Evtuguin, D. V.; Santos, L.; Coutinho, J. A. P. Thermophysical Characterization of Ionic Liquids Able to Dissolve Biomass. *J. Chem. Eng. Data* **2011**, *56*, 4813-4822.

(30) Van Niekerk, D.; Castro-Marcano, F.; Colina, C. M.; Mathews, J. P. Solvent Swelling Extent of Permian-Aged Vitrinite- and Inertinite-Rich Coals: Experiments

and Modeling Using the Perturbed-Chain Statistical Associating Fluid Theory (PC-SAFT). *Energy Fuels* **2011**, *25*, 2559-2564.

(31) Zuniga-Morena, A.; Galicia-Luna, L. A.; Betancourt-Cardenas, F. F. Compressed Liquid Densities and Excess Volumes of CO_2+ Thiophene Binary Mixtures from 313 to 363 K and Pressures up to 25 MPa. *Fluid Phase Equilib.* **2005**, *236*, 193-204.

(32) Gross, J.; Sadowski, G. Application of the Perturbed-Chain SAFT Equation of State to Associating Systems. *Ind. Eng. Chem. Res.* **2002**, *41*, 5510-5515.

(33) Pamies, J. C. *Ph.D.Thesis, Universitat Rovira i Virgili, Tarragona, Spain* **2003**.

(34) Marciniak, A. Influence of Anion Structure on the Liquid-Liquid Equilibria of 1-Ethyl-3-methyl-imidazolium Cation Based Ionic Liquid-Hydrocarbon Binary Systems. *J. Chem. Eng. Data* **2011**, *56*, 368-374.

(35) Privat, R.; Gani, R.; Jaubert, J.-N. Are Safe Results Obtained when the PC-SAFT Equation of State is Applied to Ordinary Pure Chemicals. *Fluid Phase Equilib.* **2010**, *295*, 76-92.

(36) Privat, R.; Conte, E.; Jaubert, J. N.; Gani, R. Are Safe Results Obtained when SAFT Equations are Applied to Ordinary Chemicals? Part 2: Study of Solid-Liquid Equilibria in Binary Systems. *Fluid Phase Equilib.* **2012**, *318*, 61-76.

Conclusions et perspectives

Le présent travail constitue une contribution à la représentation expérimentale des propriétés thermodynamiques des liquides ioniques en présence de composés organiques et de gaz à effet de serre, notamment le dioxyde de carbone mais aussi à l'étude théorique faisant appel à la modélisation de ces données expérimentales à l'aide de l'équation d'état PC-SAFT.

Une étude théorique dans le chapitre II a permis de vérifier la capacité de l'équation d'état PC-SAFT pour représenter la solubilité du dioxyde de carbone dans les liquides ioniques de type imidazolium. Les paramètres de l'équation PC-SAFT pour les liquides ioniques purs et les paramètres d'interaction binaires k_{ij} ont été ajustés sur des données expérimentales. Ce type de modèle est donc capable de présenter les propriétés thermodynamiques des liquides ioniques purs mais aussi le comportement thermodynamique des mélanges : {CO_2+LIs}.

Le chapitre III détaille la solubilité du dioxyde de carbone dans deux liquides ioniques spécifiques. Les mesures de solubilités du dioxyde de carbone dans ces deux liquides ioniques ont été obtenues à l'aide d'une cellule haute pression à volume variable et ont été corrélées avec précision par l'équation PC-SAFT. La solubilité du dioxyde de carbone dans ces deux liquides ioniques a été comparée à celle obtenue dans d'autres liquides ioniques ou solvants physiques. Ces deux liquides ioniques sont de bons candidats pour l'absorption du dioxyde de carbone et les cations de type phoshonium présentent une meilleure efficacité que les cations imidazolium.

Le chapitre IV a donné une vue d'ensemble sur les performances des liquides ioniques pour la capture des gaz à effets de serre. Les solubilités du dioxyde de carbone, protoxyde d'azote et méthane ont été mesurées à l'aide d'une technique de saturation isochore. Les résultats ont permis de mettre en évidence l'influence de la structure du liquide ionique sur l'efficacité de l'absorption de ces gaz. L'utilisation des liquides ioniques à tâche spécifique est préconisée afin d'améliorer la solubilité

des gaz. Une méthode de contribution de groupes a été développée afin de prédire la constante de Henry du dioxyde de carbone dans les liquides ioniques.

Dans une dernière partie, les performances de l'équation d'état PC-SAFT pour représenter le comportement thermodynamique des composés soufrés dans deux liquides ioniques ont été examinées. Les mesures d'équilibre liquide-vapeur ont été effectuées dans une cellule en verre en utilisant une méthode statique. L'équation PC-SAFT réussit à corréler ces données avec une grande précision.

A l'issue de ce travail de thèse, nous disposons donc d'un modèle (PC-SAFT) capable de restituer les équilibres liquide-vapeur, les équilibres liquide-liquide, les équilibres liquide-liquide-vapeur des systèmes binaires {dioxyde de carbone / composé soufré + liquide ionique}. Pour élargir le domaine d'application du modèle PC-SAFT et améliorer le caractère prédictif vis-à-vis des liquides ioniques, il est nécessaire d'avoir une meilleure compréhension de la nature des liquides ioniques mais aussi de compléter les banques de données expérimentales.

Application de l'équation d'état PC-SAFT à la capture du dioxyde de carbone et à la désulfuration des essences

Le remplacement des solvants organiques classiques par une nouvelle génération de solvants moins toxiques, moins inflammables et moins polluants est un défi majeur pour l'industrie chimique. Les liquides ioniques, sels liquides qui satisfont ces critères, sont envisagés comme alternatives. Le but de ce travail est d'évaluer le comportement des liquides ioniques en présence de gaz à effet de serre (CO_2, N_2O et CH_4) ou de composés organiques. Dans un premier temps, une étude théorique présente les performances du modèle thermodynamique PC-SAFT sur la représentation des équilibres liquide-vapeur de systèmes constitués de dioxyde de carbone et de liquide ionique. Ensuite, l'étude de la solubilité du méthane, du dioxyde de carbone et du protoxyde d'azote dans divers liquides ioniques a été effectuée sous basse ou haute pression. Ce travail propose un modèle basé sur le concept de contribution de groupes afin de prédire la constante d'Henry du CO_2 dans les liquides ioniques. Enfin, une étude sur les équilibres liquide-vapeur des systèmes binaires rencontrés dans la désulfuration des essences a été effectuée. Les données expérimentales ont permis d'évaluer les performances de l'équation PC-SAFT à représenter les équilibres entre phases de systèmes {composés soufrés / aromatiques + liquide ionique}.

Mots-clés: liquides ioniques, l'équation d'état PC-SAFT, dioxyde de carbone, composé soufré, solubilité et désulfuration

****

Application of PC-SAFT equation of state in the carbon dioxide capture and the gasoline desulfurization

The replacement of conventional organic solvents by a new generation of solvents less toxic, less flammable and less polluting is a major challenge for the chemical industry. Ionic liquids have been widely promoted as interesting substitutes for traditional solvents. The purpose of this work is to evaluate the behavior of ionic liquids in the presence of greenhouse gases (CO_2, CH_4 and N_2O) or organic compounds. Firstly, a theoretical study presents the performance of the thermodynamic model PC-SAFT in the representation of vapor-liquid equilibrium of systems containing ionic liquids and carbon dioxide. Then, the solubility study of methane, carbon dioxide and nitrous oxide in various ionic liquids was performed at high or low pressure. The group contribution concept is proposed in this study in order to predict the Henry's law constant of carbon dioxide in ionic liquids. Finally, a study on the vapor-liquid equilibrium of binary systems encountered in gasoline desulfurization was carried out. Experimental data were used to evaluate the performance of PC-SAFT equation of state to represent phase equilibrium of systems {sulfur / aromatic compounds + ionic liquid}.

Keywords: ionic liquids, PC-SAFT equation of state, carbon dioxide, sulfur compounds, solubility and desulfurization

UNIVERSITÉ DE LORRAINE

A Nancy, le 05 septembre 2013

No étudiant : 31001066

CHEN YUSHU
72-16-304
qianjin rue
Jiangsu
CHINE POPULAIRE

Monsieur,

Par décision en date du 04 septembre 2013, vous avez été autorisé à présenter en soutenance vos travaux en vue de l'obtention du diplôme :

Doctorat Génie des Procédés et des Produits

La soutenance aura lieu le 26 septembre 2012 à 10h00 à l'adresse suivante :

Amphithéâtre Donzelot - ENSIC, 1, rue Grandville - 54000 NANCY

La soutenance sera publique.

Je vous prie d'agréer, Monsieur, l'expression de mes salutations distinguées.

Le Président

Université de Lorraine Le Président

Pierre MUTZENHARDT

UNIVERSITÉ DE LORRAINE
34 COURS LÉOPOLD - CS 25233
54052 NANCY CEDEX
TÉL : 03 54 50 54 00
CONTACT@UNIV-LORRAINE.FR
WWW.UNIV-LORRAINE.FR

UNIVERSITÉ DE LORRAINE

Nancy, le 15 mai 2013.

PM/ML/EB/2013-04/N°107

Monsieur Jean-Louis JAUBERT
ENSIC - LRGP

Cher Collègue,

Vous avez sollicité l'Université afin d'obtenir l'autorisation d'une rédaction de mémoire en anglais pour la thèse de Monsieur Yushu CHEN.

Après avoir examiné votre dossier en collaboration avec l'Ecole Doctorale RP2E, j'ai l'honneur de vous faire connaître que j'ai décidé d'accepter votre demande, sous condition qu'un résumé substantiel de 10 pages soit rédigé en français.

Veuillez agréer, Cher Collègue, l'assurance de mes sincères salutations.

Pour le Président et par délégation,
La Vice-Présidente du Conseil Scientifique

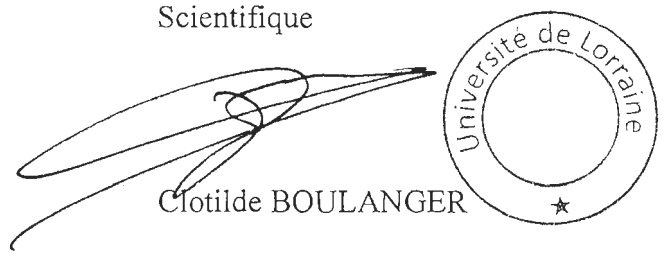

Clotilde BOULANGER

Copie à l'Ecole Doctorale RP2E

UNIVERSITÉ DE LORRAINE
34 COURS LÉOPOLD - CS 25233
54052 NANCY CEDEX
TÉL : 03 54 50 54 00
CONTACT@UNIV-LORRAINE.FR
WWW.UNIV-LORRAINE.FR